Development of a Novel Chiral Ligand: Linked-BINOL and Mechanistic Studies of Catalysis with Linked-BINOL

(新規不斉配位子 linked-BINOL の開発と触媒反応メカニズムの解析)

松永　茂樹

Abbreviation

Ac	acetyl
BINOL	2,2'-dihydroxy-1,1'-binaphthyl
Bu	butyl
cat.	catalyst
DME	dimethoxyethane
DMF	*N*,*N*-dimethylformamide
ee	enantiomeric excess
equiv	equivalent
Et	ethyl
h	hour
HPLC	high performance liquid chromatography
Ln	lanthanoides
Me	methyl
min	minute
MS 3A	molecular sieves 3A
MS 4A	molecular sieves 4A
NMR	nuclear magnetic resonance
Ph	phenyl
i-Pr	isopropyl
quant.	quantitative yield
rt	room temperature
TBS	*tert*-butyldimethylsilyl
THF	tetrahydrofuran
TMEDA	*N*,*N*,*N*,*N*-tetramethylethylenediamine
Ts	*p*-toluenesulfonyl
y.	yield

Acknowledgement

I would like to express my sincere appreciation to my supervisor, Prof. Masakatsu Shibasaki for his generous, endless, and sometimes strict, encouragement during these studies. I am sure that his enthusiasm for chemistry influenced greatly on my research style.

I also thank Dr. Takashi Ohshima, Dr. Takehiko Iida, Dr. Motomu Kanai, and Dr. Takeyuki Suzuki for their kind discussion on my research project. They often gave me clues to overcome difficulties in the research.

I wish to acknowledge Prof. Kentaro Yamaguchi and Dr. Shigeru Sakamoto for their help in the analysis of the catalysts. Without their help, I cannot accomplish my research project.

I am grateful to co-workers of mine, Mr. Naoya Kumagai, Dr. Noriyoshi Yamamoto, Mr. Shinji Harada, Mr. Tomofumi Kinoshita, Dr. Naoki Yoshikawa, Dr. Erasmus M. Vogl, Dr. Jagattaran, Das, Dr. Yun-Sik Kim, Mr. Shigemitsu Okada, Dr. Roels Jochen, Dr. Akihiro Sekine, and many other former and current members in Shibasaki's group. Especially, I thank Mr. Noriyuki Yamagiwa, Dr. Tian Jun, Mrs. Yumi Abiko, Mr. TakamasaYoshida and others in 4^{th} and 5^{th} lab for their kind support. They really helped me to start new research projects in our group. Without their patient and careful works, I could not develop anything during these three years. I am enjoying working with them. I am grateful to Dr. K. Yamada, Dr. Y. Hamashima and Dr. S. Yamasaki, they told me how attractive chemistry is when I was a undergraduate student. I also thank Dr. Takashi Mizutani, Dr. Kunihiko Fujii, Mr. Isao Sakurada and Ms. Izumi Yamamoto, who were the classmates of mine. They supported me a lot all the time.

I thank Ms. Yuko Suya and other secretaries of prof. Shibasaki, they mentally supported me everyday. Without their help, I could not continue my research.

Finally, I would like to express my sincere appreciation to my parents and family for their continuous support.

Preface

Organic chemistry can create something useful from almost nothing. That may be one of the reasons why chemistry is attractive to many chemists including me. It is like a game, once one starts the game it is difficult to stop it. Ever since the birthday of the organic chemistry in early 19th century, organic chemistry attracted many scientists. Organic chemistry, thus, witnessed a great advance during past twenty decades. Chemistry now indeed provides various commodities to us such as plastics, synthetic fibers, medicines, pesticides, odors etc, which we use everyday. Thus, many people often say, "Synthetic organic chemistry is a matured science", and "You can prepare anything you want if you have enough money and time". On the other hand, public and mass media still have rather negative impression on chemistry such as "pollution", "sick-house syndrome", "carcinogen" etc. Why? Is it because of the lack of propaganda from the chemists? Maybe, that is a part of the reason, but it is not the only reason. In my opinion, major reason is that organic chemistry is still immature. Chemistry in this century should not only provide useful products, but also should do it with least waste, money, time, energy etc. When compared with the biosynthesis of complex molecules in nature, you will immediately see how primitive the state of art in the chemistry is. I would like to continuously go ahead toward "perfect chemistry". Of course, it is a never-ending story, that is actually another reason chemistry attracts me a lot.

As a member of Faculty of Pharmaceutical Sciences, I investigated a catalytic asymmetric synthesis for my Ph. D. thesis. Asymmetric catalysis can be a useful tool for the synthesis of optically active medicine with least waste, and can contribute a lot in process chemistry. Toward "perfect" asymmetric catalysis, I considered that both the development of new asymmetric catalysis and its mechanistic study should be closely related. Either the development of new asymmetric catalysis or its mechanistic study alone is not enough. The development of new asymmetric catalysis provides me a chance to find new chemistry through mechanistic studies. Mechanistic studies, then, in turn, provides me an insight to develop a new catalysis. They are like two wheels of a bike. I can go ahead only when I have both of them—This is my favorite style to enjoy chemistry.

Although what I found so far is still far from "perfect", I believe I am going ahead step by step. Here I would like to report a part of my work during these five years, which was performed based on my philosophy about research.

September 2003
Shigeki Matsunaga

Chapter 1. Background

1-1. Introduction

Synthesis of chiral compounds using catalytic asymmetric processes is one of the most important and most rapidly growing areas in modern synthetic organic chemistry.[1] Such catalytic and asymmetric processes are more economic and more environmentally benign than processes that use stoichiometric amounts of reagents. In Shibasaki's continuing research project towards the development of practical and atom-economic[2] asymmetric catalysis, Shibasaki's group has demonstrated the usefulness of multifunctional cooperative asymmetric catalysis in a variety of enantioselective transformations,[3] such as the nitroaldol reaction,[4] direct aldol reaction,[5] Michael reaction,[6] Michael-aldol reaction,[7] hydrophosphonylation,[8] hydrophosphination,[9] protonation,[10] epoxidation of enones,[11a,11b] α,β-unsaturated carboxylic acid imidazolide,[11c] α,β-unsaturated amide[11d] and α,β-unsaturated *N*-acylpyrrole,[11e] epoxide opening reaction,[12] Diels-Alder reaction,[13] nitro-Mannich reaction,[14] cyanosilylation of aldehydes[15] and ketones,[16] Strecker reaction,[17] Reissert reaction,[18] and cyano-ethoxycarbonylation.[19] There have been great achievements in the field of asymmetric catalysis with regard to the concept of multifunctional cooperative catalysis, and many groups are now employing a multifunctional strategy in the development of new asymmetric catalysts.[20] From a practical point of view, however, some of the heterobimetallic multifunctional asymmetric complexes still have room for improvement, such as in catalyst loading and stability. To overcome these problems and to widen the scope of multifunctional bimetallic catalysis, I started my PhD work toward the development of a novel chiral ligand. The development and application of a novel linked-BINOL and mechanistic studies using linked-BINOL complexes will be discussed.

1-2. Heterobimetallic multifunctional asymmetric complexes

1,1'-Bi-naphthols (BINOLs) have an important role as chiral ligands in modern asymmetric catalysis,[21] incorporating various types of Lewis acidic metals. Heterobimetallic complexes, developed by Shibasaki and co-workers, also consist of two or three BINOLs, Lewis acidic center metals, and alkali metals, the structures of which were unequivocally determined using NMR, LDI-TOF mass spectrometry, and X-ray crystal analysis (Figure 1).[22]

Mechanistic studies[22] suggest that the heterobimetallic complexes promote the various asymmetric reactions via dual activation of both substrates (nucleophiles and electrophiles).

The Brønsted base moiety of the catalysts (alkali metal binaphthoxide) activates the nucleophiles, such as nitroalkanes, by deprotonation. At the same time, the Lewis acid moiety (lanthanides, aluminum or gallium center metals) activates the electrophiles. The dual activation occurs at positions controlled by the asymmetric catalyst, and so the substrates react with the other substrates from a defined direction, resulting in high enantioselectivity.

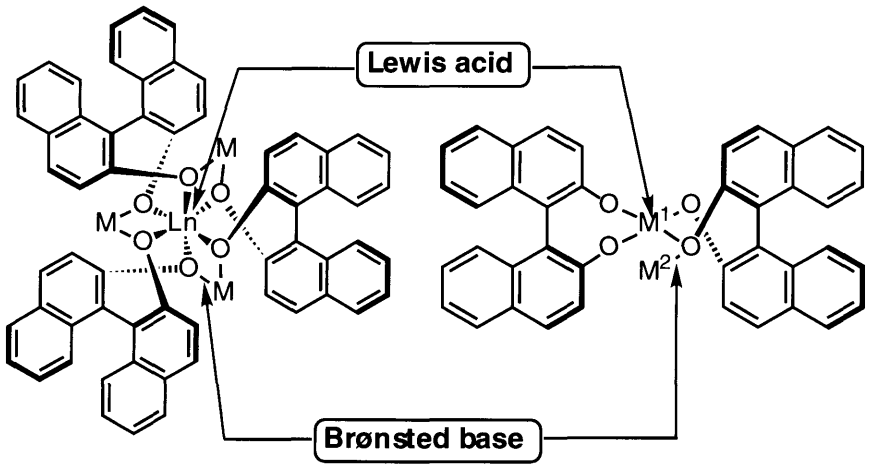

Ln = La, M = Li : LLB **1** M^1 = Al, M^2 = Li : ALB **2**

M^1 = Ga, M^2 = Li : GaLB **3**

Reviews: 1) Shibasaki, M.; Yoshikawa, N. *Chem. Rev.* **2002**, *102*, 2187.
2) Shibasaki, M.; Sasai, H.; Arai,T. *Angew. Chem., Int. Ed. Engl.* **1997**, *36*, 1236.

Figure 1. Heterobimetallic multifunctional complexes

Although the heterobimetallic complexes work well in various asymmetric reactions,[3] the structural feature of two or more ligands incorporated in the complexes sometimes causes a severe stability problem. In the worst cases, some heterobimetallic complexes decompose under the reaction conditions due to irreversible ligand exchange between BINOLs and nucleophiles, resulting in a lower chemical yield and/or enantiomeric excess of the desired products. For example, coworkers of mine and I previously reported the enantioselective epoxide opening reaction with 4-methoxyphenol promoted by GaLibis(binaphthoxide) (GaLB) complex (Figure 1. **3**).[12b] As shown in Figure 2, GaLB afforded enantiomerically enriched 1,2-diol mono ethers, which are versatile chiral building blocks, in only moderate chemical yields despite the use of more than 20 mol % of the catalyst. The poor reactivity of GaLB **3** was attributed to a ligand exchange between BINOL and 4-methoxyphenol, and the preparation of a more stable Ga-complex was an

effective solution to this problem. Thus, I first attempted to increase the stability of the GaLB complex **3** through the development of a new chiral ligand.

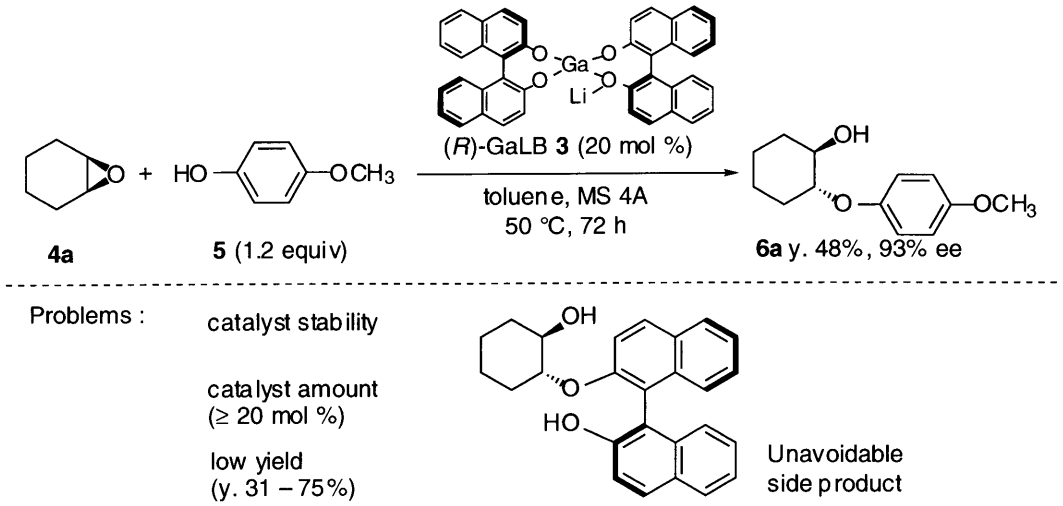

Iida, T.; Yamamoto, N.; Matsunaga, S.; Woo, H-G.; Shibasaki, M. *Angew. Chem., Int. Ed.* **1998,** *37*, 2223.

Figure 2. Problems in catalytic enantioselective epoxide ring opening with 4-methoxyphenol promoted by Ga-Li(BINOL)$_2$ (GaLB: **3**).

Chapter 2. Development of a Novel Linked-BINOL and its Application to Ga-Li-linked-BINOL Complex

2-1. Ligand Design 1: Carbon-linked-BINOL

To increase the stability of the GaLB **3**, I hypothesized that by linking the two BINOL units in GaLB, the complex would become more stable against ligand exchange without any adverse effects on the asymmetric environment. [23, 24] One of the key issues for designing a linked-BINOL is the length and flexibility of its linker. The linker should be relatively short to somewhat limit the flexibility of BINOL units, because the geometry is likely to be crucial for enantioselectivity. In addition, a linker that is too rigid would also be unfavorable because the asymmetric environment would be negatively affected. In the worst cases, even the formation of the desired 1:2 (gallium : BINOL unit) complex would be prevented by a rigid linker.

I first designed carbon linked-BINOLs (Figure 3, **7** – **9**) to evaluate the effects of the linker. As shown in Scheme 1, Ga-Li-carbon-linked-BINOL complexes were prepared using $GaCl_3$ (1 mol equiv), **7**, **8**, or **9** (1 mol equiv), and BuLi (4 mol equiv). In contrast to my initial assumption, however, none of these were effective in the enantioselective epoxide opening reaction of cyclohexene oxide (**4a**) with 4-methoxyphenol (**5**). The results were summarized in Table 1. Ga-Li-carbon-linked-BINOL complexes afforded the epoxide opening product **6a** in only low yield and enantiomeric excess (with **7**: yield 28%, 27% ee; with **8**: yield 43%, 10% ee; with **9**: y. 40%, 1% ee). These unsatisfactory results might be due to the undesired oligomeric structure of these linked-BINOL complexes. With a carbon linker, each BINOL unit of the linked-BINOLs can rotate freely during the

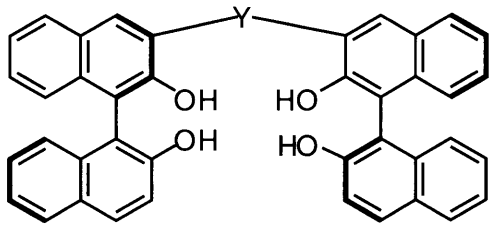

Y

7: —CH_2—

8: —$(CH_2)_2$—

9: —$(CH_2)_3$—

Figure 3. Carbon linked-BINOLs (**7**–**9**).

Scheme 1 . Catalyst Preparation.

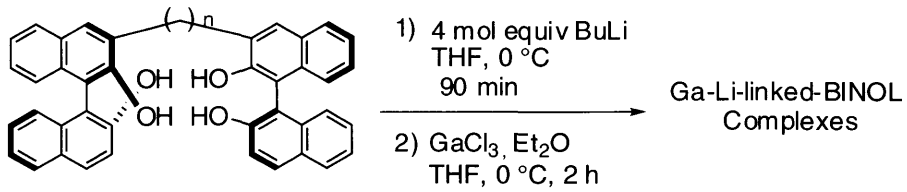

Table 1. Catalytic Enantioselective Ring Opening of Cyclohexene Oxide Promoted by Ga-Li-linked-BINOL Complexes.

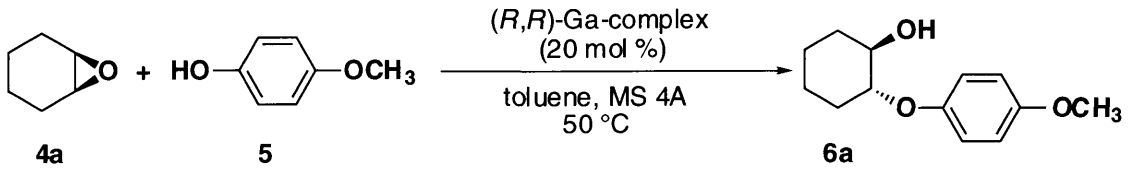

4a **5** **6a**

ligand	time (h)	yield (%)	ee (%)
7 : n = 1	78	28	27
8 : n = 2	66	43	10
9 : n = 3	72	40	1

Low yield
Low ee

cf. GaLB: 72 h, y. 48%, 93% ee

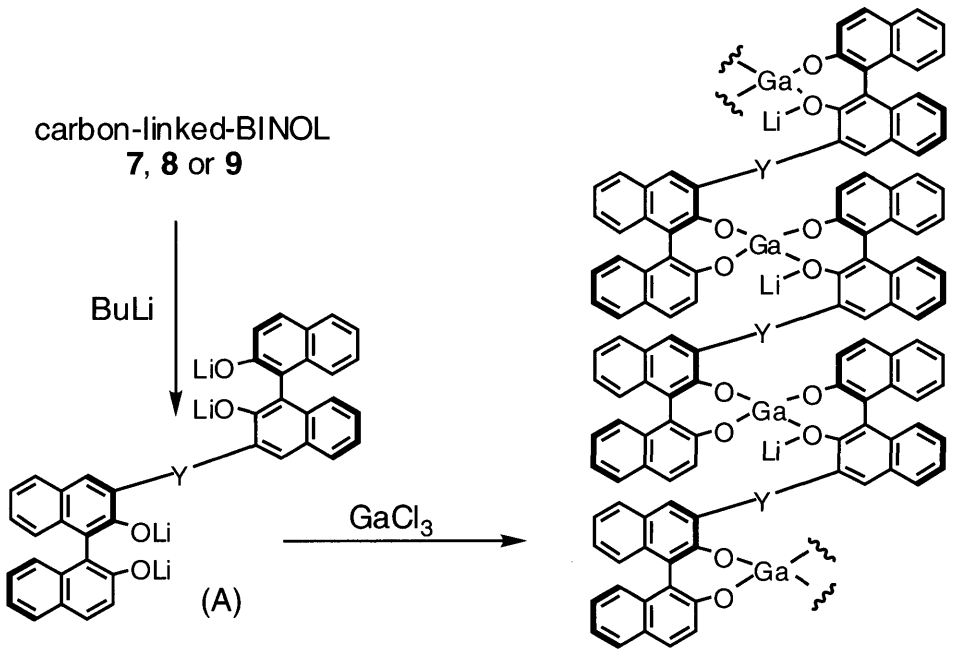

Figure 4. Possible oligomeric structure of Ga-Li-carbon-linked-BINOL complexes.

formation of Ga-complexes. As shown in Figure 4, the conformation (A) seems favored due to the steric and electronic repulsion, thus the Ga-Li-carbon-linked-BINOL would result in undesired oligomeric species, the asymmetric environment of which should be different from that of the monomeric GaLB **3**.

2-2. Ligand Design 2: Oxygen-linked-BINOL

To overcome this problem, I designed a novel oxygen-containing linked-BINOL (Figure 5, **10**). This new linked-BINOL **10** was designed based on reports by Cram et al. regarding crown ethers incorporating chiral BINOL units.[25] I assumed that the oxygen atom in the linker would coordinate to gallium during the Ga-complex formation, thus helping the formation of the desired monomeric Ga-complex. In contrast to crown ether-type cyclic ligands, this linked-BINOL, which is a kind of semi-crown ether linked only with one side of the BINOL units (3–3'' position), has a vacant coordination site around the gallium center metal. Thus, the Ga-Li-linked-BINOL complex should be still active as a Lewis acid towards epoxides. The preparation of **10** is shown in Scheme 2. Starting from optically active (*R*)-BINOL, (*R*,*R*)-linked-BINOL **10** was obtained easily in multigram scale (total yield 59% from (*R*)-BINOL). The synthetic procedure was successfully completed even by the undergraduate student, who just started to learn the experimental technique in organic chemistry, in >35 g scale of **10**.

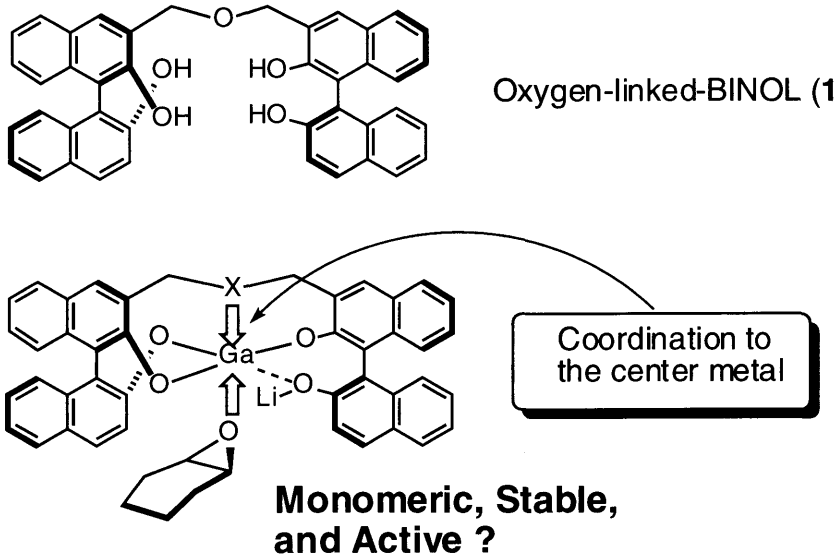

Figure 5. Further advanced design to prepare monomeric and stable complex — linked-BINOL containing coordinative heteroatom.

Scheme 2. Synthesis of Oxygen-containing-linked-BINOL **10**.

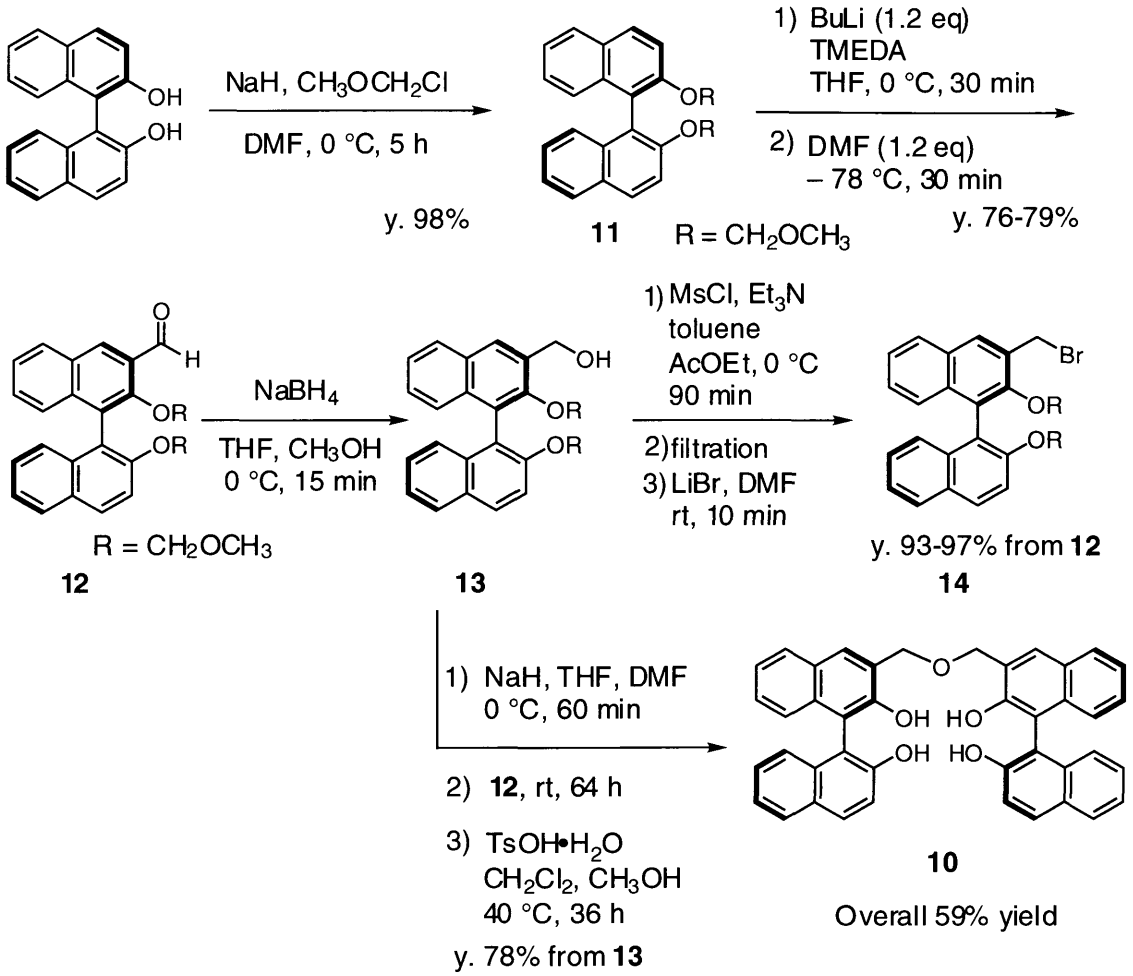

Complex **15** [prepared from $GaCl_3$ (1 mol equiv), **10** (1 mol equiv), and BuLi (4 mol equiv): Scheme 3] was far more stable than GaLB **3**, and very effective for the epoxide opening reaction. As shown in Scheme 3, **15** promoted the ring opening reaction of **4a** with **5** without any decomposition of the catalyst, affording **6a** in 73% yield and 92% ee. Encouraged by the result, I then optimized the reaction conditions as summarized in Table 2. Ga-Li-linked-BINOL complex **15** was slightly less reactive than original GaLB **3**, probably due to lower Lewis acidity of the complex. Unlike GaLB **3**, Ga-Li-linked-BINOL complex **15** was stable even in the presence of excess 4-methoxyphenol (**5**) and / or at higher temperature. By adding 3 equiv of **5** and heating the reaction mixture at 75 °C, reaction rate improved, and the reaction proceeded with reduced levels of catalyst for the first time. Under optimized conditions (toluene, 75 °C, 3 equiv of **5**), cyclohexene oxide (**4a**) reacts with 4-methoxyphenol (**5**) smoothly in the presence of 10 mol % catalyst, half the amount of GaLB, to afford **6a** (96 h, yield 72%, 91% ee, entry 5). It is noteworthy that

the Ga-Li-linked-BINOL complex **15** remained unchanged in the presence of 3 equiv of **5** at 75 ℃. With GaLB **3**, neither increased amount of **5** nor higher temperature than 50 ℃ was effective for improving the reaction rate, because decomposition of the catalyst competed.

Scheme 3. Catalyst Preparation and Enantioselective Epoxide Opening Reaction.

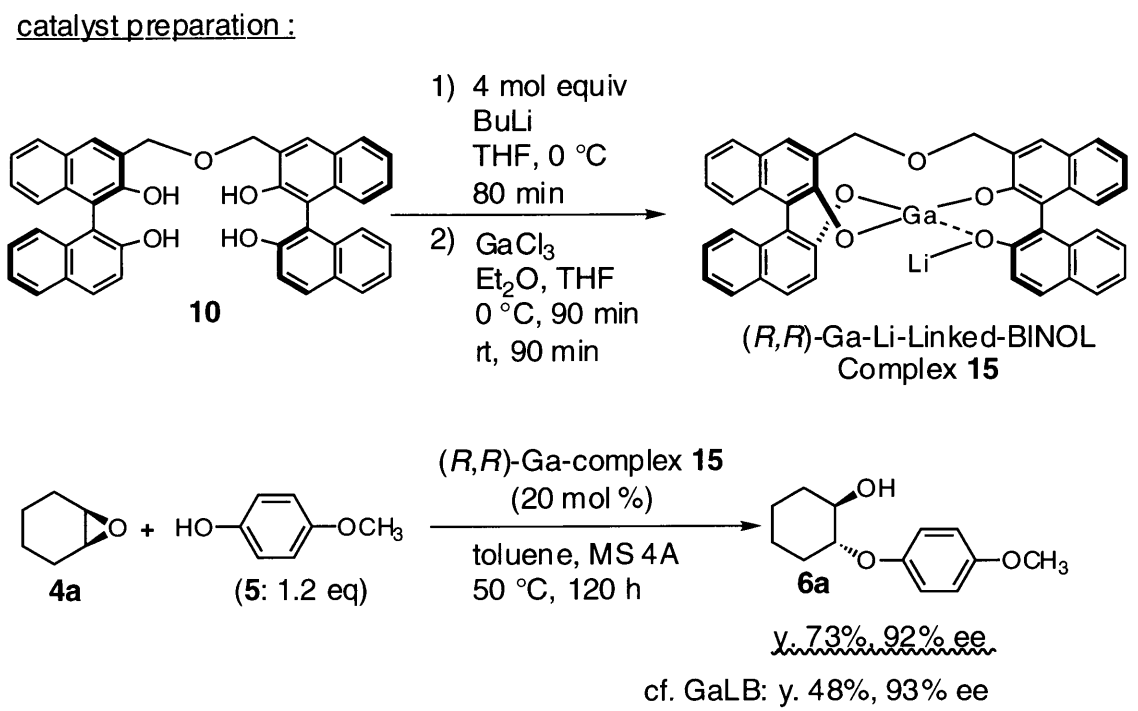

Table 2. Optimization of the Reaction Conditions with 10 mol % Catalyst **15**.

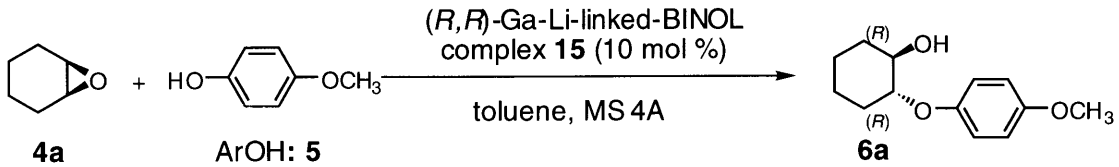

entry	catalyst (mol %)	ArOH (equiv)	temp (°C)	time (h)	yield (%)	ee (%)
1	20	1.2	50	120	73	92
2	10	1.2	50	160	44	92
3	10	3.0	50	158	41	96
4	10	1.2	75	157	79	89
5	10	3.0	75	96	72	91

Substrate scopes are summarized in Table 3, comparing with the results using GaLB **3**. Entries 1 through 5 show that the new Ga-Li-linked-BINOL complex **15** (10 mol %) afforded products (**6a–6e**) in analogous enantiomeric excess (66 – 91%) but in higher chemical yields (72 – 94%) compared to GaLB (20 mol %, Table 3, right column). After the reaction linked-BINOL **10** was recovered by extracting with 1M aq NaOH. This situation was very different from that with GaLB **3** because BINOL itself reacted with epoxide and the recovery of BINOL was impossible. The Ga-Li-linked-BINOL **15** was also effective for epoxides **4g–4i** (entry 7-9). Importantly, using only 3 mol % of catalyst **15**, epoxide **4d** gave **6d** in 80% yield and 91% ee, although the reaction time was long (117 h, entry 4 in parenthesis). All of these results can be attributed to the stability of the Ga-Li-linked-BINOL complex **15**, obtained by linking the two BINOL units in GaLB **3**. The stable catalyst **15** remained unchanged during the course of the reaction, whereas GaLB **3** decomposed due to severe ligand exchange with 4-methoxyphenol (**5**) and the reaction then stopped.

Table 3. Enantioselective Ring Opening of Various *meso*-Epoxides with 4-Methoxyphenol (**5**) Promoted by Ga-Li-Linked-BINOL Complex (**15**).

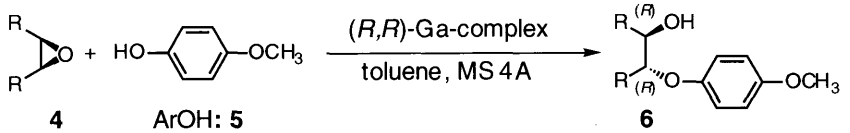

4 ArOH: **5** **6**

entry	epoxide	product	Ga-Li-Linked-BINOL (10 mol %) ArOH (equiv)	temp (°C)	time (h)	yield (%)	ee (%)	GaLB (20 mol %) ArOH (equiv)	temp (°C)	time (h)	yield (%)	ee (%)
1		**4a** **6a**	3.0	75	96	72	91	1.2	50	72	48	93
2		**4b** **6b**	3.0	60	63	88	85	1.2	50	72	75	86
3	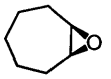	**4c** **6c**	3.0	75	108	82	66	1.2	50	72	31	67
4		**4d** **6d**	3.0 (1.2)[a]	75 (75)[a]	36 (117)[a]	94 (80)[a]	85 (91)[a]	1.2	50	72	74	87
5[b]	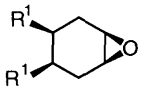	**4e** **6e**	3.0	60	96	72	79	1.2	50	96	34	80
6[c]	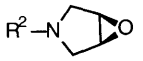	**4f** **6f**	3.0	60	160	77	78	1.2	50	160	51	90
7	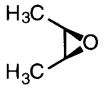	**4g** **6g**	3.0	60	140	72	91	—	—	—	—	—
8	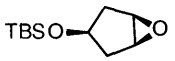	**4h** **6h**	3.0	60	48	67	87	—	—	—	—	—
9	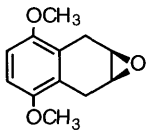	**4i** **6i**	2.0	60	70	85	96	—	—	—	—	—

a) 3 mol % catalyst was used.
b) $R^1 = CH_2OTBDPS$
c) $R^2 =$  , 30 mol % catalyst was used.

2-3. Mechanistic Studies of the Ga-Li-linked-BINOL Complex

After improving stability of the Ga-Li-complex against ligand exchange with the newly developed linked-BINOL **10**, I then attempted to determine the structure of the linked-BINOL complex because the structural information should provide clues for applying the linked-BINOL **10** to other catalytic asymmetric reactions. Although ^{13}C-NMR (Figure 6)

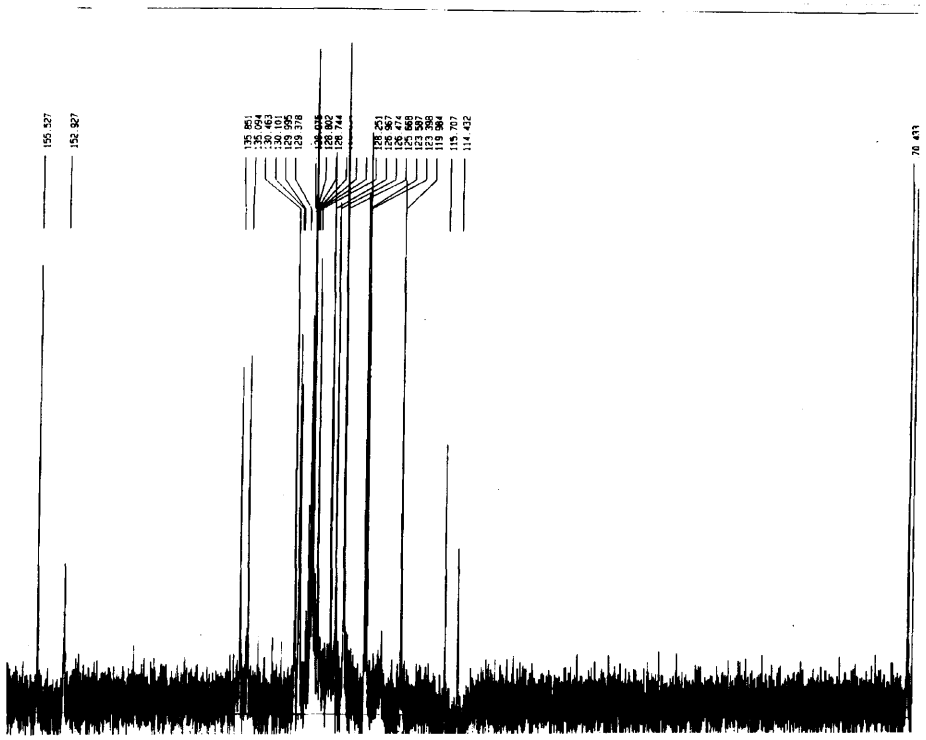

Figure 6. ^{13}C-NMR spectrum of (*R*,*R*)-Ga-Li-linked-BINOL complex **15** in THF.

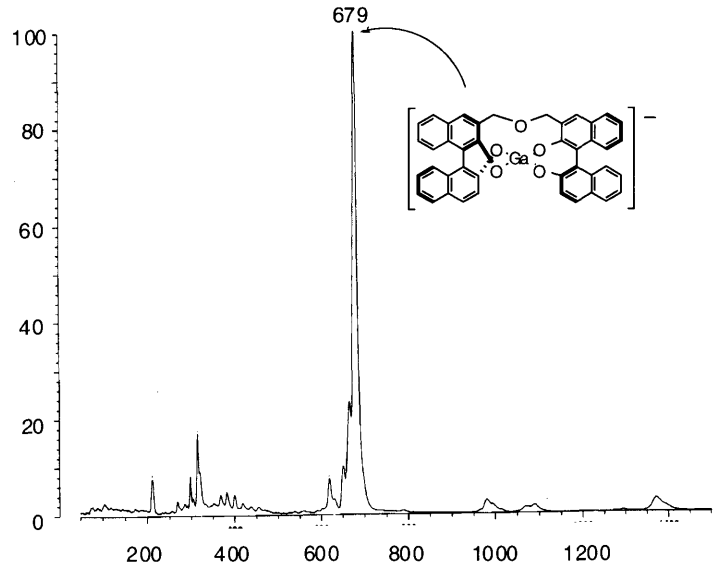

Figure 7. LDI-TOF MS(–) spectrum of (*R*,*R*)-Ga-Li-linked-BINOL complex **15** in THF.

and (–)-LDI TOF mass spectrometry [Ga-Li-linked-BINOL **15**: M – Li^+ = 679 for Ga^{69} (base peak)] data (Figure 7) suggested the assumed C_2-symmetric monomeric structures, all attempts to obtain X-ray grade crystals of the Ga-Li-linked-BINOL complex **15**, prepared from $GaCl_3$, were unsuccessful. After several trials, I obtained X-ray grade crystal of LiCl-free Ga-Li-linked-BINOL complex **16**, prepared from Ga(O-*i*-Pr)$_3$ (1 mol equiv), linked-BINOL **10** (1 mol equiv), and BuLi (1 mol equiv) (Scheme 4). The crystal was obtained from toluene solution in the presence of tiny amount of THF and diethyl ether at room temperature.

Scheme 4. Preparation of (*R*,*R*)-Ga-Li-linked-BINOL•3 LiCl Complex **15** and LiCl free (*R*,*R*)-Ga-Li-linked-BINOL Complex **16**.

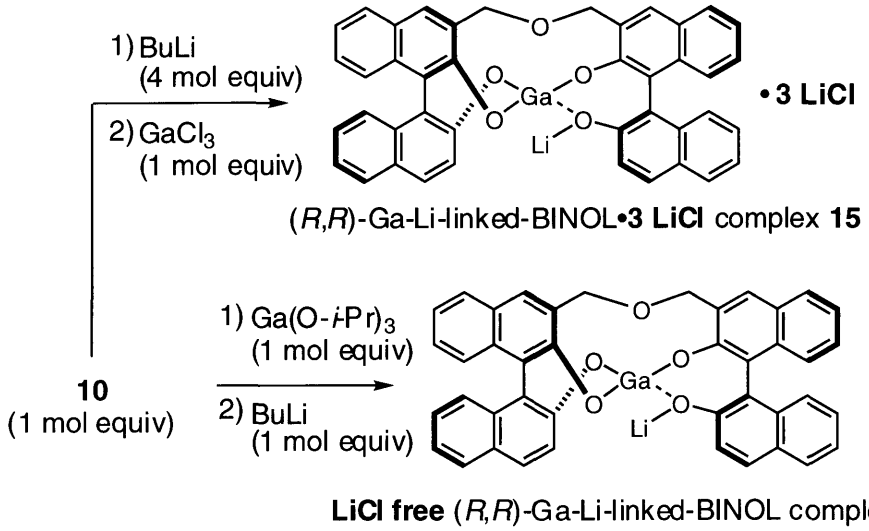

This LiCl-free Ga-Li-linked-BINOL crystal of **16** also catalyzed the ring opening reaction of epoxide **4a** to give **6a** (20 mol % catalyst, toluene, 50 ℃, 40 h, y. 85%), although in somewhat lower ee (74%) compared to catalyst **15**. By treating this crystal with 3 mol equiv LiCl in THF prior to use, the enantiomeric excess increased to 90%, suggesting the formation of the same catalyst as the one from $GaCl_3$. The role of LiCl is not clear, but it is well-known that lithium halide functions effectively as an achiral additive to increase enantioselectivity.[26] Therefore it might be possible that LiCl could coordinate to the Ga-Li-linked-BINOL complex, slightly affecting the asymmetric environment of the complex in solution phase. As shown in Figure 8, Ga-Li-linked-BINOL complex has a monomeric tetracoordinated structure, which is similar to the structure of the Al-Li-bis(binaphthoxide)(thf)$_3$ complex (ALB: **2** in Figure 1).[6a] The crystal structure indicated that, as planned initially, the linked-BINOL has no adverse effects on the asymmetric

environment constructed by the two BINOL units in GaLB **3**. Instead, the linked-BINOL **10** just provided stability against ligand exchange by linking the two BINOL units. On the other hand, in contrast to my initial assumption, the oxygen atom in the linker does not coordinate to the gallium center metal, at least in the ground state. The different results obtained by carbon-linked-BINOL **7** (**6a**, 1% ee) and linked-BINOL **10** (**6a**, 91% ee) indicate that the oxygen in the linker should have a key role in the present system. The oxygen in the linker might provide properties similar to a crown ether to the ligand, thus promoting formation of the desired monomeric species similar to GaLB **3** during the complex formation. Although X-ray structure is not C_2-symmetric, NMR spectrum suggested that the Ga-Li-linked-BINOL complex has C_2-symmetry. Thus, it is probable that the structure in solution phase is slightly different from that in solid phase. Trials to observe ^{71}Ga-NMR resulted in failure due to severe broadening of a peak.

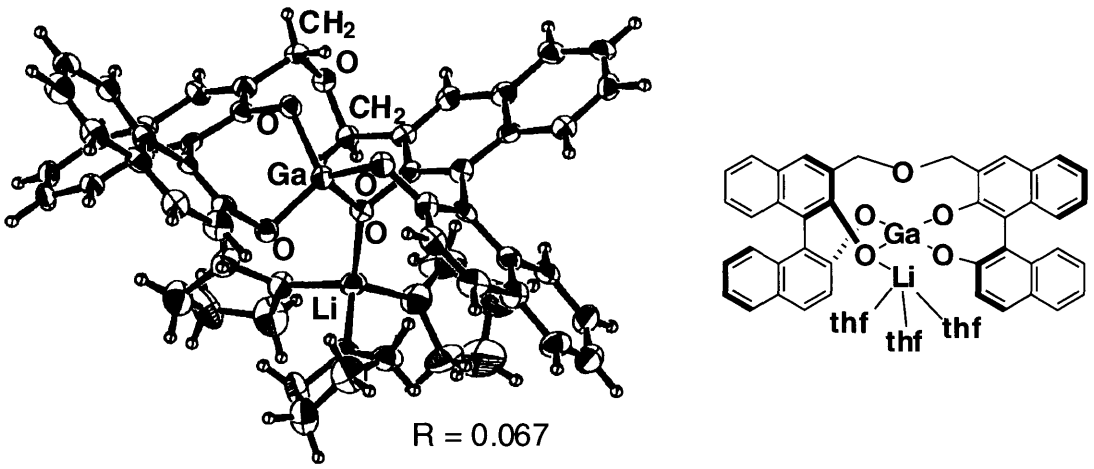

Figure 8. X-ray structure of LiCl free (*R*,*R*)-Ga-Li-linked-BINOL

The proposed mechanism of the epoxide opening reaction with 4-methoxyphenol (**5**) is shown in Scheme 5. The gallium center metal acts as a Lewis acid and activates epoxides (I), while at the same time the lithium binaphthoxide moiety functions as a Brønsted base to activate 4-methoxyphenol (**5**: ArOH) (II). The activated nucleophile would then react with epoxide to give III. Proton exchange between gallium alkoxide and an aromatic hydroxyproton leads to the epoxide opening adduct and regeneration of the catalyst. On the basis of the X-ray structure of LiCl-free (*R*,*R*)-Ga-Li-linked-BINOL complex **16** and the absolute configuration of the product obtained using this catalyst ((*R*,*R*)-**6a**), enantiomeric induction in the present system is explained by assuming the transition state shown in Figure 9: Due to the steric hindrance, the epoxide coordinating to gallium would be fixed in

(A) form rather than (B) form. Lithium binaphthoxide then activates and controls the orientation of 4-methoxyphenol (**5**: ArOH) so that lithium phenoxide attacks the epoxide selectively from one side to afford the (*R*,*R*)-1,2-diol mono ether.

Scheme 5. Working Model for the Ring Opening of Cyclohexene Oxide with 4-Methoxyphenol (ArOH) Catalyzed by Gallium Heterobimetallic Complexes

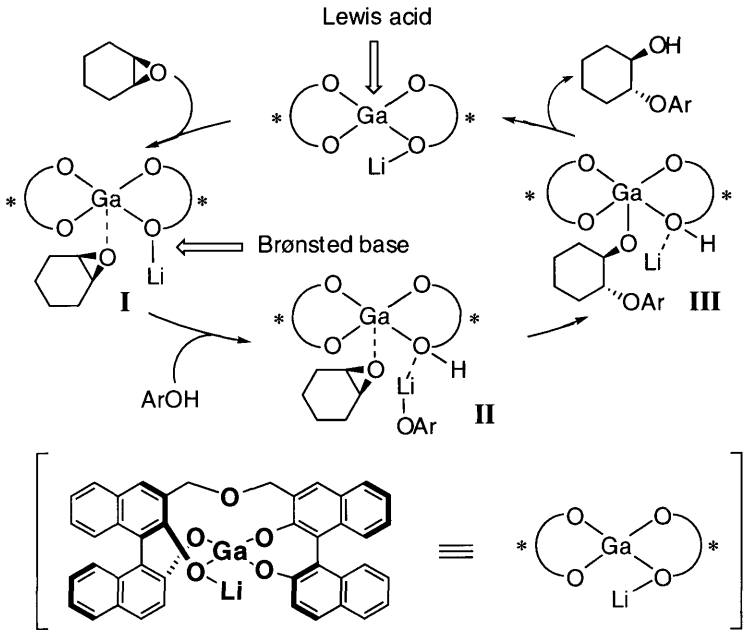

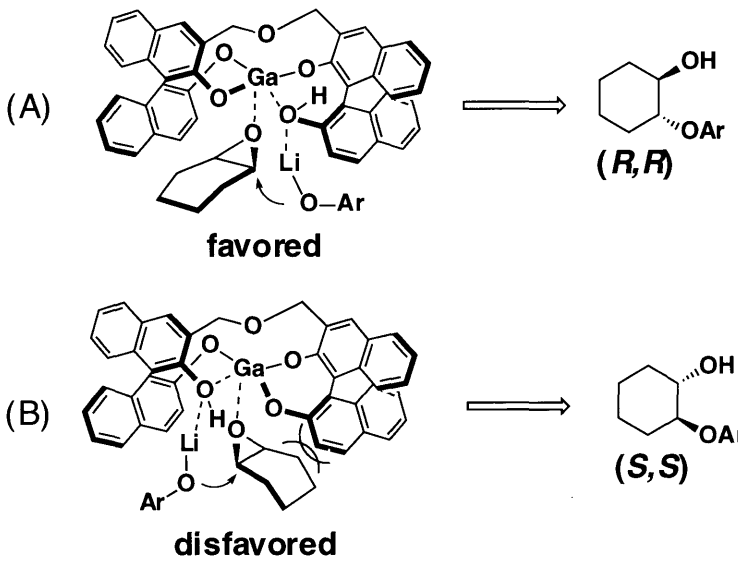

Figure 9. Working transition state model for epoxide ring opening reaction promoted by (*R*, *R*)-Ga-Li-linked-BINOL complex.

Chapter 3. Mechanistic Studies of Et_2Zn/linked-BINOL Complex

3-1. Introduction: other application of linked-BINOL

After I developed the linked-BINOL, its unique chiral environment was successfully applied to other various metal complexes.[27] Because the linker part of the ligand was relatively flexible, the linked-BINOL can incorporate metals with various ionic radii.

La(O-*i*-Pr)$_3$/linked-BINOL = 1/1 complex was effective for the Michael reaction of malonate to enones. When the reaction was performed in DME, excellent ee was achieved for cyclic enones (up to >99% ee; Scheme 6).[28] La(O-*i*-Pr)$_3$/linked-BINOL = 1/1 complex is commercially available from Strem.

Scheme 6. La(O-*i*-Pr)$_3$/linked-BINOL = 1/1 Complex: Michael Reaction in DME (Dr Kim's results).

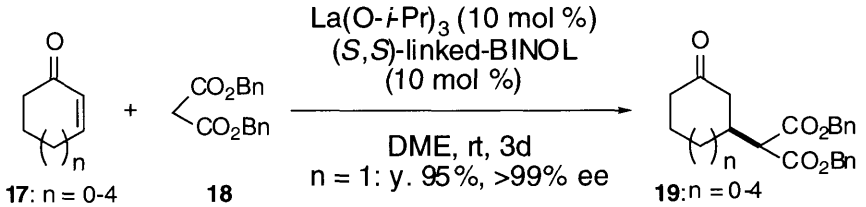

La(O-*i*-Pr)$_3$/linked-BINOL = 1/1 Complex is commercially available from Strem.

1) Kim, Y. S.; Matsunaga, S.; Das, J.; Sekine, A.; Ohshima, T.; Shibasaki, M. *J. Am. Chem. Soc.* **2000**, *122*, 6506. 2) Takita, R.; Ohshima, T.; Shibasaki, M. *Tetrahedron Lett.* **2002**, *43*, 4661.

During investigation of the La(O-*i*-Pr)$_3$/linked-BINOL = 1/1 complex (10 mol %), I found that the addition of Et_2Zn (10 mol %) was effective for the acceleration of the reaction (Scheme 7).[29] Michael reaction in THF gave Michael adducts in better yield and ee with Et_2Zn (10 mol %).

Scheme 7. La(O-*i*-Pr)$_3$/Et$_2$Zn/linked-BINOL = 1/1/1 Complex: Michael Reaction in THF.

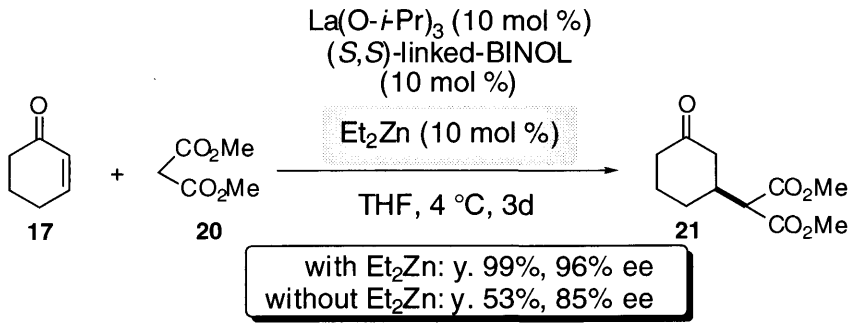

Matsunaga, S. Ohshima, T.; Shibasaki, M. *Tetrahedron Lett.* **2000**, *41*, 8463.

A coworker of mine, Kumagai, and I then became interested in the property of Zn/linked-BINOL **10** complex, and found Et$_2$Zn/linked-BINOL **10** = 2/1 complex was effective for the direct aldol reaction of hydroxyketone **23** (Scheme 8)[30, 31] and direct Michael reaction of hydroxyketone (Scheme 9).[32]

Scheme 8. Et$_2$Zn/linked-BINOL = 2/1 Complex: Direct Aldol Reaction (Mr. Kumagai and Matsunaga's results).

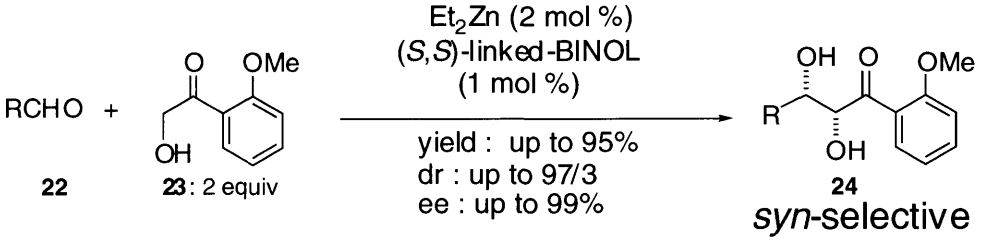

1) Kumagai, N.; Matsunaga, S.; Yoshikawa, N.; Ohshima, T.; Shibasaki, M. *Org. Lett.* **2001**, *3*, 1539.
2) Yoshikawa, N.; Kumagai, N.; Matsunaga, S.; Moll, G.; Ohshima, T.; Suzuki, T.; Shibasaki, M. *J. Am. Chem. Soc.* **2001**, *123*, 2467.

Scheme 9. Et$_2$Zn/linked-BINOL = 2/1 Complex: Direct Michael Reaction (Mr. Kumagai and Matsunaga's results).

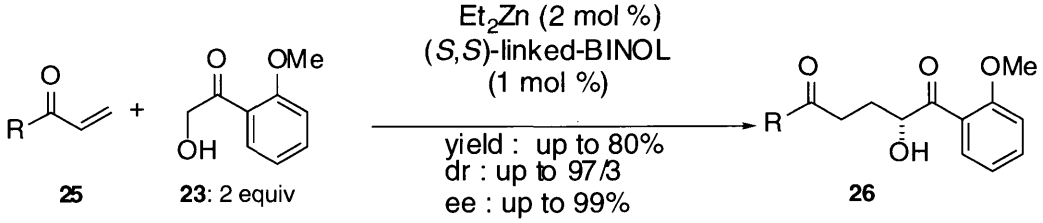

Kumagai, N.; Matsunaga, S.; Shibasaki, M. *Org. Lett.* **2001**, *3*, 4251.

In these reactions, the use of the linked-BINOL **10** was essential for high enantiomeric induction. When BINOL itself was used, product was obtained in lower chemical yield and ee depending on the reaction. Although the utility of the linked-BINOL**10** was apparent, I thought that detailed mechanistic study of linked-BINOL **10** was essential for further application and optimization of the liked-BINOL. The mechanistic study should also give me the clue for launching the new project. Thus, I decided to investigate the mechanism of the direct aldol reaction promoted by Et_2Zn /linked-BINOL **10** = 2/1 complex.

3-2. Problem in the Direct Aldol Reaction Promoted by Et_2Zn/linked-BINOL = 2/1 Complex

In the direct aldol reaction promoted by Et_2Zn /linked-BINOL = 2/1 complex (Scheme 8), there remained a few problems as shown in Figure 10. In the aldol reaction, (a) more than 2 equiv of ketone was essential for high yield (>90%); (b) it was difficult to reduce catalyst loading to less than 1 mol %; (c) ketone **27**, which afforded products with tetrasubstituted carbon, resulted in low yield. Through mechanistic studies, I searched clues to overcome these three problems.

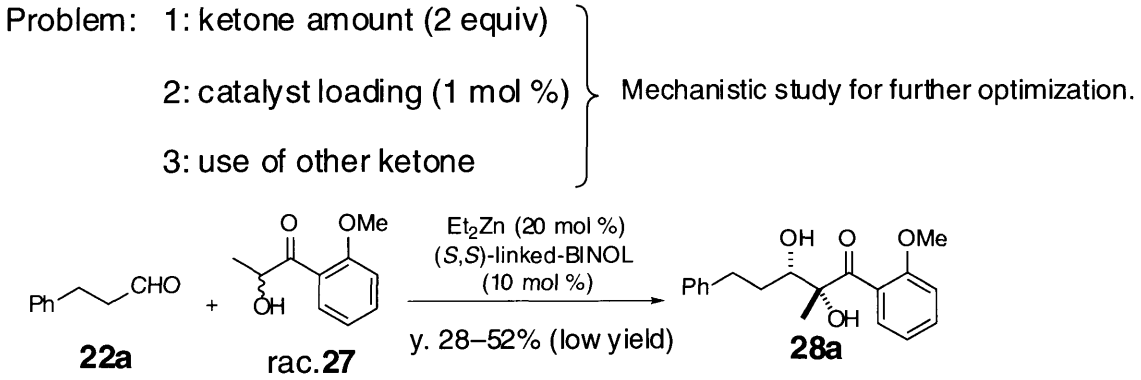

Figure 10. Problems in direct aldol reaction using Et_2Zn/linked-BINOL complex.

3-3. Analysis of Et_2Zn /linked-BINOL = 2/1 Complex

Initially, I postulated that the complex prepared from 2 equivalents of Et_2Zn and 1 equivalent of (*S*,*S*)-linked-BINOL **10** would be a bimetallic monomer[30, 32] on the basis of the related X-ray structure of a Ga-Li-linked-BINOL complex[23a] and Zn bimetallic complexes (Figure 11).[33] Unexpectedly, however, X-ray analysis of a crystal obtained from the Et_2Zn/(*S*,*S*)-linked-BINOL **10** = 2/1 solution in THF revealed that the complex consisted of Zn and **10** in a ratio of 3:2 [trinuclear Zn_3(linked-binol)$_2$thf$_3$] with C_2-

symmetry.[34] The structure of the Zn/linked-BINOL preformed complex **29** is shown in Figure 12. Three Zn atoms were aligned in almost a straight line (Zn(2)-Zn(1)-Zn(3) angle = 6.6°), and each Zn center was pentacoordinated.

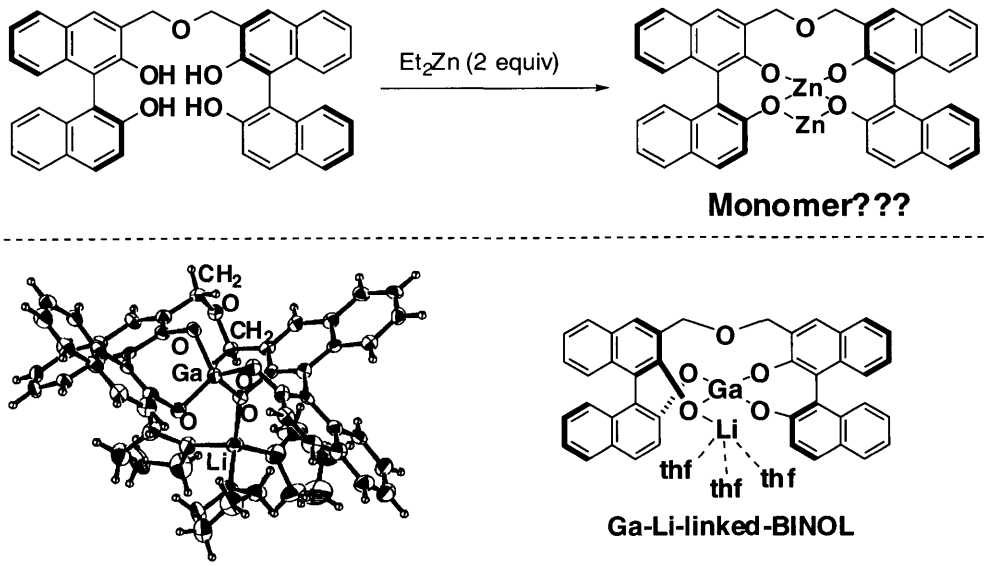

Matsunaga, S.; Das, J.; Roels, J.; Vogl, E. M.; Yamamoto, N.; Iida, T.; Yamaguchi, K.; Shibasaki, M. *J. Am. Chem. Soc.* **2000**, *122*, 2252.

Figure11. What is the Structure of Et_2Zn/linked-BINOL?

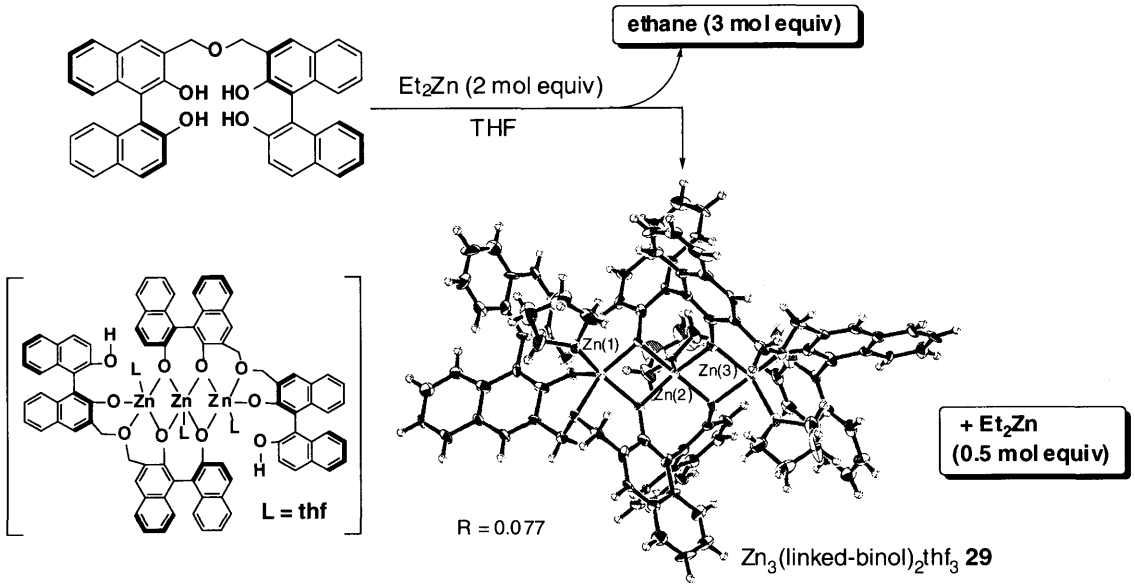

Figure 12. X-ray structure of preformed complex Zn_3(linked-binol)$_2$thf$_3$ **29**.

The existence of the trinuclear **29** in Et_2Zn/linked-BINOL **10** = 2/1 solution was confirmed by NMR (Figure 13), and cold spray ionization mass spectrometry (CSI-MS) analyses (Figure 14),[35] and by measuring ethane gas emission (Figure 12). ^{1}H NMR

spectra of (A) free (*S*,*S*)-linked-BINOL **10** and (B) the Et_2Zn/linked-BINOL **10** = 2/1 mixture in THF-d_8 are shown in Figure 13. The ^1H NMR spectrum of (B) the Et_2Zn/linked-BINOL **10** = 2/1 mixture had four different ArC*H* signals, suggesting a non-C_2-symmetric environment around each of the two linked-BINOL **10** units in **29**. ^1H NMR spectrum of crystal **29** in THF-d_8 was the same as that of Et_2Zn/linked-BINOL **10** = 2/1 solution. Free ligand **10** and **29** were mainly observed in NMR spectra of the Et_2Zn/linked-BINOL **10** = 1/1 mixture, indicating that formation of **29** is thermodynamically preferred. The presence of **29** in major and additional minor free linked-BINOL **10** was observed in the NMR spectrum of the Et_2Zn/linked-BINOL **10** = 1.5/1 mixture, even when freshly titrated Et_2Zn (1.0 M in hexanes) was used. The necessity of a slight excess Et_2Zn (≥2 equiv against **10**) to form a trinuclear Zn/linked-BINOL **10** = 3/2 complex was confirmed by NMR and ethane gas emission experiments. The presence of additional Et_2Zn (0.5 mol equiv with respect to ligand **10**) in the Et_2Zn/linked-BINOL **10** = 2/1 solution was checked by measuring ethane gas emission.

(A)^{1}H NMR spectrum of linked-BINOL **10** in THF-*d8*.

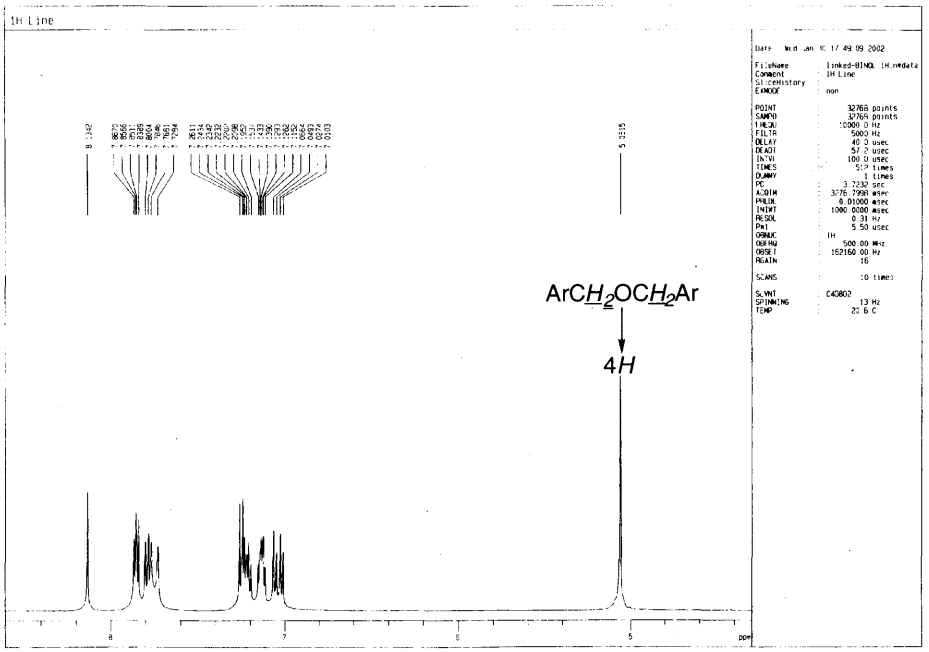

(B)^{1}H NMR spectrum of Et_2Zn/linked-BINOL **10** = 2/1 mixture in THF-*d*8.

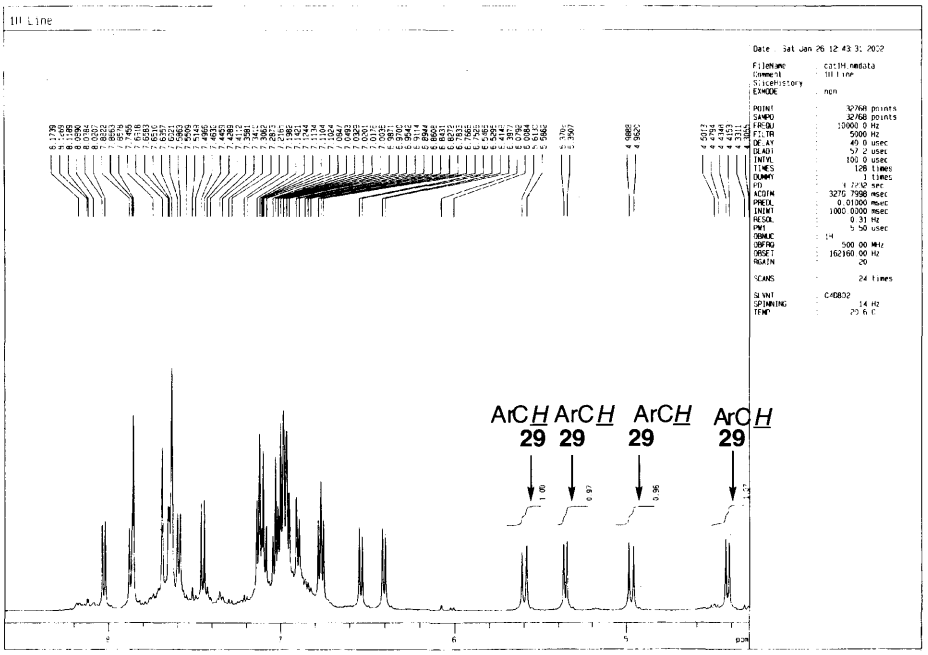

Figure 13. ^{1}H-NMR spectra of (A) (*S*,*S*)-linked-BINOL **10** and (B) Et_2Zn/(*S*,*S*)-linked-BINOL **10** = 2/1 in THF-d_8.

3 mol equiv of ethane gas emitted after addition of 2 mol equiv of Et_2Zn to ligand **10**. When concentrated H_2SO_4 was added to the mixture, an additional 1 mol equiv of ethane gas was detected, suggesting that 0.5 mol equiv of Et_2Zn remained in the Et_2Zn/linked-BINOL **10** = 2/1 solution (Figure 12). With CSI-MS, a Zn/linked-BINOL **10** = 3/2 complex (*m/z* = 1418.9) was observed as a prominent peak both in the Et_2Zn/linked-BINOL **10** = 1.5/1 and 2/1 solutions. The CSI-MS spectrum of 2/1 solution is shown in Figure 14. Observed peaks showed good agreement with theoretical ion distribution pattern derived from Zn isotopes ratio in nature.

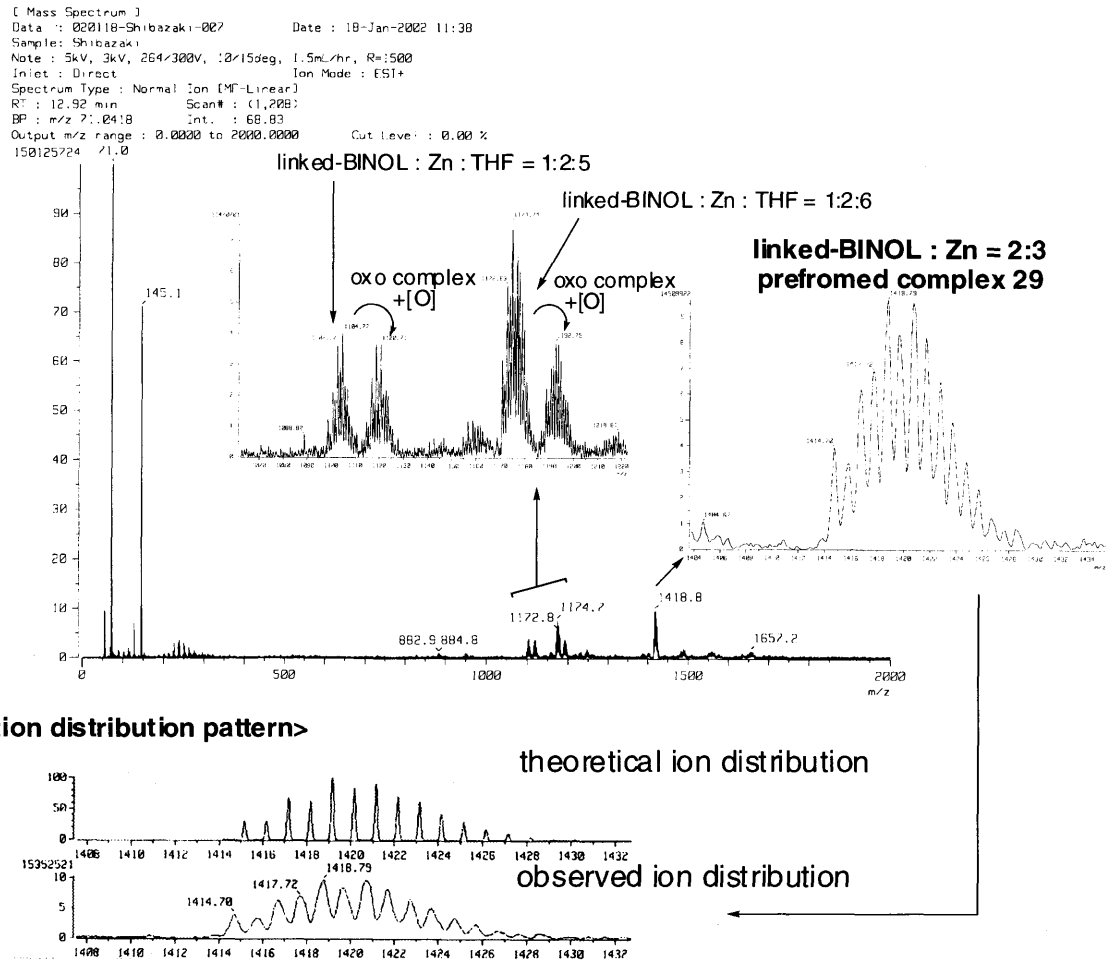

Figure 14. CSI-MS spectrum of Et_2Zn/(*S*,*S*)-linked-BINOL **10** = 2/1 in THF.

To clarify the role of small excess Et_2Zn, kinetic profiles of the reaction (a) with crystal **29** (1.5 mol %) and additional Et_2Zn (1.5 mol %) and (b) with only crystal **29** (1.5 mol %) was examined. As shown in Figure 15, additional Et_2Zn did have positive effects on reaction rate. The aldol reaction of **23** and **22a** proceeded 1.7 times faster with the additional Et_2Zn (Figure 15. (a) $v_b = 6.95 \times 10^{-6}$ Ms^{-1}, (b) $v_a = 4.06 \times 10^{-6}$ Ms^{-1}). Because ee of the products was similar in both cases, the effects of a background racemic reaction with ligand free Et_2Zn was rationally excluded. A small excess of Et_2Zn would have some interaction with the preformed complex **29** in the presence of ketone **23**, enhancing the reaction rate.

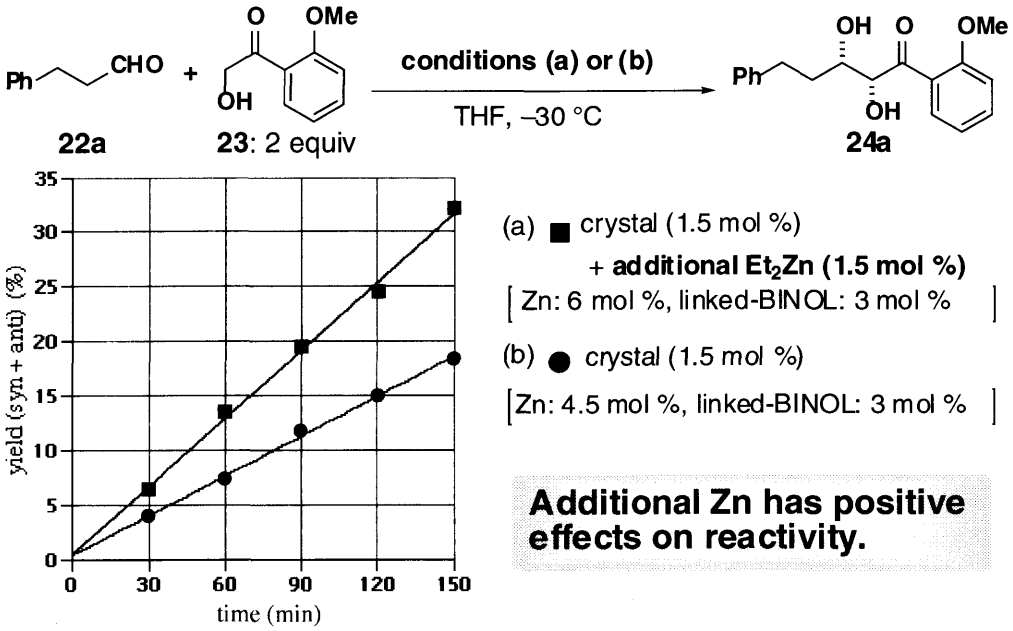

Figure 15. Reaction profile with (a) crystal **29** (1.5 mol %) + additional Et_2Zn (1.5 mol %) and (b) crystal **29** alone (1.5 mol %).

Observation of the reaction profiles with various amounts of catalyst gave me another interesting information. The initial rate of the aldol reaction using 1 mol equiv (100 mol %) of **22a**, 2 mol equiv (200 mol %) of **23**, and varied amounts of ligand **10** and Et_2Zn (Zn/**10** = 2/1) were measured. The reaction rate increased as usual when the catalyst loading (based on ligand) increased from x = 1, 3 to 5 mol % (Figure 16A). In contrast, the rate gradually decreased by increasing the catalyst loading (based on ligand) from x = 10, 20, 40, to 100 mol % (Figure 16B). The reaction rate with 100 mol % catalyst was as slow as that with 1 mol % catalyst. These results suggested that excess ketone against Et_2Zn/linked-BINOL complex is necessary for this reaction. In fact, when the reaction was

performed using just 1 mol equiv of ketone to catalyst as shown in Scheme 10, no reaction proceeded at all.

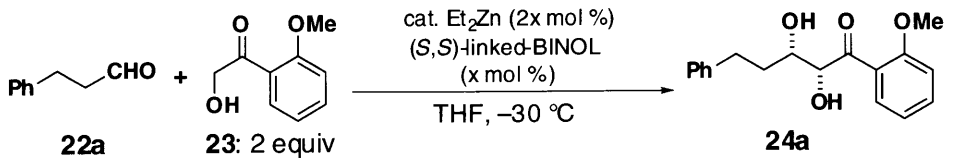

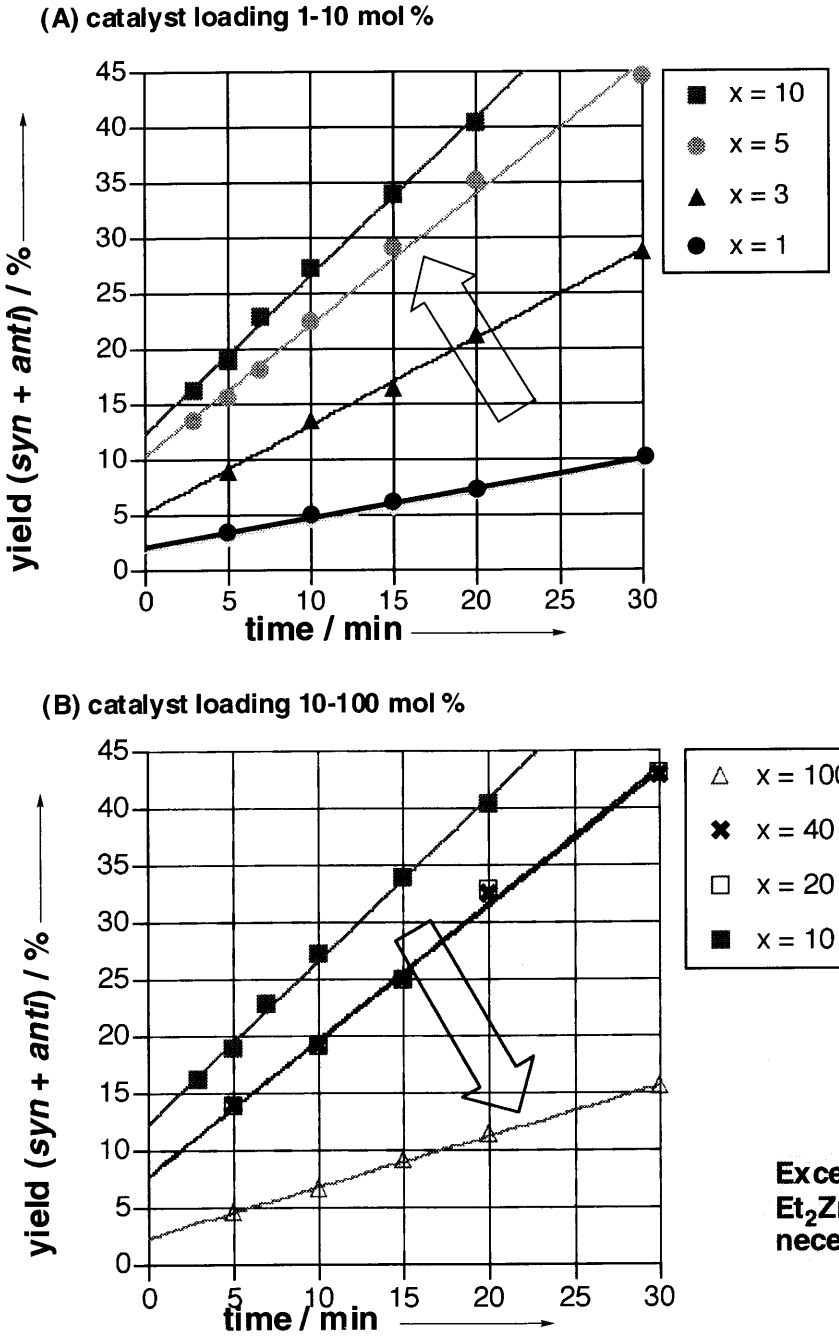

Figure 16. Reaction profile with various catalyst loading.

Scheme 10. Aldol Reaction with 1 mol Equiv of Ketone.

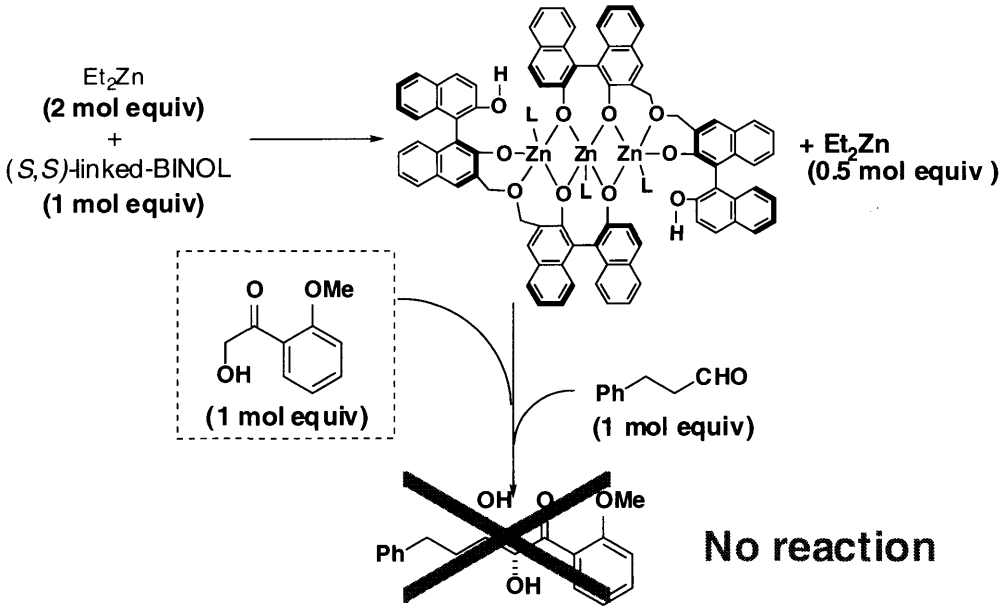

Kinetic experiments suggested that small excess of Et_2Zn and large excess of ketone **23** had important role to promote the aldol reaction. I then turned my attention to observe the formation of a Zn-ketone active species directly using CSI-MS analysis. When 1 mol equiv of ketone **23** (against ligand **10**) was added to Et_2Zn/linked-BINOL **10** = 2/1 solution, peaks derived from Zn:**10**:**23** = 3:2:1 (*m/z* = 1585.8) and 3:2:2 (*m/z* = 1750.9) appeared. As mentioned in Scheme 10, however, the addition of 1 mol equiv of aldehyde **22a** to the mixture did not afford any aldol product **24a**. Thus, neither the crystal **29** nor the Zn:**10**:**23** = 3:2:1 complex is a real catalyst but only a preformed complex. As the amount of ketone **23** increased from 1 mol equiv to 5 and 10 mol equiv, there was a drastic change in the CSI-MS spectra. With 5 mol equiv of ketone **23**, the peak corresponding to **29** diminished, and a peak derived from a novel heptanuclear Zn complexes (Zn:**10**:**23** = 7:3:4, *m/z* = 2951.1) and (Zn:**10**:**23** = 7:4:4, *m/z* = 3565.4) appeared as major peaks. The peak increased by increasing ketone **23** from 5 to 10 mol equiv. In addition, fragment peaks assigned as Zn:**10**:**23** = 7:3:3 (*m/z* = 2785.8), 7:3:2 (*m/z* = 2618.2), and 7:3:1 (*m/z* = 2454.6) were also observed. The CSI-MS chart of Et_2Zn/**10**/**23** = 2/1/10 is shown in Figure 17. Observed peaks showed good agreement with theoretical ion distribution pattern derived from Zn isotopes ratio in nature. The formation of the heptanuclear complex should be more favorable under the reaction conditions for aldol reaction (Scheme 8), because as much as 200 mol equivalent of ketone **23** exists against ligand **10**. More than 100 mol equiv of **23** remained even at the final stage of the reaction under the conditions in Scheme 8. As expected, the addition of 1 mol equiv of aldehyde **22a** to Et_2Zn/**10**/**23** = 2/1/10

solution led to the formation of aldol adduct **24a**, suggesting that a complicated oligomeric Zn-rich complex may be a putative actual active species.[36] All the trials to elucidate the exact structure of oligomeric Zn-rich active species, however, failed. For example, NMR analysis trials only afforded complex charts, suggesting the existence of several species in equilibrium in the presence of excess ketone **23**.

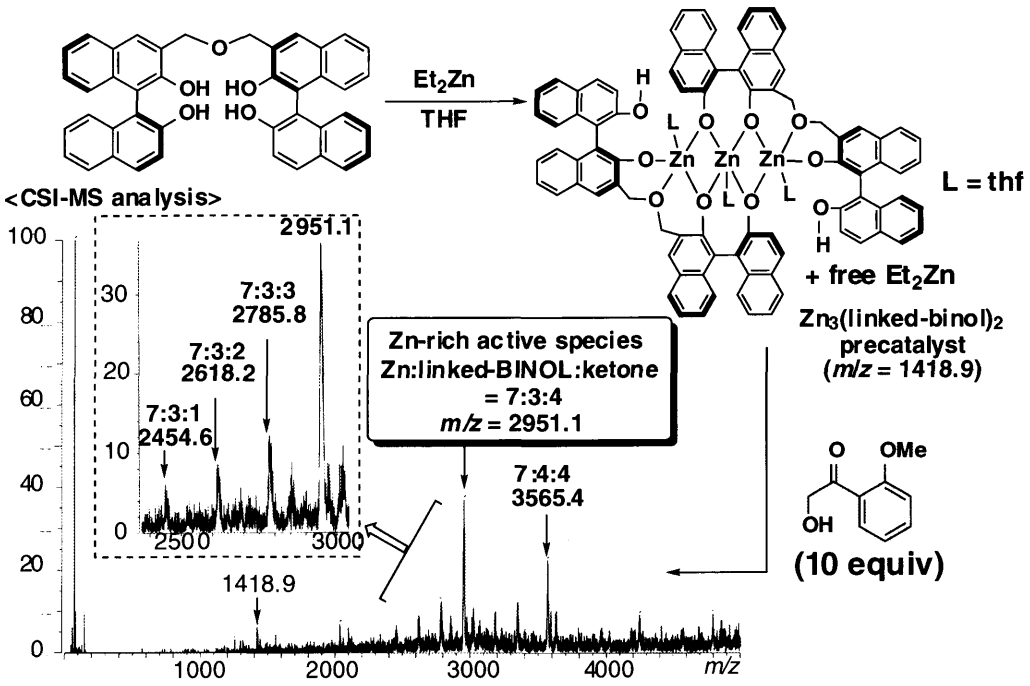

Figure 17. CSI-MS spectrum of Et_2Zn/ linked-BINOL **10**/ ketone **23** =1/2/10 solution.

On the basis of these kinetic profile and CSI-MS analysis, I suppose that Zn-rich species, like heptanuclear complex observed in CSI-MS, would be the actual active species. Additional Et_2Zn could react with hydroxyketone **23** to form Zn-alkoxide (Zn-**23**), and then react smoothly with the preformed trinuclear Zn_3(linked-binol)$_2$ complex **29** to form oligomeric Zn-rich species, increasing the total amount of putative Zn-rich active species. I also hypothesized that Zn-alkoxide (Zn-**23**) generated from small excess Et_2Zn would accelerate the catalyst turnover step, in which aldol adducts dissociate from catalyst via ligand exchange with ketone **23** or with the Zn-alkoxide (Zn-**23**) (Details are discussed in Scheme 11, *vide infra*). In fact, with 2-methoxy-2'-methoxyacetophenone (Figure 18, **30**) and 2-(*tert*-butyldimethylsilyloxy)-2'-methoxyacetophenone (Figure 18, **31**), no reaction proceeded after 25 h at –20 °C, and 12 h at 0 °C using 3 mol % of linked-BINOL **10** and 6 mol % of Et_2Zn, respectively. The results support my assumption that Zn-alkoxide (Zn-**23**) has a crucial role to enhance the reaction rate.

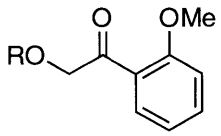

R = OMe: **30**
R = OTBS: **31**

Figure 18. Protected ketone **30** and **31**.

Absolute and relative configuration of aldol adducts also provided useful information regarding the mechanism of the present aldol reaction. Identical absolute configuration (*R*) was expressed at the α-position of both the *syn-* and *anti-* aldol products (Figure 19(A), *syn*-(2*R*,3*S*), *anti*-(2*R*,3*R*)). Both *syn-* and *anti-* isomers were obtained in similarly high ee (>84% ee), suggesting that the present catalyst differenciates the enantioface of the enolate very well and aldehydes come from the *Re*-face of the zinc enolate (Figure 19(A)). *syn*-Selectivity can be explained by assuming the transition state shown in Figure 19(B). Based on the mechanisms of related bifunctional asymmetric catalysis[3] and related achiral bimetallic zinc catalysts,[37] it seems reasonable to assume a synergistic function of two or more zinc centers in an oligomeric Zn-rich complex.

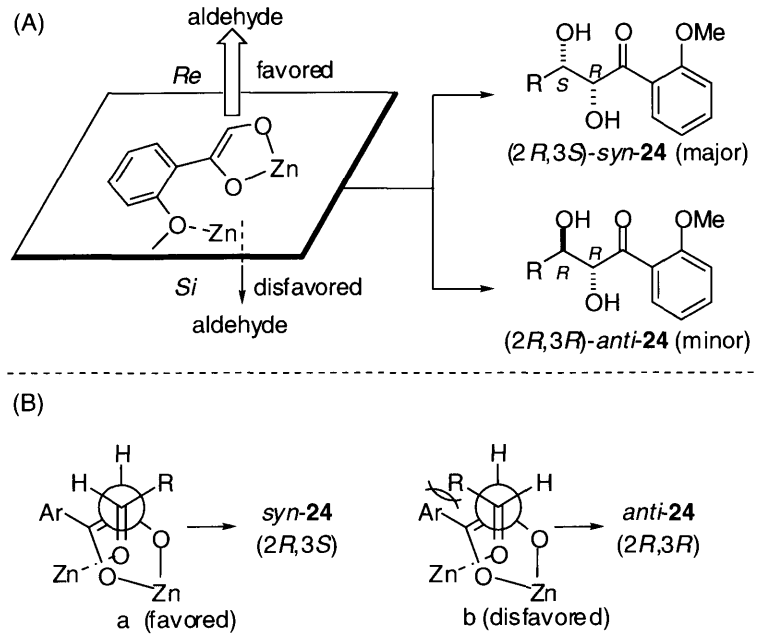

Figure 19. Stereochemical course of the direct aldol reaction of hydroxyketone **23**.

To gain more insight into the catalytic cycle of the aldol reaction, initial rate kinetics were surveyed. The reaction was first-order on ketone, first-order on the Et_2Zn/linked-BINOL **10** complex, and, importantly, zero-order on aldehyde. The results are summarized in Figure 20. For detailed experimental results, see experimental section. Thus, the possible rate determining step would be the product dissociation step to regenerate the Zn/linked-BINOL **10**/ketone **23** oligomeric putative active species.[38]

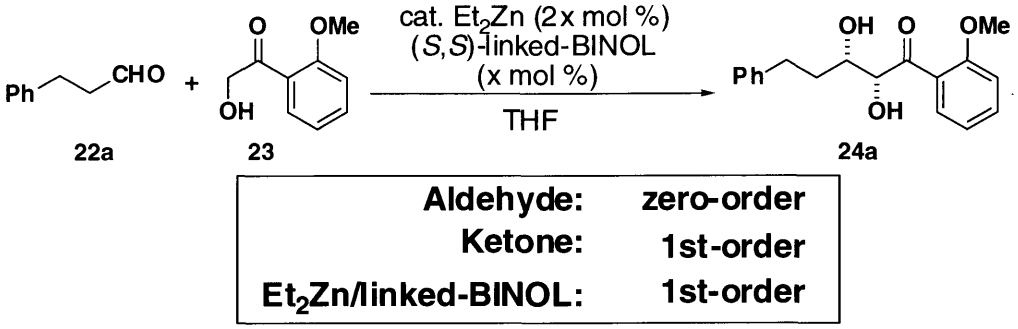

Figure 20. The results of initial rate kinetic study.

The postulated catalytic cycle for the direct aldol reaction is shown in Scheme 11. In the presence of ketone **23**, the oligomeric Zn-rich putative active complex (I) would be generated, as observed by CSI-MS analysis (I). Zn-binaphthoxide (Ar*O-Zn, Zn-**10** in Scheme 1) would function as a Brønsted base to deprotonate the α-proton in **23** to form (II). Aldehyde comes from the *Re*-face of the enolate selectively to be activated by the Lewis acidic zinc center. Initial rate kinetics suggest that the 1,2-addition step proceeds quickly to form (IV). Protonation with the phenolic proton of **10** (Ar*OH) followed by ligand exchange with **23** would regenerate (I). The catalyst turnover step would be the rate limiting step. This is consistent with the rate acceleration effects due to small excess Et_2Zn. The Zn-alkoxide (Zn-**23** complex) should react more smoothly with (IV) through transmetallation than ketone **23** itself does.[39]

Scheme 11. Postulated Catalytic Cycle for the Direct Aldol Reaction.

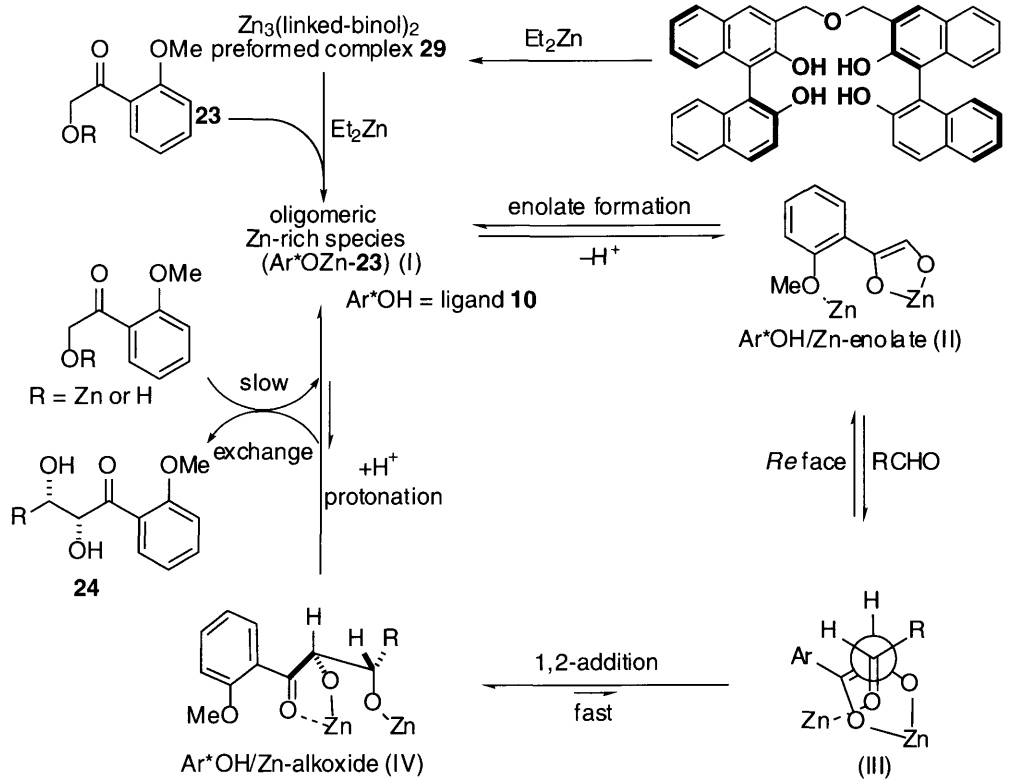

3-4. Optimization of the Aldol and Michael Reaction: a New Et_2Zn/linked-BINOL = 4/1-MS 3A System.

(A) Strategy for Optimization

Although the exact structure of putative active oligomeric species was not completely clarified, important information to improve the present asymmetric zinc catalysis was obtained through mechanistic studies: (1) The rate determining step of the present direct aldol reaction was speculated to be the product dissociation step. (2) NMR, CSI-MS, and ethane gas emission analysis revealed that small excess Et_2Zn remained in the Et_2Zn/linked-BINOL **10** = 2/1 solution. (3) Kinetic profiles using preformed trinuclear Zn complex **29** with and without additional Et_2Zn suggested that a small excess Et_2Zn accelerates the reaction rate. As shown in Figure 21, target for optimization is the catalyst turnover step. I planned to improve two of three problems as mentioned in section 3-2: amount of ketone and catalyst loading. I hypothesized that the addition of more Et_2Zn would lead to better reactivity, maintaining high selectivity. In addition, other additives to accelerate the ligand exchange were also expected to improve the reaction rate and catalyst

loading. I also assumed that the amount of ketone loading could be reduced by enhancing the catalyst turnover step, because the relative ratio of ketone/catalyst can be improved by reducing the catalyst loading.

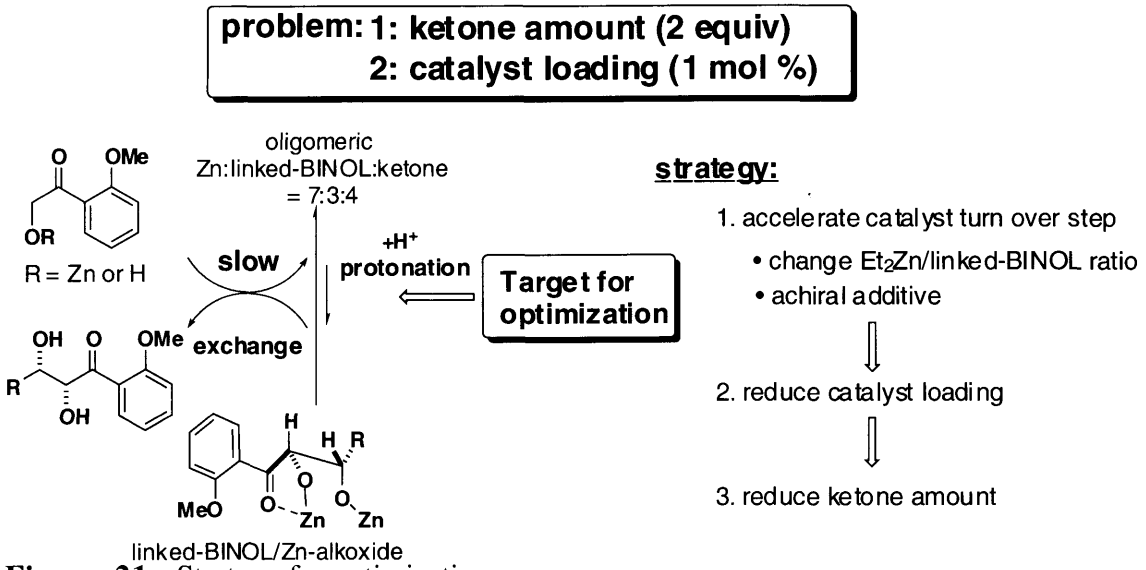

Figure 21. Strategy for optimization.

(B) Optimization of the Direct Aldol Reaction

With the first generation Zn/linked-BINOL **10** = 2/1 system, the aldol reaction proceeded smoothly in the presence of 2 equiv of ketone **23**, however the chemical yield decreased to 77% with 1.1 equiv of **23**. (Table 4, entry 1 *vs* entry 2). As the first trial, the reaction with a reduced amount of ligand **10** (0.5 mol %) was examined to increase the Zn/**10** ratio (entry 3, Zn/**10** = 4/1 *vs* entry 2, Zn/**10** = 2/1). As expected, the reaction proceeded to afford product **24a** with the same ee (93%) as in entry 2, suggesting that no racemic pathway with ligand-free Et_2Zn was involved in entry 3. Considering the efficiency, it is important that the same results (93% ee, y. 78% in entry 3) were obtained with only half the amount of chiral ligand, however the chemical yield with 1.1 equivalent of ketone **23** was still unsatisfactory. To further improve the turnover step, we surveyed various achiral additives to find activated MS 3A as the best additive.[40] MS 3A was used after activation at 160 °C under reduced pressure (ca. 0.7 kPa) for 3 h prior to use. In the presence of MS 3A, the Zn/ linked-BINOL **10** = 4/1 system promoted the direct aldol reaction of **22a** smoothly using 0.5 mol % (entry 4) or 0.25 mol % (entry 5) of ligand **10** to give **24a** in high yield (entry 4: 93%, entry 5: 90%), good dr (*syn*/*anti* = 89/11) and high ee (entry 4: 94%, entry 5: 96%) after 18 h. The reaction also proceeded smoothly with 0.1 mol % ligand loading to

afford **24a** in high ee (92% ee) although reaction time became longer (36h, 84% yield; entry 6). The optimized conditions were applicable to α-substituted aldehyde **22b** to afford **24b** in high yield, dr, and ee (entry 7, y. 92%, dr = 98/2, 96% ee). To demonstrate the practical utility of the present reaction, a direct aldol reaction was performed on a 200 mmol scale with aldehyde **24b** (entry 8). Using 0.25 mol % of **10** (0.5 mmol, 307 mg), 1 mol % of Et_2Zn (2 mL, 2 mmol, 1.0 M in hexanes), and 1.1 equiv of ketone **23**, the reaction proceeded smoothly and 53.7 g of **24b** (y. 96%) was obtained in high dr (*syn*/*anti*=98/2) and ee (94% ee) after 12h. By using the new Et_2Zn/(*S*,*S*)-linked-BINOL **10** = 4/1 with MS 3A system, the substrate/chiral ligand ratio was successfully improved from 100 (1 mol % with prior 2/1 system) to 400 to 1000 (0.25–0.1 mol %). This is the most efficient, in terms of catalyst loading, asymmetric catalyst for the direct catalytic asymmetric aldol reaction. Considering that the standard catalyst loading for the direct catalytic asymmetric aldol reaction is 5 to 20 mol %,[31] the exceptionally low catalyst loading in the present asymmetric zinc catalysis is remarkable.

Table 4. Optimization of Direct Aldol Reaction of **23** with the New Zn/**10** = 4/1 System.

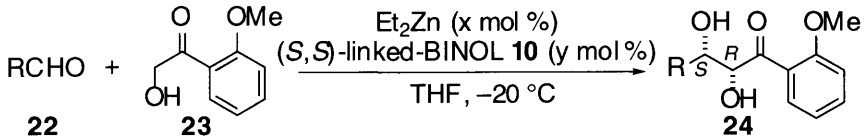

22 23 24

entry	aldehyde R	product	ketone (equiv)	additive	Et_2Zn (mol %)	ligand (mol %)	time (h)	yield (%)	dr (*syn*/*anti*)	ee (%) (*syn*)
1	Ph⁄⁄CHO	**22a** **24a**	2	none	2	1	18	92	90/10	93
2		**22a** **24a**	1.1	none	2	1	18	77	90/10	93
3		**22a** **24a**	1.1	none	2	0.5	18	78	90/10	93
4		**22a** **24a**	1.1	MS 3A	2	0.5	18	93	89/11	94
5		**22a** **24a**	1.1	MS 3A	1	0.25	18	90	89/11	96
6		**22a** **24a**	1.1	MS 3A	0.4	0.1	36	84	89/11	92
7	⬡CHO	**22b** **24b**	1.1	MS 3A	1	0.25	17	92	98/2	96
8[a]		**22b** **24b**	1.1	MS 3A	1	0.25	12	96	98/2	94

[a] Reaction was run on a 200 mmol scale (53.7 g of **24b** was obtained).

With the new 4/1 with the MS 3A system, aldol adduct **24c** from the sterically hindered α,α-disubstituted aldehyde **22c** was also obtained in excellent dr (>98/2) and high ee (92% ee, Scheme 12). In case of **22c**, thermodynamic stability of **22c** and **24c** appeared to be almost same. Thus, more forcing conditions were necessary to make the

equilibrium toward the product **24c**. 5 mol % of ligand **10** and 2 equiv of ketone **23** were necessary to achieve **24c** in moderate chemical yield (75%). Because **24c** was unstable, the aldol adduct was isolated after conversion into acetonide.

Scheme 12. Direct Aldol Reaction of α,α-Disubstituted aldehyde **22c**.

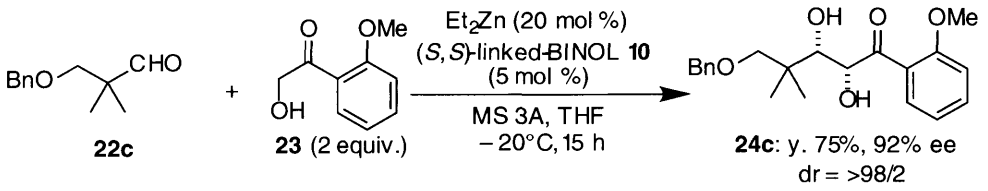

(C) Optimization of the Direct Michael Reaction

After succeeded in optimizing the direct aldol reaction, I then examined the utility of the new catalyst system in the direct Michael reaction of **23**. As shown in Table 5, in the case of the previously used Et_2Zn/linked-BINOL **10** = 2/1 without MS 3A system (see, also Scheme 9), addition of 2 mol equivalent of ketone **23** was essential to achieve satisfactory chemical yield (entry 1: 86% with 2 equiv of **23**, entry 2: 53% with 1.1 equiv), probably due to problems in the catalyst turnover step. With the new Et_2Zn/linked-BINOL **10** = 4/1 with MS 3A system, however, there was no difficulty in catalyst turnover with only 1.1 equivalent of ketone **23**. With 0.5 mol % of (*S*,*S*)-linked-BINOL **10**, 2 mol % of Et_2Zn, and 1.1 equivalents of **23**, the reaction reached completion within 3 h to give product **26** in better yield and ee (entry 3: y. 90%, 96% ee). With reduced catalyst loading (entry 4: 0.25 mol % and entry 5: 0.1 mol %), the reaction proceeded efficiently to afford **26** in good yield and high ee after 5 h (entry 5: y. 86%, 96% ee, entry 6: y. 83%, 96% ee). With 0.05 mol % (entry 6) and 0.02 mol % (entry 7), the reaction rate and chemical yield decreased at 4 ℃. At room temperature, the reaction proceeded smoothly even with 0.02 mol % of (*S*,*S*)-linked-BINOL **10** (substrate/chiral ligand = 5000) to afford **26** in good yield (entry 8: 90%) after 13 h, maintaining high enantiomeric excess (entry 8: 91% ee). With 0.01 mol % loading (substrate/chiral ligand = 10,000), **26** was obtained in moderate yield (78%) and good ee (89%). It is noteworthy that the substrate/chiral ligand ratio improved by two orders of magnitude from substrate/chiral ligand = 100 with prior Zn/linked-BINOL **10** = 2/1 ratio system to 5000 to 10,000 with the new Zn/linked-BINOL **10** = 4/1 ratio and MS 3A system even with reduced amounts of ketone **23**. The results in entries 8 and 9 indicate that the new system is exceptionally efficient in terms of catalyst loading among reported catalytic asymmetric carbon-carbon bond-forming reactions. Using as little

as 1.5 mg of (*S*,*S*)-linked-BINOL **10** and 10 μL of commercially available Et_2Zn solution in hexanes (1.0 M, 0.01 mmol), 4.63 g of product **26** was obtained (entry 9).

Table 5. Optimization of 1,4-Addition Reaction of Vinyl Ketone **26** with the Second Generation Et_2Zn/ (*S*,*S*)-linked-BINOL **10** = 4/1 with MS 3A System.

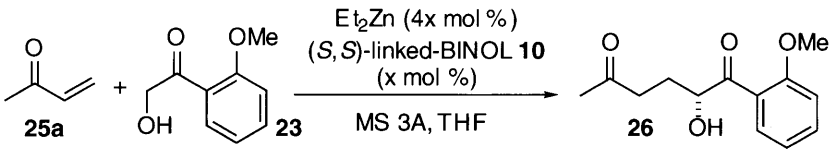

entry	ketone (equiv)	ligand (mol %)	Et_2Zn (mol %)	additive	temp. (°C)	time (h)	yield (%)	ee (%)
1	2	1	2	none	4	4	86	93
2	1.1	1	2	none	4	4	53	97
3	1.1	0.5	2	MS 3A	4	3	90	96
4	1.1	0.25	1	MS 3A	4	5	86	96
5	1.1	0.1	0.4	MS 3A	4	5	83	96
6	1.1	0.05	0.2	MS 3A	4	16	72	95
7	1.1	0.02	0.08	MS 3A	4	30	74	88
8	1.1	0.02	0.08	MS 3A	rt	13	90	91
9	1.1	0.01	0.04	MS 3A	rt	28	78	89

(D) Construction of Chiral Tetrasubstituted Carbon Stereocenter

Catalytic asymmetric construction of a chiral tetrasubstituted carbon stereocenter,[41] which is not accessible via asymmetric hydrogenation reactions,[42] is one of the most important topics in recent synthetic organic chemistry. I envisioned that the present asymmetric zinc catalysis would also differentiate the enantioface of tetrasubstituted enolate derived from 2-hydroxy-2'-methoxypropiophenone (Figure 22, **27**). The aldol adduct and 1,4-adduct would then be chiral *tert*-alcohol. Optimization for the Michael reaction of **27** is shown in Table 6. The ratio of Et_2Zn/(*S*,*S*)-linked-BINOL **10** and the addition of MS 3A were again important to achieve high yield. With 2.2 mol equivalent of racemic ketone **27** and the Et_2Zn/(*S*,*S*)-linked-BINOL **10** = 2/1 complex, **32a** was obtained in 15% yield in the absence of MS 3A (entry 1) and 35% yield in the presence of MS 3A (entry 2). With a 4/1 ratio, chemical yield improved to 51%, maintaining high ee (96% ee, entry 3). By increasing the amount of *rac*-**27**, chemical yield was improved to 88%(entry 4, 96% ee). Interestingly, the recovered ketone **27** was optically active in all cases (entries 1-4).

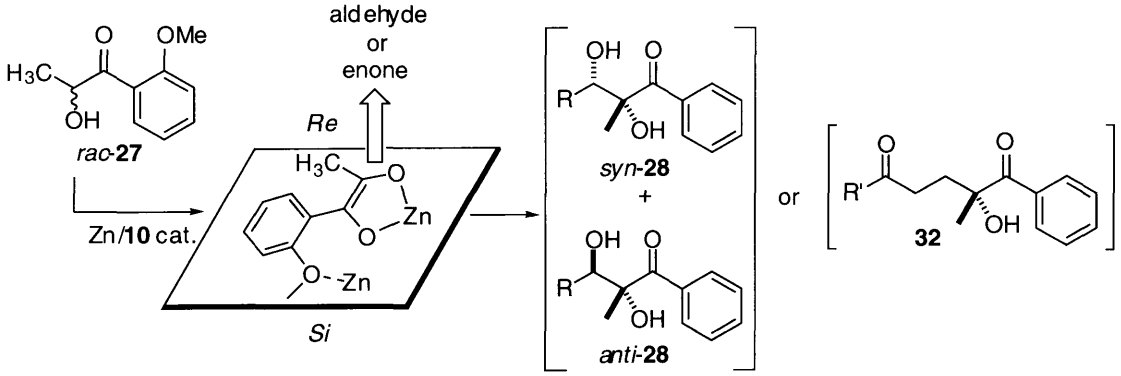

Figure 22. Concept for the construction of tetrasubstituted carbon stereocenter via direct aldoland Michael reaction of hydroxyketone **27**.

Table 6. Optimization of 1,4-Addition Reaction of Vinyl Ketone **25a** with *rac*-2-Hydroxy-2'-methoxypropiophenone (*rac*-**27**).

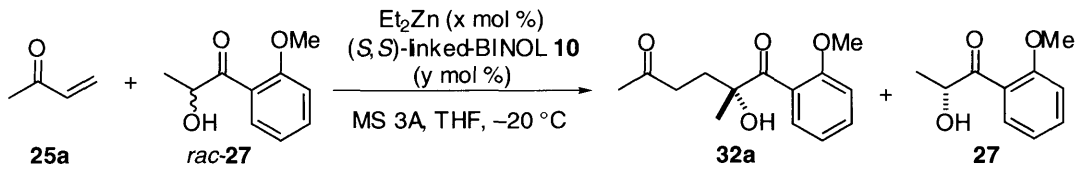

entry	Et_2Zn (mol %)	ligand **10** (mol %)	ketone **27** (equiv)	additive	time (h)	yield (%)	ee (%) **32a**	ee (%) **27**
1	10	5	2.2	none	16	15	93	8
2	10	5	2.2	MS 3A	16	35	96	22
3	20	5	2.2	MS 3A	16	51	96	35
4	20	5	5	MS 3A	16	88	96	33

Under the optimized conditions, the 1,4-addition reaction of ketone **27** to various vinyl ketones proceeded smoothly as shown in Table 7 (entries 1-6). The present reaction provides a new methodology to synthesize optically active chiral *tert*-alcohol in a catalytic asymmetric manner. Good yield (78-95%) and high ee (90%-96%) were achieved with vinyl ketones, however, the reaction did not proceed with other acceptors with β-substituents, probably due to steric hindrance.

Table 7. 1,4-Addition Reaction of Various Vinyl Ketones **25** with racemic ketone **27**.

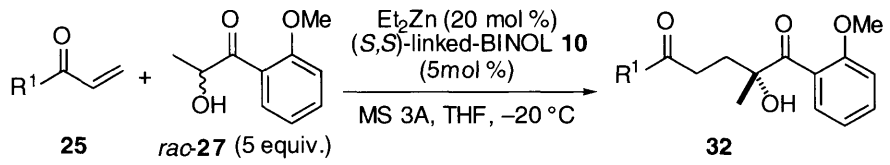

25 *rac*-**27** (5 equiv.) **32**

entry	R^1	vinyl ketone	product	time (h)	yield (%)	ee (%)
1	*p*-$MeOC_6H_4$	**25b**	**32b**	12	95	90
2	C_6H_5	**25c**	**32c**	24	82	93
3	*o*-$MeOC_6H_4$	**25d**	**32d**	24	78	91
4	*p*-BrC_6H_4	**25e**	**32e**	24	82	93
5	CH_3	**25a**	**32a**	16	88	96
6	CH_3CH_2	**25f**	**32f**	24	86	90

The fact that recovered ketone **27** was optically active with the (*R*)-configuration (8-35% ee; Table 6) provided a clue to the mechanism of the present asymmetric zinc catalysis. To obtain more precise results, reaction profiles using optically active (*S*)-**27** (>99% ee, 2.5 equiv)[43] with (a) Et_2Zn/(*S*,*S*)-linked-BINOL **10** and (b) Et_2Zn/(*R*,*R*)-linked-BINOL were examined. The results are shown in Figure 23. With (b) (*R*,*R*)-linked-BINOL, only trace amount of **32a** was obtained (y. <2% determined by ^1H NMR), and the ee of recovered ketone **27** was still 99% ee, suggesting that trace, if any, enolization occurred under the reaction conditions. On the other hand, with (a) (*S*,*S*)-linked-BINOL **10**, the reaction proceeded smoothly to afford product **32a** in 97% ee and the ee of the recovered ketone was lower (97% ee) than that of starting ketone **27** (>99% ee). These results indicate that the Et_2Zn/linked-BINOL complex recognizes the absolute configuration of α-hydroxyketone very well. In addition, the 1,4-addition reaction proceeded smoothly even when the racemic-**27** was used and the ee of the product was similarly high as summarized in Table 7 (**32a**, 96% ee, Table 7, entry 5). Thus, it seemed that one enantiomer, (*S*)-**27**, was involved in the reaction pathway using (*S*,*S*)-linked-BINOL **10**, while the other enantiomer, (*R*)-**27**, would not interact with Zn/(*S*,*S*)-linked-BINOL complex at all. The (*R*)-**27** enantiomer had no adverse effects on the reaction with (*S*,*S*)-linked-BINOL **10**. The results are also consistent with the exceptionally low catalyst loading for the 1,4-addition reaction of **25a** with ketone **23** (Table 5, 0.01 mol %, substrate/chiral ligand = up to 10,000). The absolute configuration of the 1,4-adduct **26** was *R*, which should not interact well with the Zn/(*S*,*S*)-linked-BINOL **10**/ketone **23** complex. Thus, product inhibition was not problematic in the case of the present 1,4-addition reaction, unlike many other common asymmetric catalyses by chiral Lewis acids.[44]

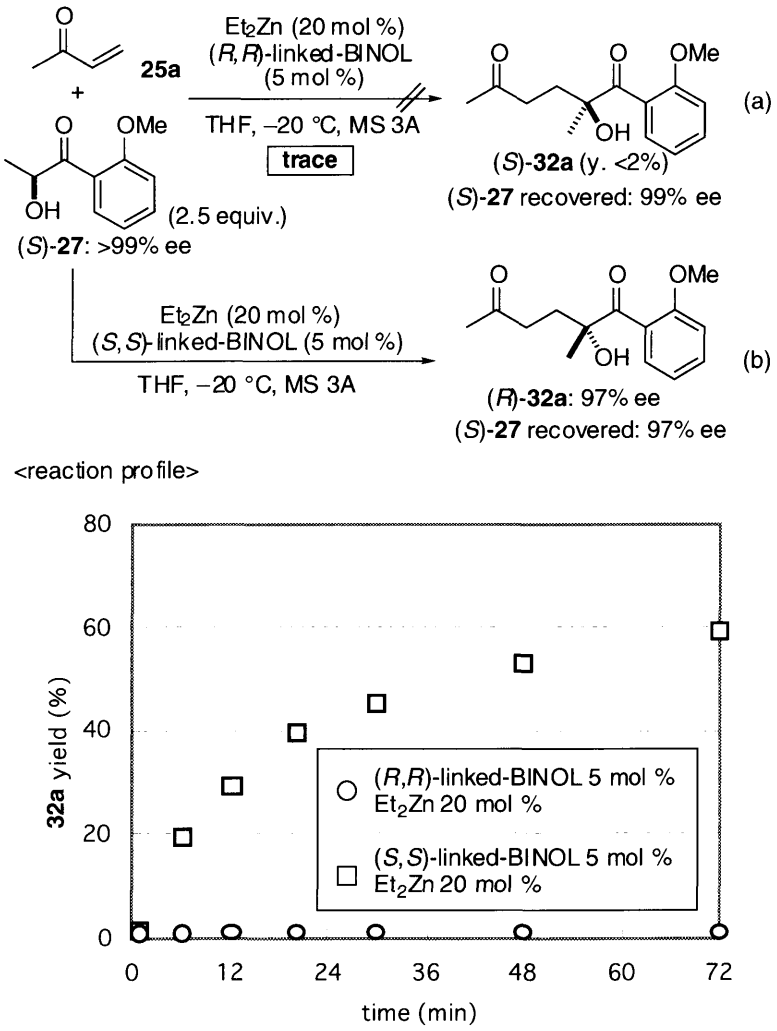

Figure 23. Reaction profiles of 1,4-addition reaction with optically active ketone (*S*)-**27** (99% ee) catalyzed by (a) Et_2Zn/(*R*,*R*)-linked-BINOL and (b) Et_2Zn/(*S*,*S*)-linked-BINOL.

The aldol reaction of **27** also afforded products with a chiral tetrasubstituted carbon stereocenter. As shown in Table 8, the ratio of Et_2Zn/(*S*,*S*)-linked-BINOL **10** and the addition of MS 3A were important to achieve high yield. With 2.2 equivalents of **27**, the aldol reaction of aldehyde **22a** was examined using Et_2Zn/(*S*,*S*)-linked-BINOL **10** = 2/1, 3/1, 4/1, and 6/1 ratio (entries 1-4). The chemical yield increased by increasing the ratio from 2/1 (entry 1, 39%) to 4/1 (entry 3, 65%) to afford **28a** in high ee (entry 3, *syn* 84% ee, *anti* 93% ee), albeit with modest diastereoselectivity. With a 6/1 ratio (entry 4), the enantiomeric excess decreased (*syn* 76% ee, *anti* 87% ee), probably due to the racemic pathway being promoted by too much excess Et_2Zn. Interestingly, with the same amount of Et_2Zn (20 mol %), less (*S*,*S*)-linked-BINOL **10** afforded a better chemical yield (entry 3: 5

mol % of **10**, y. 65%, entry 5: 10 mol % of **10**, y. 52%), suggesting the effectiveness of the new 4/1 ratio to improve the reactivity. With the optimized Et_2Zn/(*S*,*S*)-linked-BINOL **10** = 4/1 ratio, chemical yield was improved by using 5 equiv of ketone **27** to afford **28a** in 78% yield (entry 6). The addition of activated MS 3A (entries 7-8) further improved reactivity and the product was obtained in excellent yield (entry 8, 97%) and high ee (entry 8, *syn* 87% ee, *anti* 95% ee) at –20 °C.

Table 8. Optimization of Direct Aldol Reaction of 2-Hydroxy-2'-methoxypropiophenone (**12**).

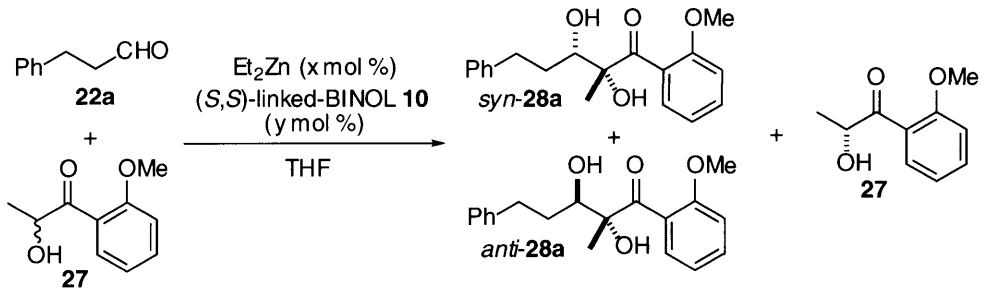

entry	Et_2Zn (mol %)	ligand **10** (mol %)	ketone **27** (equiv)	additive	temp. (°C)	time (h)	yield (%)	dr (*syn*/*anti*)	ee (%) *syn*	ee (%) *anti*	ee (%) ketone **27** recovered
1	10	5	2.2	none	–10	24	39	62/38	88	92	26
2	15	5	2.2	none	–10	24	51	62/38	88	93	36
3	20	5	2.2	none	–10	24	65	64/36	84	93	61
4	30	5	2.2	none	–10	24	64	65/35	76	87	60
5	20	10	2.2	none	–10	24	52	67/33	88	92	41
6	20	5	5	none	–10	24	78	64/36	85	91	25
7	20	5	5	MS 3A	–10	6	94	67/33	75	85	31
8	20	5	5	MS 3A	–20	16	97	62/38	87	95	27

The optimized reaction conditions, Et_2Zn 20 mol %, (*S*,*S*)-linked-BINOL **10** 5 mol %, and MS 3A, were applied to various α-unsubstituted aldehydes. As shown in Table 9, both linear (entries 1-3) and branched (entry 4) α-unsubstituted aldehydes afforded products in moderate to high yield (72-97%) and in moderate to excellent ee (68-96% ee). Aldehydes with oxygen functionality were also applicable substrates (entries 5-7) and products were obtained in good yield (80-92%) and high ee (85-97% ee). In all cases, diastereoselectivity was moderate (*syn*/*anti* = 59/41-71/29). With α-substituted aldehyde **22b**, no reaction proceeded, probably because the aldol adduct **22b** was thermodynamically unfavorable under the reaction conditions.

Table 9. Direct Aldol Reaction of Various Aldehydes with 2-Hydroxy-2'-methoxypropiophenone (**27**).

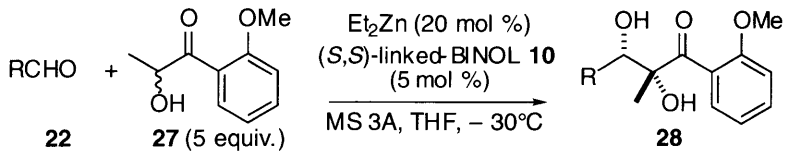

22 **27** (5 equiv.) **28**

entry	R		product	time (h)	yield (%)	dr[a] (*syn*/*anti*)	ee (*syn*/*anti*)
1	Ph⌒CHO	**22a**	**28a**	16	97	62/38	87/96
2	Ph⌒⌒CHO	**22d**	**28d**	19	72	64/36	78/90
3	⌒CHO	**22e**	**28e**	12	88	71/29	68/86
4	⌒CHO	**22f**	**28f**	10	80	68/32	72/87
5	PMBO⌒CHO	**22g**	**28g**	13	89	59/41	86/95
6	BOMO⌒CHO	**22h**	**28h**	10	92	69/31	87/97
7	BnO⌒CHO	**22i**	**28i**	18	80	65/35	85/92
8	⌒CHO	**22b**	**28b**	24	0	—	—

[a] Determined by ^{1}H NMR of mixture (entries 1-3, 5-7), determined after isolation (entry 4).

During the investigation to improve diastereoselectivity of the direct aldol reaction of **27**, I found that the heteroatom in the linker part of linked-BINOL affected the diastereoselectivity. With a new (*S*,*S*)-sulfur-linked-BINOL **35** (Scheme 13), the aldol reaction of **27** proceeded *anti*-selectively (Table 10). The synthetic scheme for the new ligand **35** is shown in Scheme 13. Reactivity with **35** was somewhat lower than that with oxygen-linked-BINOL **10**, and aldol adducts were obtained in moderate to good yield (56-82%) by using 10 equiv of **27**. Major *anti*-isomers were obtained in high ee (81-93% ee), although ee of minor *syn*-isomers was rather low (48-60% ee). I believe that heteroatoms in the linker would coordinate to the Zn atom, affecting the structure of the putative active oligomeric complex. It is difficult to explain precisely the effect of heteroatoms in the linker, however, because the exact structure of the putative oligomeric

active species is not clarified yet.

Scheme 13. Synthesis of a New (*S*,*S*)-Sulfur-linked-BINOL **35**.[a]

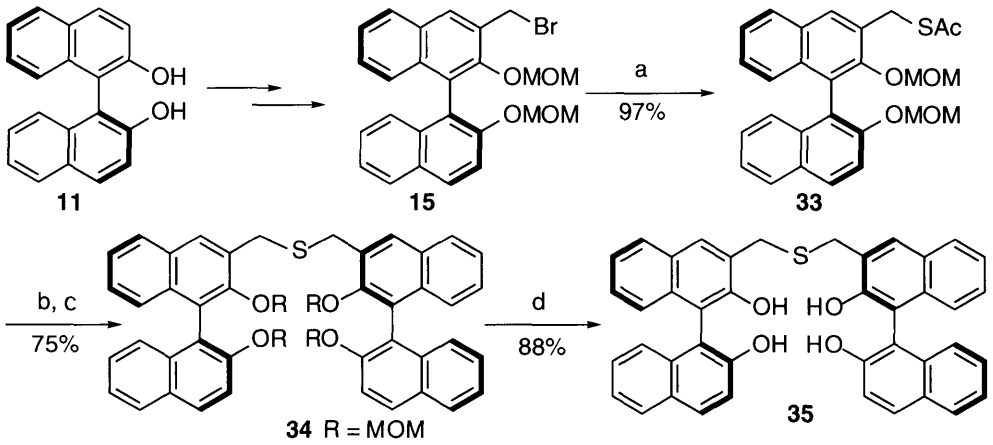

[a] (a) AcSK, DMF, 0 ℃, 10 min, 97%; (b) NaOMe, MeOH, THF 0 ℃, 5 min; (c) **15**, NaH, THF, 0 ℃, 30 min, 75% (2 steps); (d) TsOH•H_2O, CH_2Cl_2, MeOH, 40 ℃, 12 h, 88%.

Table 10. Direct Aldol Reaction with 2-Hydroxy-2'-methoxypropiophenone (**27**) Using (*S*,*S*)-Sulfur-linked-BINOL **35**.

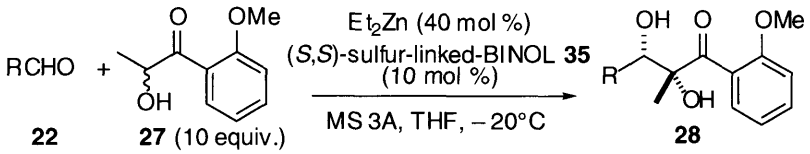

entry	R		product	time (h)	yield (%)	dr[a] (*syn*/*anti*)	ee (*syn*/*anti*)
1	Ph⌒⌒CHO	**22a**	**28a**	45	82	35/65	60/92
2	Ph⌒⌒⌒CHO	**22d**	**28d**	24	63	41/59	45/86
3	⌒⌒CHO	**22e**	**28e**	24	56	41/59	48/87
4	PMBO⌒⌒CHO	**22g**	**28g**	24	73	41/59	58/93
5	BOMO⌒⌒CHO	**22i**	**28i**	24	72	39/61	52/81

[a] Determined by ^{1}H NMR of mixture.

4. Summary

(1) I developed a novel chiral ligand linked-BINOL **10**. Heteroatom in the linker part was effective for the construction of unique chiral environment.[23a]

(2) In the epoxide opening reaction with Ga-Li-linked-BINOL complex, linked-BINOL **10** was effective for stabilizing the Ga-Li complex against ligand exchange with 4-methoxyphenol.

(3) The structure of Ga-Li-linked-BINOL complex was confirmed by X-ray single crystal analysis.

(4) Mechanistic study of the direct aldol reaction of 2-hydroxy-2'-methoxyacetophenone **23** catalyzed by Et_2Zn/linked-BINOL = 2/1 complex was performed, through X-ray, NMR, CSI-MS, and kinetics.[45]

(5) On the basis of the results from mechanistic studies, the new catalyst system: Et_2Zn /linked-BINOL = 4/1-MS 3A system was developed. Catalyst/substrate ratio in both the aldol reaction (up to 1000/1)[45] and Michael reaction (up to 10000/1)[46] was improved. The amount of ketone was also reduced to 1.1 equiv without any problem.

(6) With the new Et_2Zn /linked-BINOL = 4/1-MS 3A system, 2-hydroxy-2'-methoxypropiophenone **27** was successfully used as a donor, affording optically active *tert*-alcohol in high ee. Both linked-BINOL **10** and *sulfur*-linked-BINOL **35** were effective for the aldol reaction, giving either *syn*- or *anti*- diastereoselectivity.

Appendix:

Et_2Zn /linked-BINOL = 4/1-MS 3A system was recently found effective for an anti-selective direct catalytic asymmetric Mannich-type reaction by coworkers of mine.[47]

Appendix: *anti*-Selective Direct Mannich-type Reaction (Mr. Kumagai and Mr. Harada)

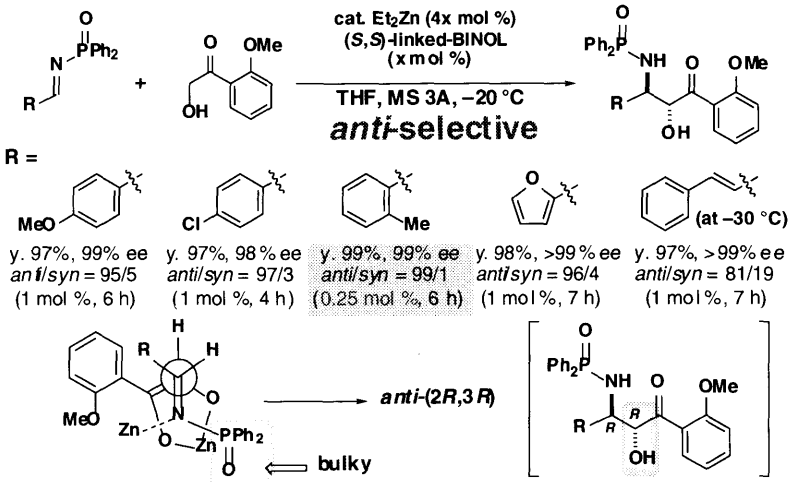

Matsunaga, S; Kumagai, N.; Harada, S.; Shibasaki, M. J. *Am. Chem. Soc.* **2003**, *125*, 4712.

Experimental Section

General: Infrared (IR) spectra were recorded on a JASCO FT/IR 410 Fourier transform infrared spectrophotometer. NMR spectra were recorded on a JEOL JNM-LA500 spectrometer, operating at 500 MHz for ^{1}H NMR and 125.65 MHz for ^{13}C NMR. Chemical shifts in $CDCl_3$ were reported downfield from TMS (= 0) for ^{1}H NMR. For ^{13}C NMR, chemical shifts were reported in the scale relative to $CHCl_3$ (77.00 ppm for ^{13}C NMR) as an internal reference. Chemical shifts in C_6D_6 were reported downfield from TMS (= 0) or in the scale relative to C_6D_6 (7.15 ppm) for ^{1}H NMR. For ^{13}C NMR, chemical shifts were reported in the scale relative to C_6D_6 (128.0 ppm) for ^{13}C NMR as an internal reference. Optical rotations were measured on a JASCO P-1010 polarimeter. EI and FAB mass spectra were measured on JEOL JMS-DX303 or JMS-BU20 GCmate. LDI-TOF mass spectra were measured on Shimadzu MALDI IV. ESI mass spectra were measured on Waters micromass ZQ. Column chromatography was performed with silica gel Merck 60 (230–400 mesh ASTM). The enantiomeric excess (ee) was determined by HPLC analysis. HPLC was performed on JASCO HPLC systems consisting of the following: pump, 880-PU or PU-980; detector, 875-UV or UV-970, measured at 254 nm; column, DAICEL CHIRALCEL OD, OD-H, OJ, OJ-H, CHIRALPAK AS, AS-H, AD, AD-H; mobile phase, hexane–2-propanol; flow rate, 0.50–1.0 mL/min. Reactions were carried out in dry solvents under an argon atmosphere, unless otherwise stated. Tetrahydrofuran (THF) and diethyl ether were distilled from sodium benzophenone ketyl. Toluene was distilled from sodium. $GaCl_3$ and $Ga(O\text{-}i\text{-}Pr)_3$ were purchased from Kojundo Chemical Laboratory Co., LTD., 5-1-28, Chiyoda, Sakado-shi, Saitama 350-0214, Japan (fax, ++(81)-492-84-1351). Et_2Zn (1.0 M, in hexanes) was purchased from Aldrich, which was titrated prior to use. Other reagents were purified by the usual methods.

Experimental Section for Chapter 2: Development of a Novel Linked-BINOL and its Application to Ga-Lilinked-BINOL Complex

Synthesis of linked-BINOL 10.

2,2'-bis(Methoxymethyloxy)-1,1'-binaphthalene-3-carboxaldehyde (12) :

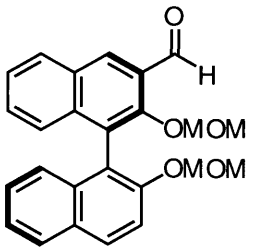

To a stirred solution of MOM-protected (*R*)-binaphthol (32.05 g, 85.6 mmol), in THF (320 mL) at – 78 ℃ was added TMEDA (15.5 mL, 103 mmol) , then BuLi (60.8 mL, 96.7 mmol, 1.59 M in hexane) over 15 min. The mixture was warmed up to 0 ℃ and stirred for 30 min. After cooling down to –78 ℃, DMF (7.58 ml, 103 mmol) in THF (40 mL) was added dropwise over 10 min. The mixture was stirred at the same temperature for 30 min, and then was warmed up to 0 ℃ and stirred for further 40 min. The resultant yellow solution was quenched with sat. aq NH_4Cl (50 mL). After addition of 1 M aq HCl (50 mL), the solution was extracted with diethyl ether (500 mL), and the combined organic layers were washed with sat. aq $NaHCO_3$ (50 mL) and brine, and then dried over $MgSO_4$. The solvent was evaporated under reduced pressure, and the residue was purified by flash column chromatography (SiO_2, hexane/ethyl acetate 10/1) to give **13**(26.03 g, 64.7 mmol, y. 76 %). **12** has already been reported. See ref 11a.

3-Hydroxymethyl-2,2'-bis(methoxymethyloxy)-1,1'-binaphthalene (13) :

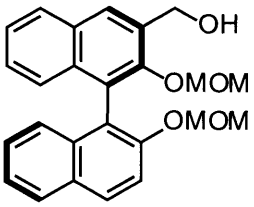

To an ice-cooled solution of **12** (5.15 g, 12.8 mmol) in THF (80 mL) / CH_3OH (80 mL) was added $NaBH_4$ (485 mg, 12.8 mmol), and the mixture was stirred at 0 ℃ for 15 min. H_2O was added and the mixture was concentrated under reduced pressure and then extracted with ethyl acetate (100 mL x 2). The combined organic extracts were washed with brine, dried over $MgSO_4$ and evaporated under reduced pressure. The residue was then dried *in vacuo* to afford **13** (ca. 5.1 g) as a colorless foam, which was used for next step without further purification. **13** has already been reported. See ref 11a.

3-Bromomethyl-2,2'-bis(methoxymethyloxy)-1,1'-binaphthalene (14) :

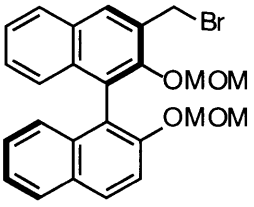

To an ice-cooled solution of crude **13** (5.1 g) in toluene (50 mL) / ethyl acetate (50 mL) were added successively Et_3N (7.14 mL,

51.2 mmol) and MsCl (1.98 mL, 25.6 mmol). The mixture was stirred at 0 ℃ for 90 min. The resultant suspension was filtered to remove solid $Et_3NH^+Cl^-$ and the solid was washed with ethyl acetate (50 mL). The combined filtrate and washings were cooled down to 0 ℃ and then LiBr (11.1 g, 128 mmol) and DMF (100 mL) were added. The mixture was stirred at room temperature for 10 min. It was diluted with diethyl ether (200 mL) and washed with water (100 mL x 2), 1 M aq HCl (50 mL x 2), sat. aq $NaHCO_3$ (50 mL) and brine. It was dried over $MgSO_4$ and evaporated *in vacuo* to give **14** as colorless solid (5.568 g, 11.9 mmol, y. 93% from **12**) which was used in next step without further purification as a crude material.

3,3''-(Oxydimethylene)-di-1,1'-bi-2-naphthol (10):

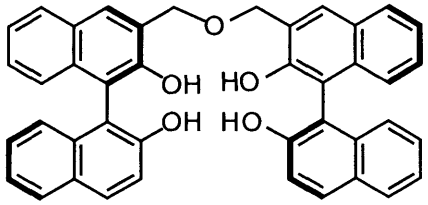

To a stirred solution of **13** (4.0 g, 9.89 mmol), in THF (50 mL) / DMF (30 mL) at 0 °C, was added NaH in oil (482 mg, 12.6 mmol as 60% purity). The mixture was stirred at the same temperature for 60 min, and then **14** (4.62 g, 9.89 mmol) in DMF (30 mL) was added. The mixture was stirred at room temperature for 64 h and then cooled down to 0 ℃ and quenched with H_2O. It was diluted with diethyl ether (400 mL), washed with H_2O (100 mL), brine (100 mL) and then dried over $MgSO_4$. After evaporation of solvent, the residue was purified by flash column chromatography (SiO_2, hexane/ethyl acetate 4/1) to give MOM-protected linked-BINOL (6.63 g(4.0 w/w % ethyl acetate was included based on ^1H NMR), 8.04 mmol, y. 82%) as a yellow foam.

To a stirred solution of this yellow foam (3.01 g, 3.65 mmol) in CH_2Cl_2 (40 mL) / CH_3OH (40 mL) was added $TsOH•H_2O$ (300 mg, 1.58 mmol). The solution was stirred at 40 ℃ for 36 h. It was then diluted with CH_2Cl_2 (250 mL), washed with sat. $NaHCO_3$ (100 mL) and brine (100 mL), and dried over $MgSO_4$. After removing the solvent under reduced pressure the residue was purified by flash column chromatography (SiO_2, hexane/ethyl acetate 4/1). The product was further purified by recrystallization using diethyl ether/hexane to give **10** (2.03 g(5.6 w/w % diethyl ether and hexane were included based on ^1H NMR), 3.12 mmol, y. 85%) as a colorless powder : IR (KBr) ν 3375, 3069, 1507, 1106 cm^{-1}; ^1H NMR ($CDCl_3$) δ 5.00 (brs, 2H), 5.05 (d, J = 12.6 Hz, 2H), 5.06 (d, J = 12.6 Hz, 2H), 6.31 (s, 2H), 7.10 (d, J = 8.3 Hz, 2H), 7.14 (d, J = 8.5 Hz, 2H), 7.22 (ddd, J = 1.5, 6.8, 8.3 Hz, 2H), 7.28-7.38 (m, 8H), 7.85 (d, J = 8.0 Hz, 2H), 7.87 (d, J = 7.3 Hz, 2H), 7.93 (d, J = 8.9 Hz, 2H), 7.98 (s, 2H); ^{13}C NMR ($CDCl_3$) δ 70.2, 112.1, 112.5, 117.7, 123.7, 124.2, 124.4, 125.6, 127.1, 127.4, 128.2, 128.3, 128.9, 129.3, 130.0, 130.8, 133.4, 133.6, 151.8, 152.2; MS *m/z* 614 [M^+], 299; $[\alpha]_D^{27}$ + 67.4 (c =

0.90 $CHCl_3$); HPLC (DAICEL CHIRALPAK AS, 2-propanol/hexane 1/4, flow 0.75) t^R 24.8 and 46.5 min; Anal. Calcd. for $C_{42}H_{30}O_5$ (1.00 mol eq), diethyl ether ($C_4H_{10}O$, 0.265 mol eq), and hexane (C_6H_{14}, 0.200 mol eq): C, 81.59; H, 5.48 Found: C, 81.30; H, 5.51.

Procedure for the preparation of (*R*,*R*)-Ga-Li-linked-BINOL complex 15.

To a stirred solution of (*R*,*R*)-linked-BINOL **10** (1.09 g(15.5 w/w % diethyl ether and hexane), 1.5 mmol), in THF (22.7 mL) at 0 °C, was added BuLi (4.0 mL, 6.0 mmol, 1.50 M in hexane) and the mixture was stirred at 0 °C for 2 h. $GaCl_3$ (3.3 mL, 1.5 mmol, 0.455 M in diethyl ether) was then added at 0 °C. After stirring for 90 min at 0 °C, the reaction mixture became a white suspension, and was then stirred at room temperature for another 90 min. The resultant suspension was used as (*R*,*R*)-Ga-Li-linked-BINOL catalyst. This catalyst suspension can be stored for at least one month under an argon atmosphere at 0 °C. $GaCl_3$ can be stored as diethyl ether solution for several months at – 20 °C.

General procedure for the catalytic enantioselective epoxide ring opening reactions with 4-methoxyphenol using Ga-Li-linked-BINOL complex 15.

A mixture of powdered MS 4A (100 mg), dried at 180 °C under reduced pressure (ca. 5 mmHg) for 6 h prior to use, and a 0.05 M suspension of (*R*,*R*)-Ga-Li-linked-BINOL complex **15** (1.0 mL, 0.05 mmol) [prepared by the procedure described above] was evaporated *in vacuo*. A solution of 4-methoxyphenol (**5**) (186 mg, 1.5 mmol) in toluene (2.0 mL), and cyclopentene oxide (**4b**) (43.7 μL, 0.50 mmol) were added to the residue at room temperature, and the mixture was stirred at 75 °C for 96 h. The resultant mixture was diluted with diethyl ether (30 mL) and filtered over a celite pad to remove MS 4A. The organic layer was washed successively with 5% aq citric acid (10 mL), 1 *N* aq NaOH (15 mL x 2), sat. aq NH_4Cl (10 mL), and brine (10 mL), and then dried over $MgSO_4$. After evaporation, the residue was purified by flash column chromatography (SiO_2, hexane/diethyl ether 5/1) to give **6b** (91.8 mg, 0.44 mmol, y. 88%) in 85% ee as colorless oil; Linked-BINOL **10** was recovered in the following manner; aq NaOH layers were acidified with 1 *N* aq HCl, then extracted with diethyl ether (20 mL). The organic layer was washed with sat. aq $NaHCO_3$ (10 mL) and brine (10 mL), then dried over $MgSO_4$. After evaporation, the residue was purified by flash column chromatography (SiO_2, hexane/diethyl ether 2/1) to give **10** in quantitative yield.

Synthesis of the 1,2-diol mono ethers 6 using Ga-Li-linked-BINOL complex 15.

The absolute configurations of **6a** and **6b** were determined by converting them into known chiral diols. **6d** was transformed into **6a**, and **6f** was transformed into a known compound.[a] Mosher's method[b] was used for **6c**, **6e** and **6i**.

(a) Ballini, R.; Marcantoni, E.; Petrini, M. *J. Org. Chem.* **1992**, *57*, 1316; (3*S*,4*S*)-1-Benzyl-3,4-bis(methoxymethoxy)pyrrolidine : $[\alpha]_D^{20} = +11.9$ °(c = 2.4, $CHCl_3$).

(b) Dale, J. A.; Dull, D.L.; Mosher, H. S. *J. Org. Chem.* **1969**, *34*, 2543.; Ohtani, I.; Kusumi, T.; Kashman, Y.; Kakisawa, H. *J. Org. Chem.* **1991**, *56*, 1296.

(1*R*, 2*R*)-2-(4-Methoxyphenyloxy)cyclohexanol

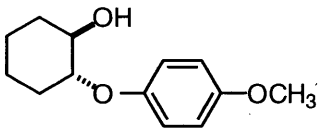

(6a) ; colorless solid ; mp 84-86 °C; IR (KBr) ν 3398, 2933, 2056, 1982 cm^{-1}; ^1H NMR ($CDCl_3$) δ 1.21-1.43 (m, 4H), 1.73 (m, 2H), 2.02-2.17 (m, 2H), 2.62 (br, 1H), 3.68 (ddd, *J* = 4.6, 8.6, 10.5 Hz, 1H), 3.76 (s, 3H), 3.84 (ddd, *J* = 4.6, 8.6, 10.5 Hz, 1H), 6.79-6.92 (m, 4H); ^{13}C NMR ($CDCl_3$) δ 23.9, 24.0, 29.3, 32.0, 55.7, 73.5, 83.6, 114.6, 118.1, 151.7, 154.4; MS *m/z* 222 [M^+]; $[\alpha]_D^{25}$ – 56.6 (c = 1.10 $CHCl_3$); HPLC (DAICEL CHIRALCEL OJ, 2-propanol/hexane 1/9, flow 1.0) t^R 14.2 and 16.5 min; Anal. Calcd. for $C_{13}H_{18}O_3$: C, 70.24; H, 8.16 Found: C, 69.95; H, 8.29.

(1*R*, 2*R*)-2-(4-Methoxyphenyloxy)cyclopentanol

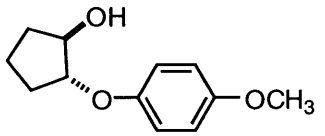

(6b) ; colorless oil ; IR (neat) ν 3408, 2954, 1507 cm^{-1}; ^1H NMR ($CDCl_3$) δ 1.58-1.84 (m, 4H), 2.01-2.16 (m, 3H), 3.75 (s, 3H), 4.28 (m, 1H), 4.43 (m, 1H), 6.83 (m, 4H); ^{13}C NMR ($CDCl_3$) δ 21.0, 29.8, 32.5, 55.7, 77.2, 85.2, 114.6, 116.6, 151.9, 153.8; MS *m/z* 208 [M^+]; $[\alpha]_D^{25}$ – 36.0 (c = 1.08 $CHCl_3$); HPLC (DAICEL CHIRALPAK AS, 2-propanol/hexane 1/9, flow 1.0) t^R 10.1 and 25.5 min; HRMS [M^+] Calcd. for $C_{12}H_{16}O_3$: 208.1100; Found: 208.1099.

(1*R*, 2*R*)-2-(4-Methoxyphenyloxy)cycloheptanol

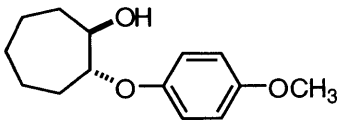

(6c) ; colorless solid ; mp 89-91 °C; IR (KBr) ν 3457, 2936, 1509 cm^{-1}; ^1H NMR ($CDCl_3$) δ 1.42-1.76 (m, 8H), 1.89-2.00 (m, 2H), 2.70 (br, 1H), 3.77 (s, 3H), 3.86 (dt, *J* = 4.0, 8.5 Hz, 1H), 3.96 (dt, *J* = 3.1, 8.9 Hz, 1H), 6.84 (m, 4H); ^{13}C NMR ($CDCl_3$) δ 22.27, 22.34, 27.3, 28.2, 31.8, 55.7, 75.9, 85.7, 114.8, 117.8, 151.5, 154.3; MS *m/z* 236 [M^+]; $[\alpha]_D^{23}$ – 28.1 (c = 0.206 $CHCl_3$(67% ee)); HPLC (DAICEL CHIRALPAK AD, 2-propanol/hexane 1/9, flow 1.0) t^R 13.0 and 16.0 min; HRMS [M^+] Calcd. for $C_{14}H_{20}O_3$: 236.1413; Found: 236.1412.

(1*R*, 2*R*)-2-(4-Methoxyphenyloxy)-4-cyclohexen-1-ol (6d) ; colorless solid ; mp 98-100 ℃; IR (KBr) ν 3376, 2925, 1508 cm^{-1}; ^1H NMR ($CDCl_3$) δ 2.08-2.22 (m, 2H), 2.55-2.63 (m, 2H), 3.77 (s, 3H), 4.02 (ddd, *J* = 5.9, 9.2, 9.2 Hz, 1H), 4.19 (ddd, *J* = 5.7, 9.2, 9.2 Hz, 1H), 5.52-5.56 and 5.59-5.62 (m, 1H each), 6.82-6.94 (m, 4H); ^{13}C NMR ($CDCl_3$) δ 30.3, 32.5, 55.7, 69.9, 79.6, 114.7, 117.9, 123.8, 124.6, 151.7, 154.5; MS *m/z* 220 [M^+]; $[\alpha]_D^{25}$ – 56.5 (c = 0.74 $CHCl_3$ (47% ee)); HPLC (DAICEL CHIRALCEL OJ, 2-propanol/hexane 1/9, flow 1.0) t^R 18.5 and 26.3 min; HRMS [M^+] Calcd. for $C_{13}H_{16}O_3$: 222.1100; Found: 222.1099.

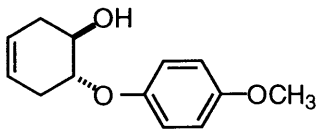

(1*R*, 2*R*, 4*R*, 5*S*)-4,5-bis((*tert*-Butyldiphenylsilyloxy)methyl)-2-(4-methoxyphenyloxy)cyclohexanol (6e) ; colorless foam ; IR (neat) ν 3437, 2930, 1507 cm^{-1}; ^1H NMR ($CDCl_3$) δ 0.96 (s, 9H), 0.98 (s, 9H), 1.37 (m, 1H), 1.45 (m, 1H), 1.97 (m, 1H), 2.21 (brs, 1H), 2.59 (m, 1H), 3.48 (d, *J* = 6.4 Hz, 2H), 3.68 (dd, *J* = 9.8, 10.1 Hz, 1H), 3.74 (s, 3H), 3.73-3.81 (m, 3H), 4.19 (ddd, *J* = 4.3, 8.5, 11.6 Hz, 1H), 6.75 (dt, *J* = 4.0, 9.2 Hz, 2H), 6.91 (dt, *J* = 3.7, 9.2 Hz, 2H), 7.24-7.42 (m, 12H), 7.52-7.62 (m, 8H); ^{13}C NMR ($CDCl_3$) δ 19.1, 26.8, 29.8, 30.9, 37.5, 39.8, 55.7, 62.1, 65.6, 73.3, 80.0, 114.7, 117.8, 127.66, 127.72, 129.6, 129.7, 133.4, 133.5, 135.5, 151.8, 154.3; MS *m/z* 758 [M^+]; $[\alpha]_D^{21}$ – 13.9 (c = 1.07 $CHCl_3$(80% ee)); HPLC (DAICEL CHIRALPAK AD, 2-propanol/hexane 1/99, flow 1.0) t^R 21.0 and 26.0 min; HRMS [M^+] Calcd. for $C_{47}H_{58}O_5Si_2$: 758.3823; Found: 758.3821.

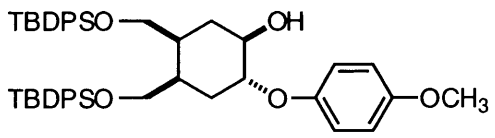

(1*R*, 2*R*)-4-(4-Methoxyphenyloxy)-1-(2,4,6-trimethylphenylsulfonyl)-3-pyrrolidin-3-ol (6f) MS 4A was used without prior activation.; colorless solid; IR (KBr) ν 3449, 2960, 1509, 1315, 1146 cm^{-1}; ^1H NMR ($CDCl_3$) δ 2.31 (s, 3H), 2.64 (s, 6H), 3.36 (dd, *J* = 2.0, 11.5 Hz, 1H), 3.42 (brs, 1H), 3.53 (dd, *J* = 4.0, 12.0 Hz, 1H), 3.76 (s, 3H), 3.81 (dd, J = 5.0, 11.5 Hz, 1H), 4.38 (m, 1H), 4.64 (m, 1H), 6.81 (s, 4H), 6.96 (s, 2H); ^{13}C NMR ($CDCl_3$) δ 20.9, 22.8, 50.0, 52.7, 55.7, 73.8, 82.0, 114.8, 116.9, 131.9, 132.3, 140.2, 142.8, 150.6, 154.6; MS *m/z* 391 [M^+]; $[\alpha]_D^{27}$ – 19.6 (c = 1.04 $CHCl_3$(79% ee)); HPLC (DAICEL CHIRALCEL OD, 2-propanol/hexane 1/9, flow 1.0) t^R 26.4 and 31.6 min; HRMS [M^+] Calcd. for $C_{20}H_{25}O_5$: 391.1453; Found: 391.1450.

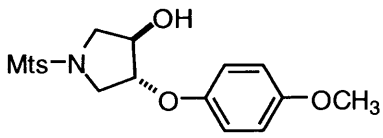

(2*R*,3*R*)-3-(4-Methoxyphenyloxy)-2-butanol (6g); 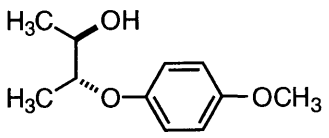

colorless oil; IR (neat) ν 3433, 2976, 1507 cm^{-1}; ^1H NMR ($CDCl_3$) δ 1.18 (d, *J* = 6.1 Hz, 3H), 1.22 (d, *J* = 6.1 Hz, 3H), 2.63 (brs, 1H), 3.75 (S, 3H), 3.79 (dq, *J* = 6.1, 6.4 Hz, 1H), 3.98 (dq, *J* = 6.1, 6.4 Hz, 1H), 6.79-6.86 (m, 4H); ^{13}C NMR ($CDCl_3$) δ 15.6, 18.4, 55.6, 70.9, 80.3, 114.7, 117.8, 151.6, 154.3; MS *m/z* 196 [M^+]; $[\alpha]_D^{26}$ – 52.3 (c = 1.93 $CHCl_3$(91% ee)); HPLC (DAICEL CHIRALPAK AS, 2-propanol/hexane 1/9, flow 1.0) t^R 7.3 and 28.9 min; HRMS [M^+] Calcd. for $C_{11}H_{16}O_3$: 196.1099; Found: 196.1104.

(1*R*, 2*R*, 4*S*)-4-(*tert*-Butyldimethylsilyloxy)-2-(4-methoxyphenyloxy) cyclopentanol (6h) 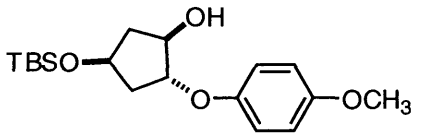

; colorless oil; IR (neat) ν 3508, 2930, 1507 cm^{-1}; ^1H NMR ($CDCl_3$) δ 0.10 (s, 6H), 0.90 (s, 9H), 1.86 (ddd, *J* = 1.5, 1.8, 14.0 Hz, 1H), 1.97 (ddd, *J* = 4.3, 4.7, 15.0 Hz, 1H), 2.05 (ddd, J = 4.9, 4.9, 14.0 Hz, 1H), 2.34 (dddd, *J* = 1.8, 1.8, 7.0, 15.0 Hz, 1H) 3.24 (brs, 1H), 3.75 (s, 3H), 4.19 (brd, *J* = 4.9 Hz, 1H), 4.51-4.53 (m, 1H), 4.71-4.73 (m, 1H), 6.80-6.87 (m, 4H); ^{13}C NMR ($CDCl_3$) δ – 5.0, – 4.9, 17.9, 25.7, 41.5, 42.2, 55.7, 74.3, 77.0, 84.8, 114.7, 116.3, 151.9, 153.8; MS *m/z* 338 [M^+]; $[\alpha]_D^{25}$ – 6.2 (c = 1.08 $CHCl_3$(87% ee)); HPLC (DAICEL CHIRALPAK AD, 2-propanol/hexane 1/9, flow 1.0) t^R 9.9 and 10.9 min; HRMS [M^+] Calcd. for $C_{30}H_{18}O_4Si$: 338.1913; Found: 338.1906.

(1*R*, 2*R*)-5,8-Dimethoxy-3-(4-methoxyphenyloxy)-1,2,3,4-tetrahydronaphthalene-2-ol (6i) ; 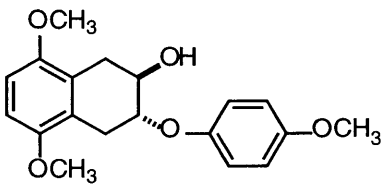

colorless foam ; mp 155-156 °C; IR (KBr) ν 3406, 2942, 1508 cm^{-1}; ^1H NMR ($CDCl_3$) δ 2.56 (dd, *J* = 9.2, 17.1 Hz, 1H), 2.64 (dd, *J* = 9.2, 17.7 Hz, 1H), 3.37 (dd, *J* = 6.1, 17.1 Hz, 1H), 3.38 (dd, *J* = 5.5, 17.7 Hz, 1H), 4.15 (ddd, *J* = 6.1, 9.2, 9.2 Hz, 1H), 4.32 (ddd, *J* = 5.5, 9.2, 9.2 Hz, 1H), 6.63 (d, *J* = 8.9 Hz, 1H), 6.65 (d, *J* = 8.9 Hz, 1H), 6.83-6.98 (m, 4H); ^{13}C NMR ($CDCl_3$) δ 28.1, 30.4, 55.5, 55.7, 69.8, 79.2, 107.4, 107.7, 114.8, 117.9, 123.7, 124.1, 151.1, 151.2, 151.8, 154.5; MS *m/z* 330 [M^+], 207; $[\alpha]_D^{25}$ –131.93 (c = 0.42 $CHCl_3$(96% ee)); HPLC (DAICEL CHIRALCEL OD, 2-propanol/hexane 1/9, flow 0.5) t^R 39.0 and 42.7 min; Anal. Calcd. for $C_{19}H_{22}O_5$: C, 69.07; H, 6.71 Found: C, 68.89; H, 6.59.

Preparation of LiCl free (*R*,*R*)-Ga-Li-linked-BINOL complex 16 for the X-ray structure analysis

To a stirred solution of (*R*,*R*)-linked-BINOL **10** (357.2 mg (14.2 w/w % diethyl ether and hexane included), 0.5 mmol), in THF (4.6 mL) at 0 ℃, was added Ga(O-*i*-Pr)$_3$ (123.49 mg, 0.5 mmol) in THF (5 mL), and the solution was stirred for 12 h at room temperature. It was cooled down to 0 ℃ and BuLi (0.333 mL, 0.5 mmol, 1.5 M in hexane) was added. The reaction mixture was stirred at room temperature for 3 h. Ga(O-*i*-Pr)$_3$ CANNOT be stored as a THF solution, it should be stored as a toluene solution or powder under an argon atmosphere.

Preparation of the crystal of (*R*,*R*)-Ga-Li-linked-BINOL(thf)$_3$

The LiCl free Ga-Li-linked-BINOL complex **16** in THF (0.05 M, 1 mL) was evaporated *in vacuo*. The resulting foam was dissolved in toluene (0.4 mL). An X-ray quality crystal of LiCl free Ga-Li-linked-BINOL(thf)$_3$ complex (colorless prism) was grown at room temperature from toluene solution (0.125 M, 0.4 mL) under argon in the presence of trace amount of THF and diethyl ether.

(*R*,*R*)-Ga-Li-linked-BINOL(thf)$_3$

collected at 135 K: $C_{65}H_{70}O_{10}GaLi$ = 1087.92, colorless prism, a = 10.013(5) Å, b = 19.02(1) Å, c = 15.34(1) Å, β = 106.32(3)°, V = 2802(3) Å^3, monoclinic, $P2_1$ (Z = 2), Dx = 1.289 g/cm^3, R(F) = 0.067. Other than (thf)$_3$, diethyl ether x 1, water x 1, and toluene x 1 were incorporated in the crystal.

Crystal data

Empirical Formula	$C_{65}H_{70}O_{10}GaLi$
Formula Weight	1087.92
Crystal Color, Habit	clear, prism
Crystal Dimensions	0.38 X 0.25 X 0.20 mm
Crystal System	monoclinic
Lattice Type	Primitive
Lattice Parameters	a = 10.013(5) Å
	b = 19.02(1) Å
	c = 15.34(1) Å

	β = 106.32(3) °
	V = 2802(3) Å^3
Space Group	$P2_1$ (#4)
Z value	2
D_{calc}	1.289 g/cm^3
F_{000}	1148.00
m(MoKa)	5.51 cm^{-1}

B. Intensity Measurements

Diffractometer	RAXIS-II
Radiation	MoKa (l = 0.71070 Å) graphite monochromated
Detector Aperture	200 mm x 200 mm
Data Images	20 exposures @ 4.0 minutes
Oscillation Range	7.0°
Detector Position	80.00 mm
Detector Swing Angle	0.00°
$2\theta_{max}$	50.0°
No. of Reflections Measured	Total: 4229 Unique: 12661 (R_{int} = 0.150)
Corrections	Lorentz-polarization Secondary Extinction (coefficient: 3.09304e-06)

C. Structure Solution and Refinement

Structure Solution	Direct Methods (SIR92)
Refinement	Full-matrix least-squares on F
Function Minimized	$\Sigma\ \omega\ (\|Fo\| - \|Fc\|)^2$
Least Squares Weights	$\omega = 1/\sigma^2(Fo) = [\sigma^2(Fo)+p^2/4Fo^2]^{-1}$
p-factor	0.0350
Anomalous Dispersion	All non-hydrogen atoms
No. Observations (I>1.50s(I))	3759

No. Variables	695
Reflection/Parameter Ratio	5.41
Residuals: R; Rw	0.067 ; 0.077
Residuals: R1	0.067
No of Reflections to calc R1	3759
Goodness of Fit Indicator	2.84
Max Shift/Error in Final Cycle	0.72
Maximum peak in Final Diff. Map	0.50 $e^-/Å^3$
Minimum peak in Final Diff. Map	-0.45 $e^-/Å^3$

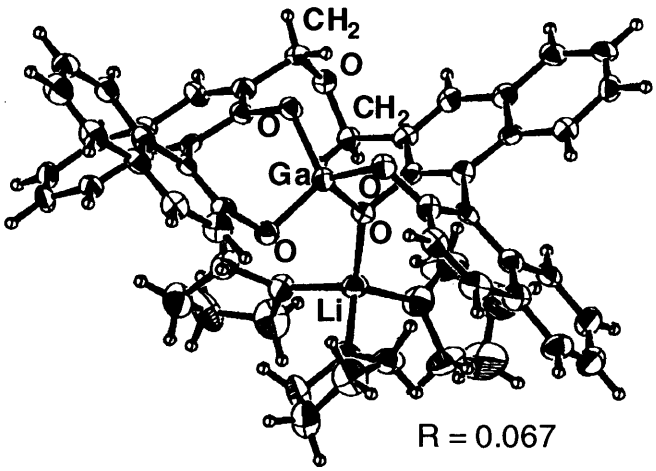

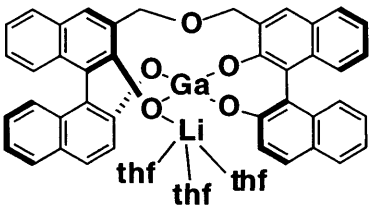

Experimental Section for Chapter 3. Mechanistic Studiues of Et_2Zn/linked-BINOL Complex

(S3-1) X-ray Crystallographic Analysis of Preformed Complex 29: Preparation of X-ray grade single crystal 29.

To a solution of (*S*,*S*)-linked-BINOL **10** (32.94 mg, 6.7w/w% diethyl ether and hexane included, 0.05 mmol) in THF (0.2 mL) at –20 ℃ in a flame-dried glass tube, was added Et_2Zn (100 μL, 0.1 mmol, 1.0 M in hexanes). The resulting mixture was vigorously shaken by vortex mixer, and left at –20 ℃ for several hours. After some needle like crystal emerged in the glass tube, the solvent was evaporated to the dryness. The residue was recrystallized from THF (0.25 mL, 0.2M in Linked-BINOL) at room temperature for a few days to give clear prisms **29**.

X-ray Crystallographic Data Collections and Refinement of the Structures.

Crystals suitable for X-ray analysis were obtained from the procedure described above. The crystals were selected under ambient conditions, attached to the tip of a glass fiber, and transferred to a Bruker SMART CCD diffractometer equipped with use of the SADABS program. The data were collected at –100 ± 1 ℃ to a maximum 2q value of 56.9°. The structure was solved by direct methods and expanded using Fourier techniques. The non-hydrogen atoms were refined anisotropically. Hydrogen atoms were included but not refined.

Crystal data

Empirical Formula	$C_{116}H_{118}O_{18}Zn_3$
Formula Weight	1996.34
Crystal Color, Habit	clear, prism
Crystal Dimensions	0.30 X 0.20 X 0.10 mm
Crystal System	orthorhombic
Lattice Type	Primitive
Lattice Parameters	a = 14.304(2) Å
	b = 18.552(2) Å
	c = 36.827(4) Å
	V = 9772.7(16) $Å^3$
Space Group	$P2_12_12_1$ (#19)
Z value	4

D_{calc}	1.357 g/cm^3
F_{000}	4192.00
m(MoKa)	8.01 cm^{-1}

B. Intensity Measurements

Diffractometer	CCD
Radiation	MoKa (l = 0.71069 Å) graphite monochromated
Detector Aperture	94 mm x 94 mm
Data Images	1265 exposures @ 10.0 seconds
Detector Position	50.00 mm
Detector Swing Angle	-28.00^o
2q$_{max}$	56.9^o
No. of Reflections Measured	Total: 58829 Unique: 12661 (R_{int} = 0.150)
Corrections	Lorentz-polarization Absorption (trans. factors: 0.5847 - 0.8156)

C. Structure Solution and Refinement

Structure Solution	Direct Methods (SIR92)
Refinement	Full-matrix least-squares on F
Function Minimized	S w (|Fo| - |Fc|)^2
Least Squares Weights	1/s^2(Fo) = 4Fo^2/s^2(Fo^2)
p-factor	0.0300
Anomalous Dispersion	All non-hydrogen atoms
No. Observations (I>1.50s(I))	6913
No. Variables	1235
Reflection/Parameter Ratio	5.60
Residuals: R; Rw	0.077 ; 0.084
Goodness of Fit Indicator	2.08
Max Shift/Error in Final Cycle	9.56
Maximum peak in Final Diff. Map	0.84 e$^-$/Å^3

Minimum peak in Final Diff. Map -1.39 $e^-/Å^3$

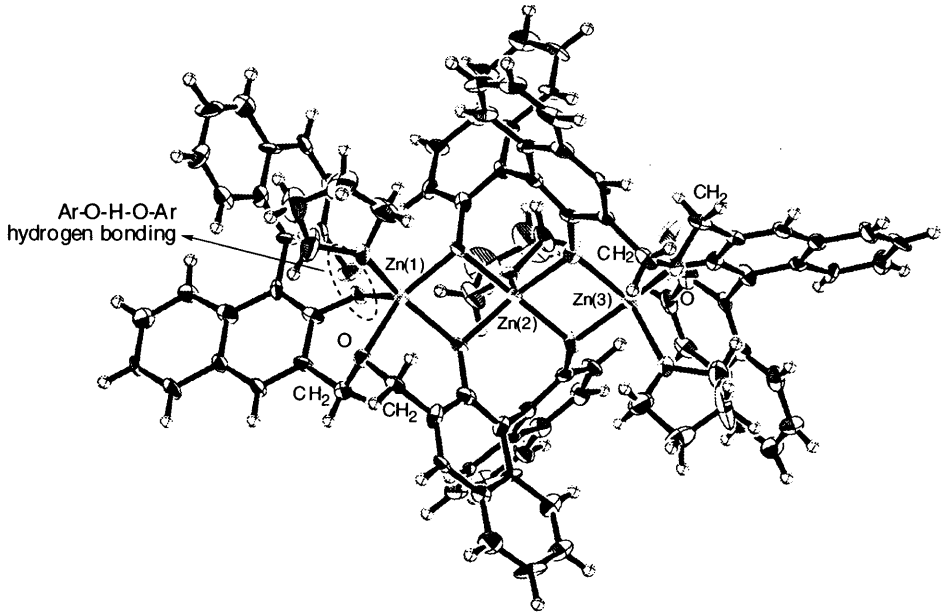

Figure (S3-1)-1. The ortep diagram of the crystal **29**.

The crystal **29** consists of linked-BINOL **10** and Zn in a ratio 2:3(Zn_3(linked-binol)$_2$thf$_3$) with C_2-symmetry. Three Zn atoms are aligned in an almost straight line, and each Zn center are penta-coordinated. Two phenolic hydrogens exist, and which are involved in hydrogen bonding. Thus, the acidity of these hydrogens seemed to decrease enough to resist deprotonation in the presence of small excess EtZn-species. See, the results of NMR and ethane gas emission experiments described in the section (S3-2) and (S3-3) of this Supporting Information.

(S3-2) NMR Experiments to Verify the Structure of Preformed Complex 29 in Solution Phase:

Freshly opened Et_2Zn (1.0 M in hexanes, Aldrich) was always used with titration prior to use. ^{1}H NMR spectra of the mixture solutions of linked-BINOL **10** and Et_2Zn in THF-d_8 are shown in Chart (S3-2)-1 ((*S*,*S*)-linked-BINOL **10** only), (S3-2)-2 (Et_2Zn/**10** = 1/1), (S3-2)-3 (Et_2Zn/**10** = 1.5/1) and (S3-2)-4 (Et_2Zn/**10** = 2/1). ^{1}H NMR spectrum of crystal **29** in THF-d_8 is shown in Chart (S3-2)-5.

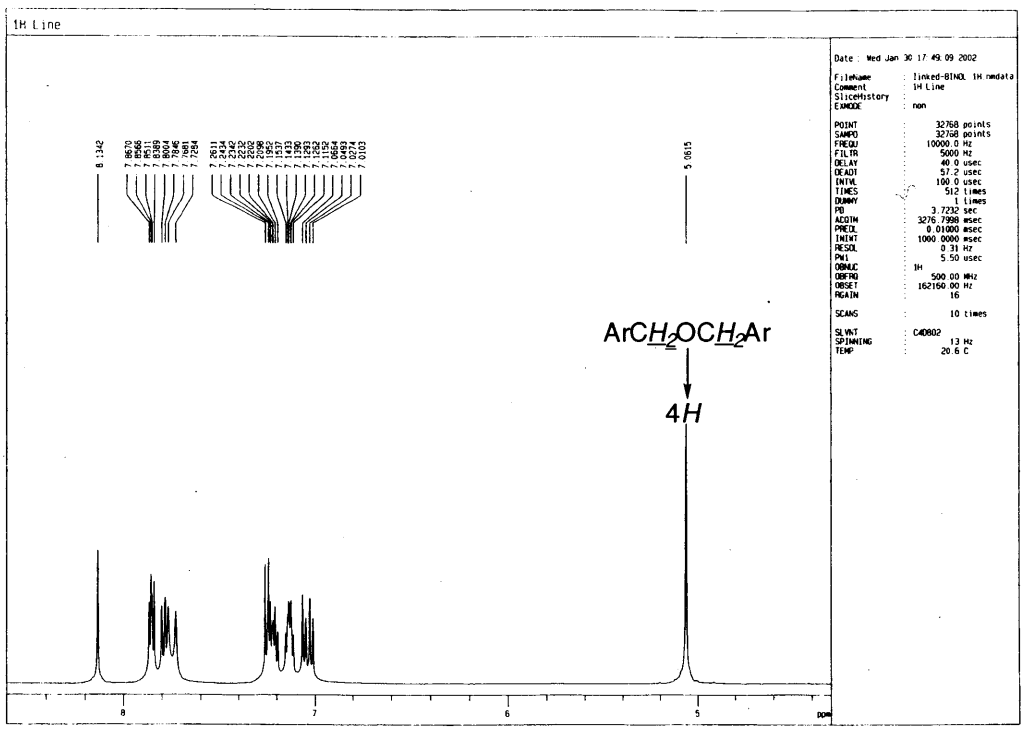

Chart (S3-2)-1. ^{1}H NMR spectrum of linked-BINOL **10** in THF-*d8*.

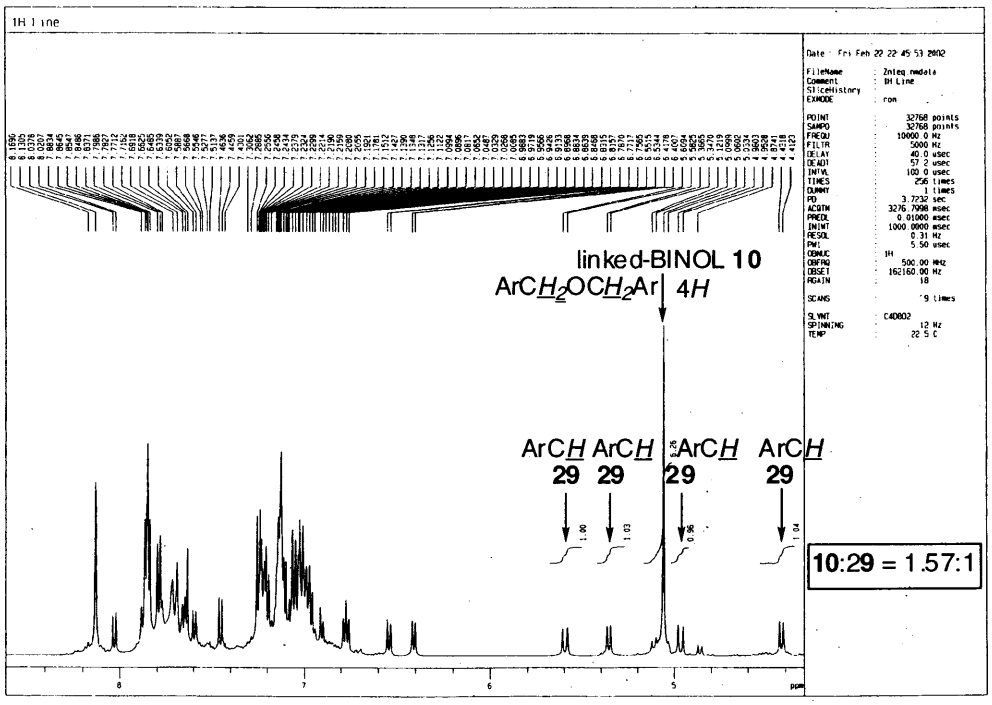

Chart (S3-2)-2. ^{1}H NMR spectrum of Et_2Zn/linked-BINOL **10** = 1/1 mixture in THF-*d*8.

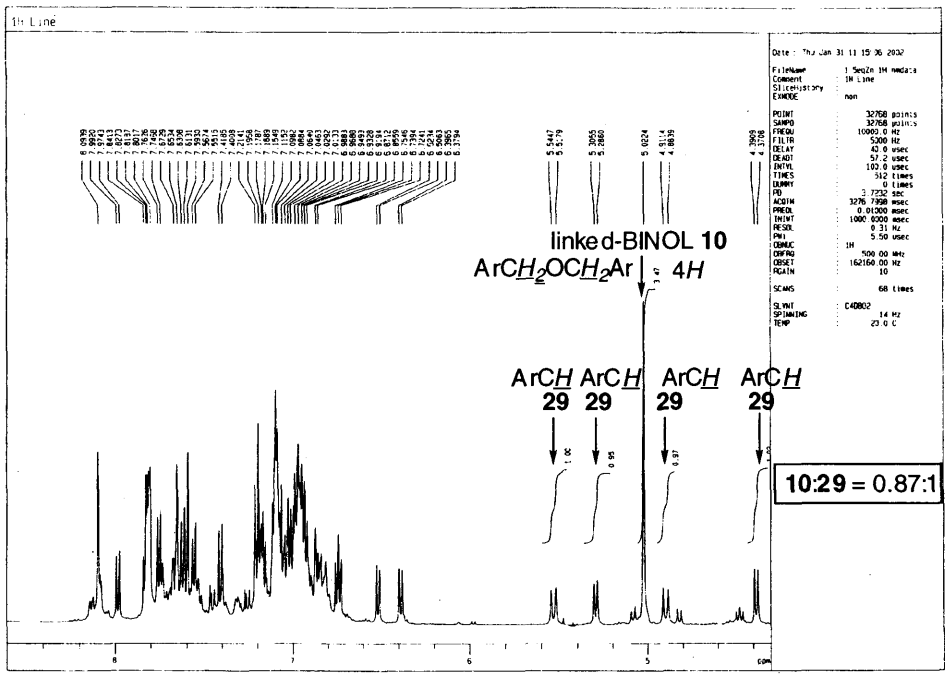

Chart (S3-2)-3. ^{1}H NMR spectrum of Et_2Zn/linked-BINOL **10** = 1.5/1 mixture in THF-*d*8.

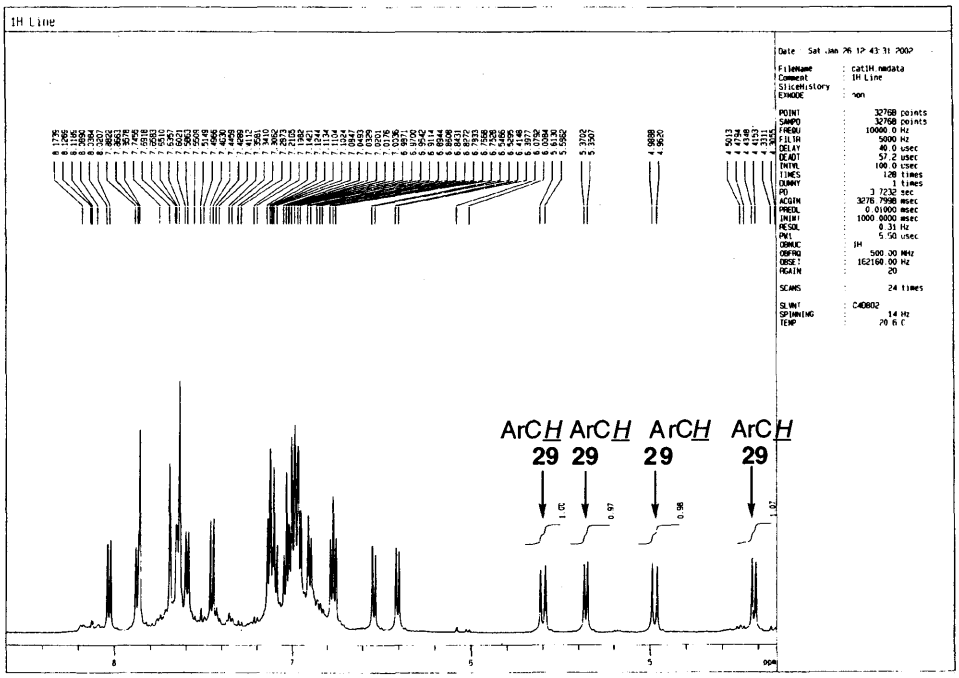

Chart (S3-2)-4. ^{1}H NMR spectrum of Et_2Zn/linked-BINOL **10** = 2/1 mixture in THF-*d*8.

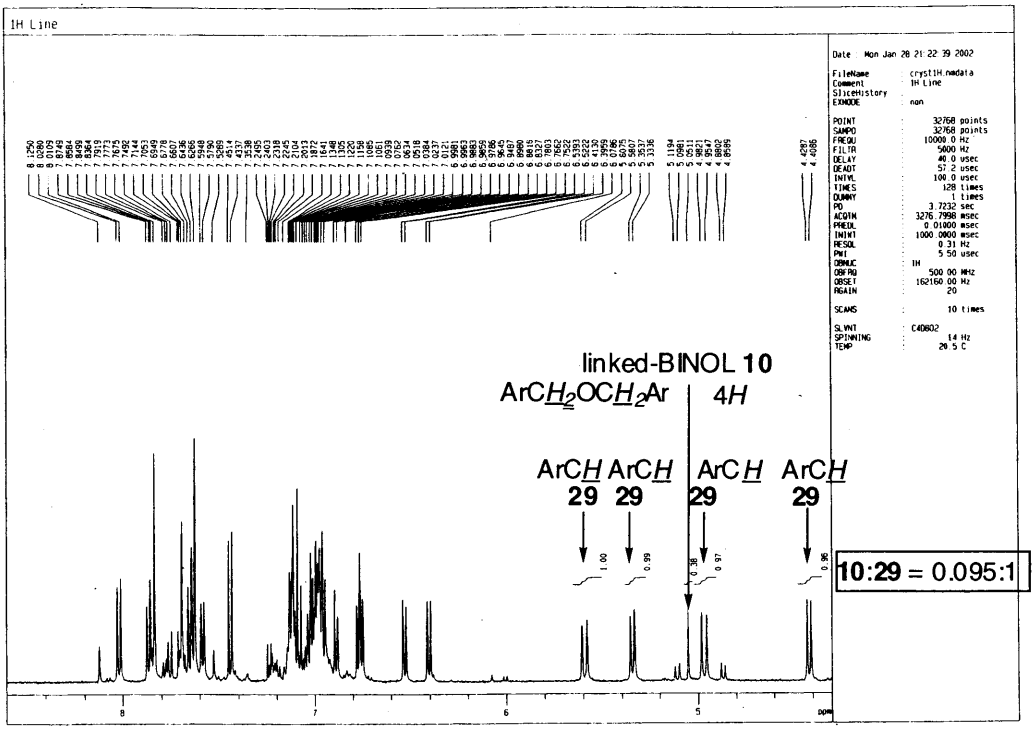

Chart (S3-2)-5. ^{1}H NMR spectrum of the crystal **29** in THF-*d*8.

In Chart (S3-2)-4 (Et_2Zn/**10** = 2/1), single species was observed, which is same as the major species in Chart (S3-2)-5 (crystal **29**). Four different benzylic protons (ArC*H*) were observed in the NMR spectrum of Chart (S3-2)-4, suggesting the non-C_2-symmetric environment around one linked-BINOL unit. The observed results in NMR spectrum matched well with the observed X-ray single crystal structure. In Chart (S3-2)-5 (crystal **29**), linked-BINOL **10** (<10%) and other minor species were observed, probably because some of the crystal **29** was hydrolyzed during operation.

The NMR experiments indicated that ≥2 mol eq of Et_2Zn was necessary for the complete complexation of linked-BINOL **10** and Zn to form preformed complex **29**. The existence of remaining Et_2Zn in Et_2Zn/**10** = 2/1 were confirmed by measuring ethane gas emission, which is described in the section (S3-3) of this Experimental Section. The two remaining phenolic protons (ArO*H*) seemed to be stabilized by hydrogen bonding, which was observed in X-ray crystal structure of preformed complex **29**.

In Chart(S3-2)-2 (Et_2Zn/**10** = 1/1) and Chart(S3-2)-3 (Et_2Zn/**10** = 1.5/1), free (*S*,*S*)-linked-BINOL **10** and **29** (Zn_2(linked-binol)$_3$) were observed as main peaks. The results indicated that the formation of **9** is thermodynamically favorable, thus desirable preformed complex **29** exists even in shortage of Zn source.

(S3-3) Ethane Gas Emission Measurement:

Freshly opened Et_2Zn (1.0 M in hexanes, Aldrich) was always used with titration prior to use. Ethane gas emission was measured by following the procedure in the literature. (Ref. Brown, H. C., *Organic Synthesis via Boranes*, Wiley-Interscience, **1975**, pp241.)

To a stirred solution of linked-BINOL **10** (131.8 mg, 0.2 mmol) in THF (6 mL) at 21 °C was successively added portions of Et_2Zn (1.0 M in hexanes), (a) 0.3 mL (0.3 mmol) and (b) 0.1 mL (0.1 mmol). After addition of Et_2Zn, ethane gas emission was measured. In (a) (Et_2Zn/linked-BINOL **10** = 1.5/1), ethane 0.37 mmol was detected, in (b) (Et_2Zn/linked-BINOL **10** = 2/1), additional ethane 0.11 mmol was detected (subtotal: 0.48 mmol). To the resulting mixture (Et_2Zn/linked-BINOL **10** = 2/1) was added conc. H_2SO_4 (0.1 mL) to afford further ethane (0.22 mmol) emission.

Scheme (S3-3)-1. Ethane Gas Emission Measurement.

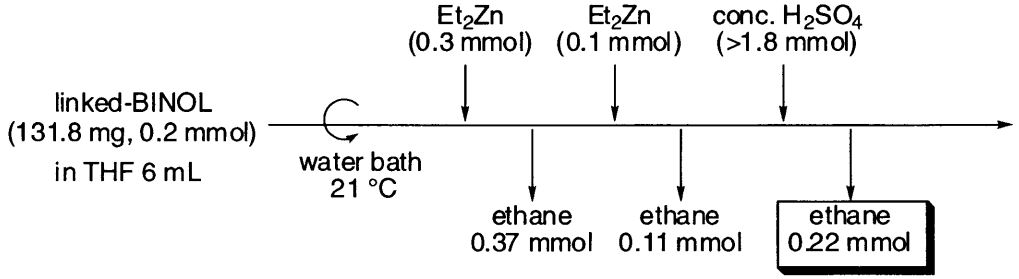

The results suggested that Et_2Zn remains in the Et_2Zn/linked-BINOL **10** = 2/1 solution. Total gas emission was 0.70 mmol (theoretically 0.80 mmol), it is probably due to technical error. Another ethane gas measurements by adding excess Et_2Zn revealed that ≥3 mol eq Et_2Zn was necessary for complete deprotonation of all four ArOH groups in linked-BINOL **10** at room temperature.

(S3-4) CSI-MS (Coldspray Ionization Mass Spectrometry) Experiments:

Preparation of CSI-MS sample of Figure (S3-4)-1.

To a stirred solution of (*S*,*S*)-linked-BINOL (16.47 mg, 6.7w/w% diethyl ether and hexane included, 0.025 mmol) in THF (0.5 mL) at –20°C, was added Et_2Zn (50 μL, 0.05 mmol, 1.0 M in hexanes). After stirring for 30 minutes at this temperature, the resulting mixture was diluted with dry THF to give CSI-MS sample (THF solution, 2 mM on linked-BINOL).

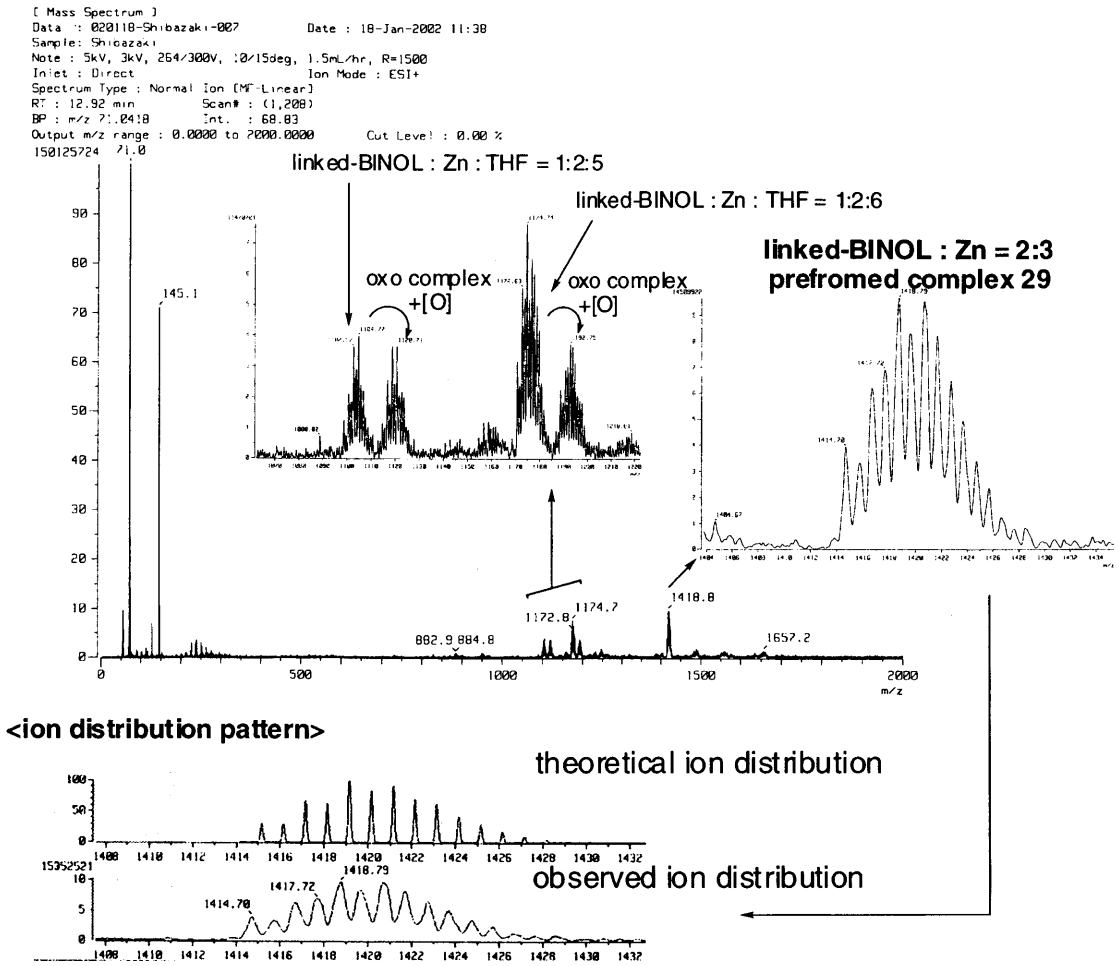

Figure (S3-4)-1. CSI-MS spectrum of Et_2Znlinked-BINOL **10** = 2/1.

In addition to linked-BINOL **1**:Zn =2:3 (*m/z* = 1418.8), fragment peaks assigned as linked-BINOL **10**:Zn =1:2 were also observed. Ion distribution pattern depending on Zn isotopes matched nicely for all assigned peaks. The existence of linked-BINOL **10**:Zn =2:3 complex was confirmed by this CSI-MS and NMR (section (S3-2)) analyses.

Preparation of CSI-MS sample in Figure (S3-4)-2

To a stirred solution of (*S*,*S*)-linked-BINOL **10**(16.47 mg, 6.7w/w% diethyl ether and hexane included, 0.025 mmol) in THF (0.5 mL) at –20℃, was added Et_2Zn (37.5 μL, 0.0375 mmol, 1.0 M in hexanes). After stirring for 30 minutes at this temperature, the resulting mixture was diluted with dry THF to give CSI-MS sample (THF solution, 2 mM on linked-BINOL).

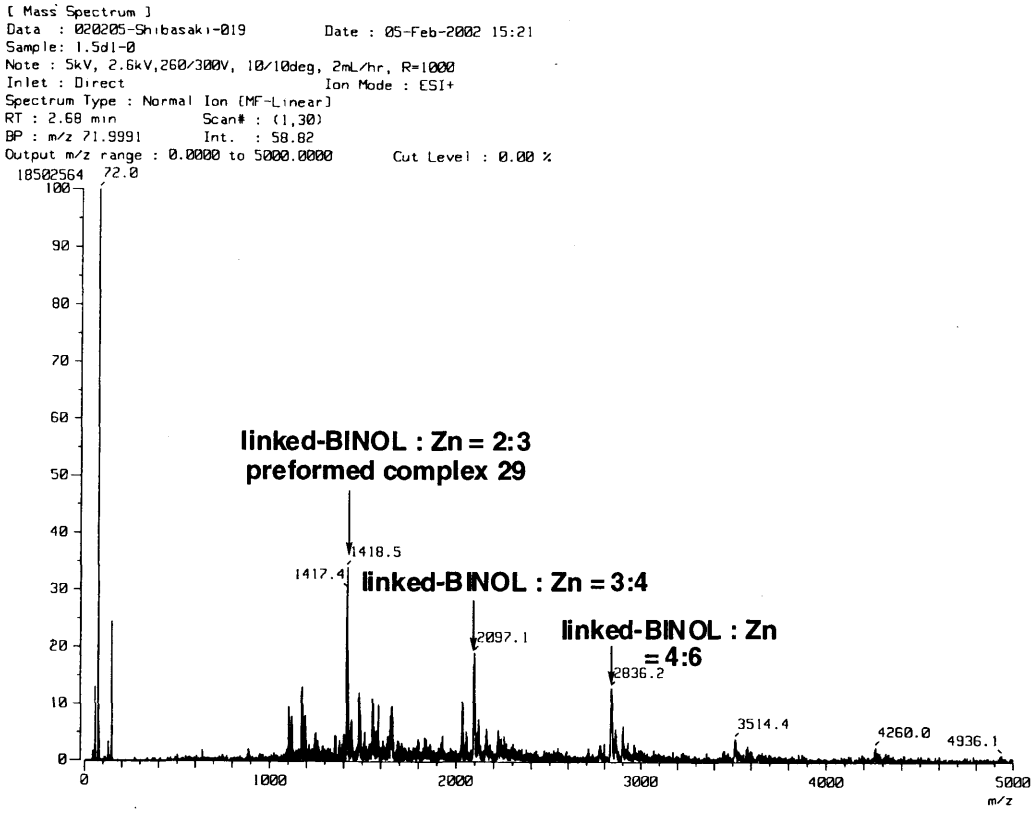

Figure (S3-4)-2. CSI-MS spectrum of Et_2Znlinked-BINOL **10** = 1.5/1.

Peaks corresponding to linked-BINOL:Et_2Zn = 3:4 and 4:6 may form under conditions to take CSI-MS.

Preparation of CSI-MS sample of Figure (S3-4)-3–(S3-4)-5.

To a THF solution of (*S*,*S*)-linked-BINOL : Zn = 1:2 mixture (2 mM in linked-BINOL) prepared by the procedure described above, was added appropriate amount of 2-hydroxy-2'-methoxyacetophenone (**23**) (1.0 M in THF) at room temperature.

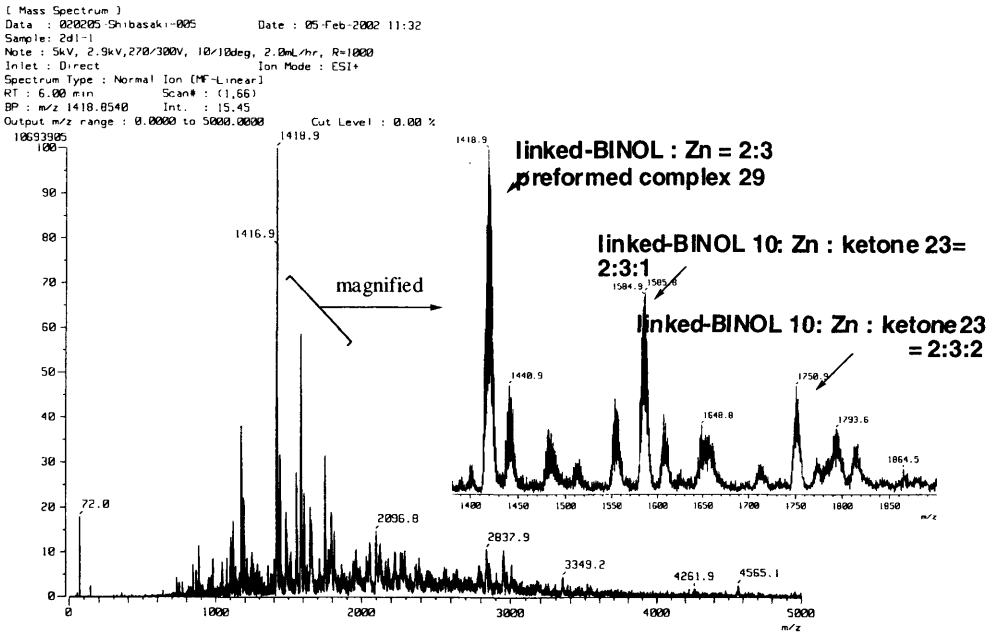

Figure (S3-4)-3. CSI-MS spectrum of linked-BINOL **10** : Et_2Zn : ketone **23** = 1:2:1

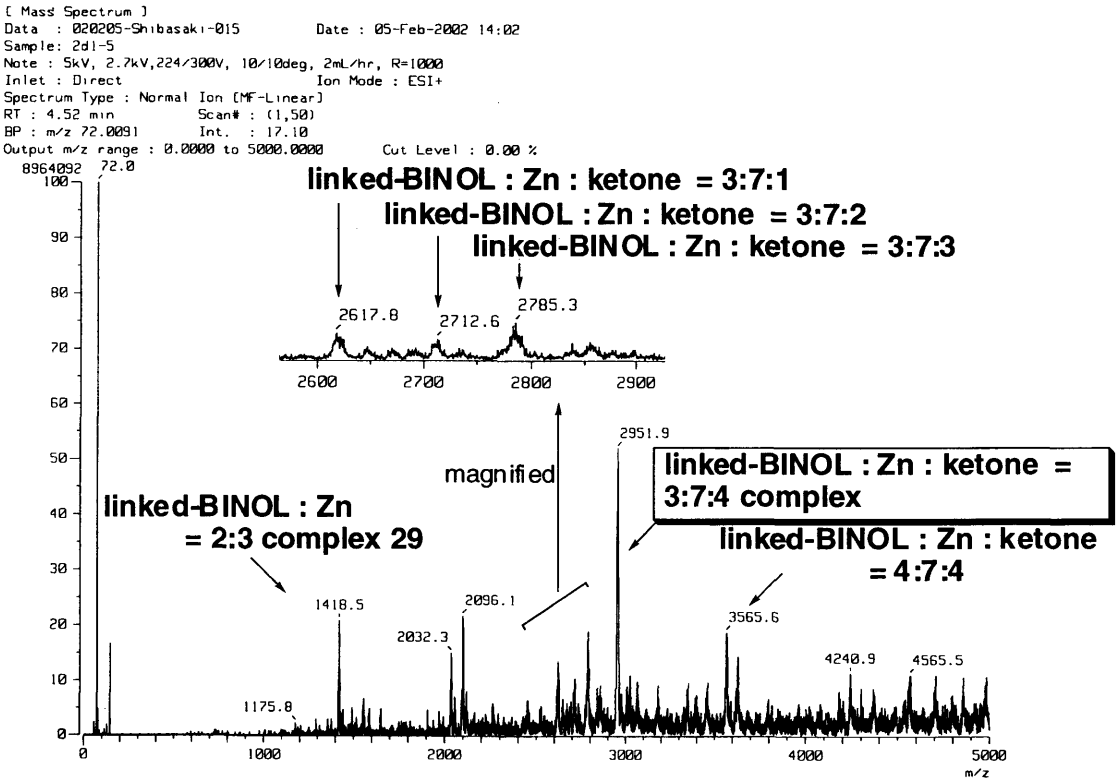

Figure (S3-4)-4. CSI-MS spectrum of linked-BINOL : Et_2Zn : ketone **23** = 1:2:5

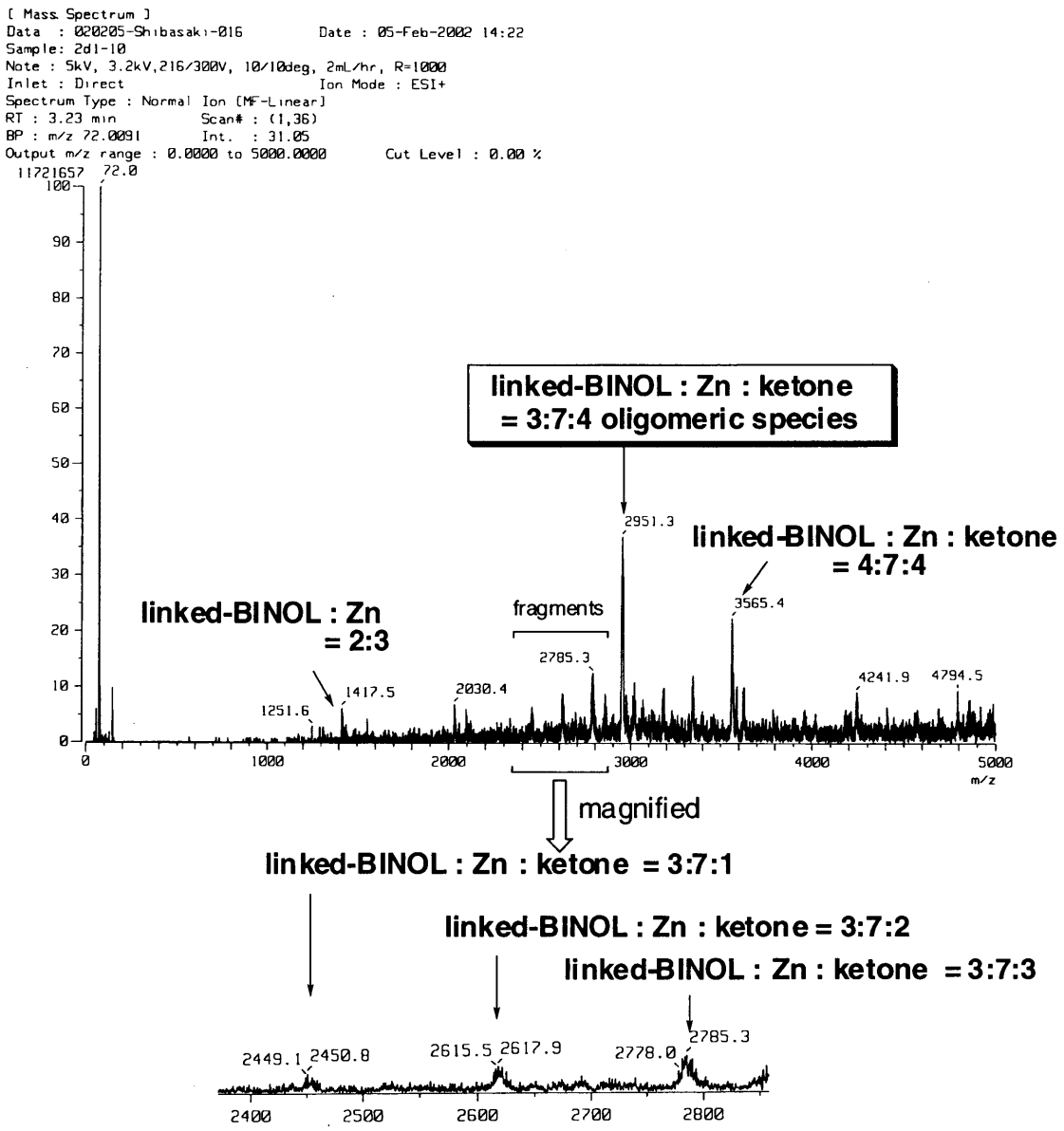

Figure (S3-4)-5. CSI-MS spectrum of linked-BINOL **10**: Et_2Zn : ketone **23** = 1:2:10

Preparation of CSI-MS sample in Figure (S3-4)-6.

To a THF solution of Zn/ (*S*,*S*)-linked-BINOL **10** = 1.5/1 mixture (2 mM in linked-BINOL) prepared by the procedure described above, was added appropriate amount of 2-hydroxy-2'-methoxyacetophenone (**23**) (1.0 M in THF) at room temperature.

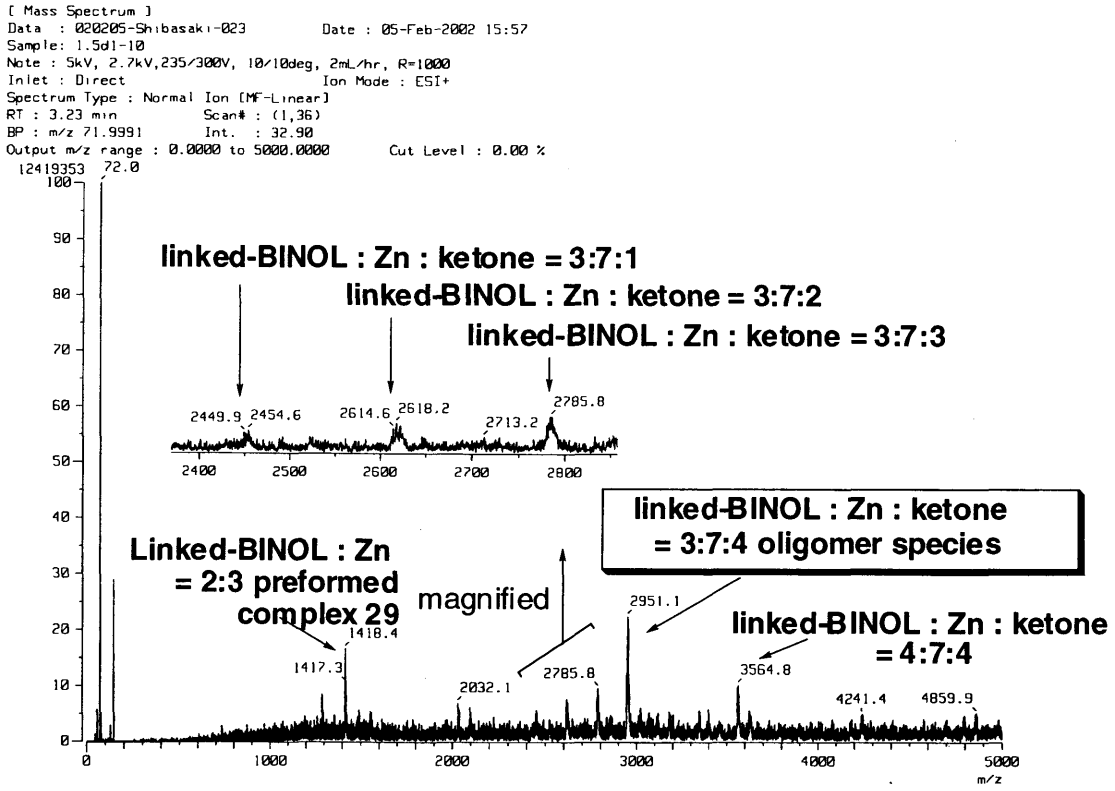

Figure (S3-4)-6. CSI-MS spectrum of linked-BINOL : Et_2Zn ketone **23**= 1:1.5:10

(S3-5) Kinetic Study:

(S3-5)–A: Initial rate kinetics in various catalyst amount.

Procedure for the reaction with 1 mol % of linked-BINOL 10 and 2 mol % of Et_2Zn.

To a stirred solution of (*S*,*S*)-linked-BINOL **10** (6.58 mg, 6.7w/w% diethyl ether and hexane included, 0.01 mmol) in THF (0.3 mL) at –20 °C, was added Et_2Zn (20 μL, 0.02 mmol, 1.0 M in hexanes). After stirring for 30 min at the same temperature, a solution of **23** (322.3 mg, 2.0 mmol) in THF (4.7 mL) was added. The resulting mixture was cooled to –30 ℃, and **22a** (1.0 mmol) was added. The reaction mixtue was stirred at –30 ℃. Samples were taken at recorded times according to the following procedure: 0.2 mL of the reaction mixture was taken with a syringe filled with 0.3 mL of saturated aqueous NH_4Cl solution and was immediately poured onto saturated aqueous NH_4Cl (2.0 mL). The resulting mixture was extracted with ether. After evaporating solvents, the crude residue was analyzed by ^1H NMR. Yields of the products **24a** were measured by comparison of integrated area of methylene proton of **23** (4.75 ppm) and a proton at C-2 position of the **24a** (4.99 ppm). Numerical data for determining initial rate are summarized in each section.

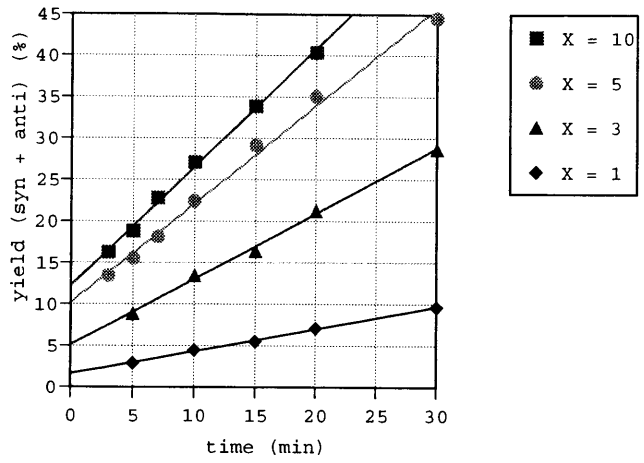

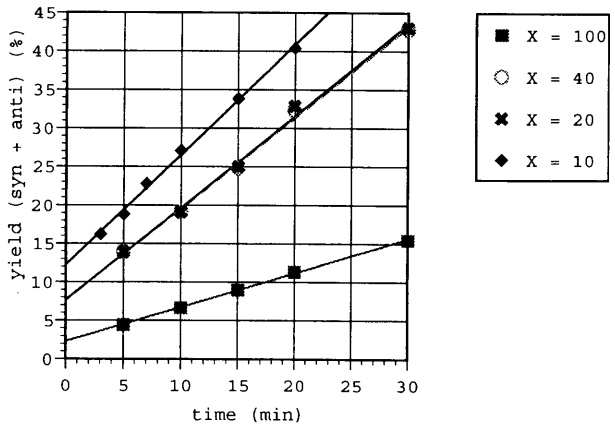

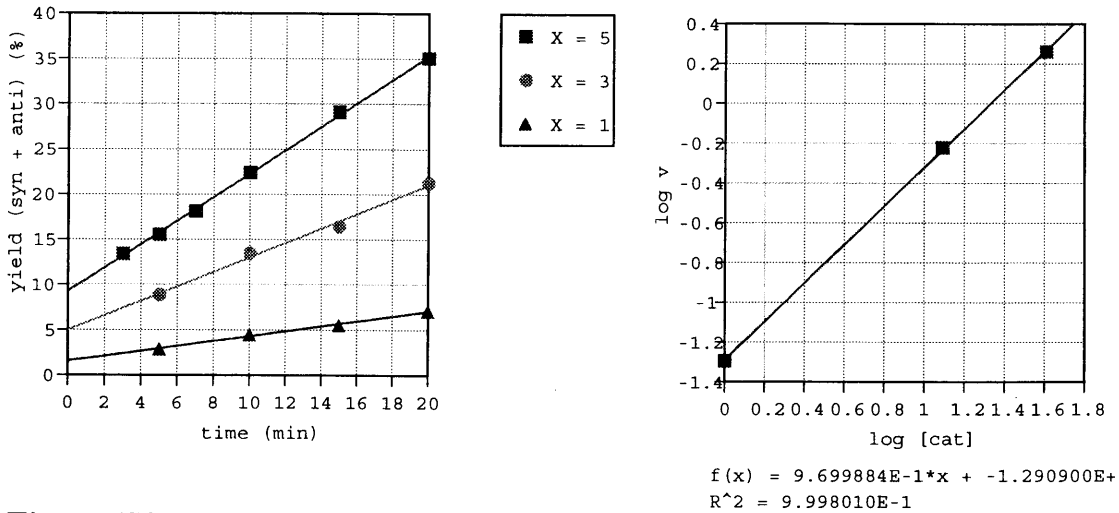

Figure (S3-5)-3. Initial rate kinetics on catalyst concentration (x = 1,3 and 5)

Table (S3-5)-1. Numerical Data for Plots in Figure (S3-5)-1, (S3-5)-2, and (S3-5)-3.

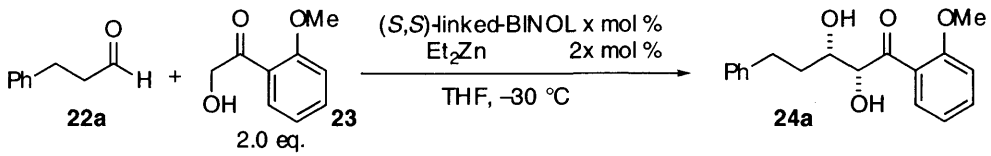

x = 1: linked-BINOL (1 mol %), Et_2Zn (2 mol %)

time (min)	5	10	15	20	30
yield (%)	2.9	4.5	5.5	7.1	9.7

f(x) = 2.691081E-1*x + 1.620270E+0
R^2 = 9.978689E-1

x = 3: linked-BINOL (3 mol %), Et_2Zn (6 mol %)

time (min)	5	10	15	20	30
yield (%)	8.9	13.5	16.4	21.3	28.7

f(x) = 7.885946E-1*x + 5.136486E+0
R^2 = 9.971096E-1

x =5: linked-BINOL (5 mol %), Et_2Zn (10 mol %)

time (min)	3	5	7	10	15	20	30
yield (%)	13.4	15.6	18.1	22.4	29.1	35.1	44.6

f(x) = 1.183913E+0*x + 1.024540E+1
R^2 = 9.938757E-1

x = 10: linked-BINOL (10 mol %), Et_2Zn (20 mol %)

time (min)	3	5	7	10	15	20
yield (%)	16.3	18.8	22.8	27.1	33.9	40.4

f(x) = 1.428942E+0*x + 1.226058E+1
R^2 = 9.969986E-1

x = 20: linked-BINOL (20 mol %), Et_2Zn (40 mol %)

time (min)	5	10	15	20	30
yield (%)	13.9	19.1	25.0	329	43.1

f(x) = 1.194800E+0*x + 7.689000E+0
R^2 = 9.950462E-1

x = 40: linked-BINOL (40 mol %), Et_2Zn (80 mol %)

time (min)	5	10	15	20	30
yield (%)	13.9	19.1	24.8	32.3	42.9

f(x) = 1.180318E+0*x + 7.727570E+0
R^2 = 9.967889E-1

x = 100: linked-BINOL (100 mol %), Et_2Zn (200 mol %)

time (min)	5	10	15	20	30
yield (%)	4.5	6.7	9.0	11.4	15.5

f(x) = 4.437649E-1*x + 2.298162E+0
R^2 = 9.991626E-1

As long as catalyst amount was less than x = 10 (linked-BINOL **10** = 10 mol %, Et_2Zn = 20 mol %), the higher amount of catalyst was used (x = 1, 3, 5 to 10), the faster reaction

rate was observed ($v_{x=1} = 8.97 \times 10^{-6} < v_{x=3} = 2.63 \times 10^{-5} < v_{x=5} = 3.95 \times 10^{-5} < v_{x=10} = 4.76 \times 10^{-5}$). In contrast, the reaction rate decreased by increasing x from 10, 20, 40, to 100 ($v_{x=10} = 4.76 \times 10^{-5} > v_{x=20} = 3.98 \times 10^{-5} > v_{x=40} = 3.93 \times 10^{-5} > v_{=100} = 1.48 \times 10^{-5}$ Ms^{-1}). This result was consistent with the observation in CSI-MS analysis. According to the CSI-MS spectra, excess ketone **23** compared to preformed complex **29** was required to form active catalyst linked-BINOL : Zn : ketone **23** = 3:7:4 complex. When the aldol reaction was performed with low catalyst loading (1-5 mol %), ketone **23** exists in sufficiently excess amount compared to the preformed complex **29**. **29** would be almost completely converted to linked-BINOL : Zn : ketone **23** = 3:7:4 complex. When, and first-order rate dependency was observed on linked-BINOL **10** concentration. On the other hand, more than 10 mol % of catalyst loading (based on linked-BINOL **10**) caused prevention of sufficient formation of **10**.

(S3-5)–B: Initial rate kinetics using the crystal 29 as a catalyst.

The crystals were prepared under argon atmosphere by the procedure described in section (S3-1). The solvent was removed from the glass tube and the crystal **29** was washed with dry THF (1.0 mL) x 4 times. After drying under reduced pressure, the crystal **29** was weighed in dry-box and was transferred into a test tube.

(a) [crystal 29 (1.5 mol %) with additional Et_2Zn (1.5 mol %) as a catalyst]

To the crystal **9** (7.0 mg, 0.0035 mmol) at 0℃ in a test tube under argon atmosphere, was added THF (0.5 mL), Et_2Zn (3.5 μL, 0.0035 mmol, 1.0 M in hexanes) and ketone **23** (77.4 mg, 0.466 mmol, in 0.665 mL THF). After the crystal dissolved completely, the mixture was cooled to –30℃. To the stirred solution of resulting mixture, was added **22a** (28.7 μL, 0.233 mmol) and the mixture was stirred at –30°C. Sampling and determination of chemical yields were carried out by the same procedure as described in section (S3-5)-A. Background reaction with free Et_2Zn is negligible, because only trace aldol adduct (<9%) was obtained by using as much as 10 mol % of Et_2Zn alone at –20 ℃ for 10 h.

(b) [crystal 29 alone (1.5 mol %) as a catalyst]

To the crystal **29** (7.0 mg, 0.0035 mmol) at 0℃ in a test tube under argon atmosphere, was added THF (0.5 mL) and ketone **23** (77.4 mg, 0.466 mmol, in 0.665 mL THF). After the crystal dissolved completely, the mixture was cooled to –30℃. To the stirred solution of resulting mixture, was added **22a** (28.7 μL, 0.233 mmol) and the mixture was stirred at –30℃. Sampling and determination of chemical yields were carried out by the same procedure as described in section (S3-5)-A.

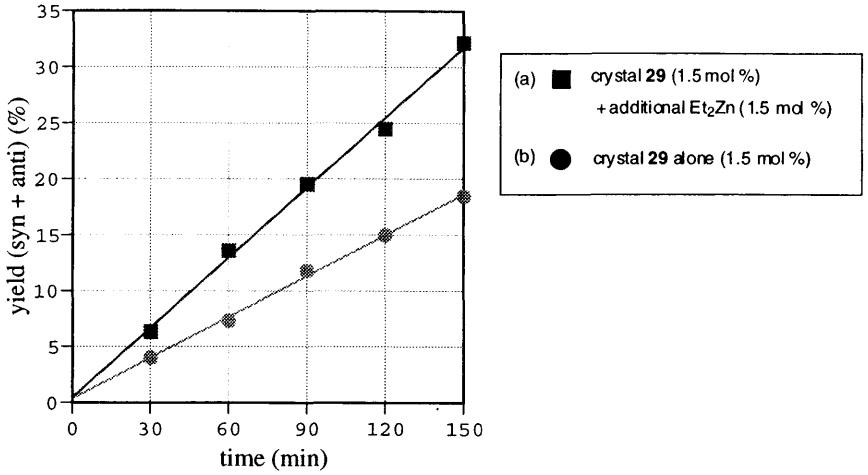

Figure (S3-5)-4. Reaction profile with (a) crystal **29** (1.5 mol %) + additional Et_2Zn (1.5 mol %)(b) crystal **29** alone (1.5 mol %)

Table (S3-5)-2. Numerical Data for Plots in Figure (S3-5)-4.

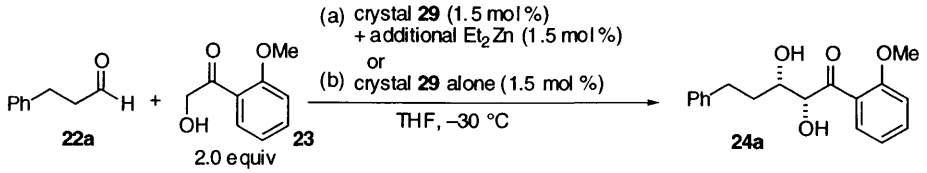

(a) [crystal **29** (1.5 mol %) + additional Et_2Zn (1.5 mol %)]

time (min)	30	60	90	120	150
yield (%)	6.3	13.6	19.5	24.5	32.1

f(x) = 2.084000E-1*x + 4.720000E-1
R^2 = 9.953906E-1

(b) [crystal **29** alone (1.5 mol %)]

time (min)	30	60	90	120	150
yield (%)	4.0	7.3	11.8	15.0	18.5

f(x) = 1.218333E-1*x + 3.610000E-1
R^2 = 9.970544E-1

(S3-5)-C: Initial rate kinetics on ketone 23 concentration.

Procedure for the aldol reaction with 0.4 M ketone 23 concentration.

To a stirred solution of (*S*,*S*)-linked-BINOL (19.74 mg, 6.7w/w% diethyl ether and hexane included, 0.03 mmol) in THF (0.9 mL) at –20 ℃, was added Et_2Zn (60 μL, 0.02 mmol, 1.0 M in hexanes). After stirring for 30 min at –20 °C, a solution of **23** (322.3 mg, 2.0 mmol) in THF (4.7 mL) was added. The resulting mixture was cooled to –30 ℃, and **22a** (1.0 mmol) was added. The reaction mixture was stirred at –30 ℃. Sampling and determination of chemical yields were carried out by the same procedure as described in section (S3-5)-(A).

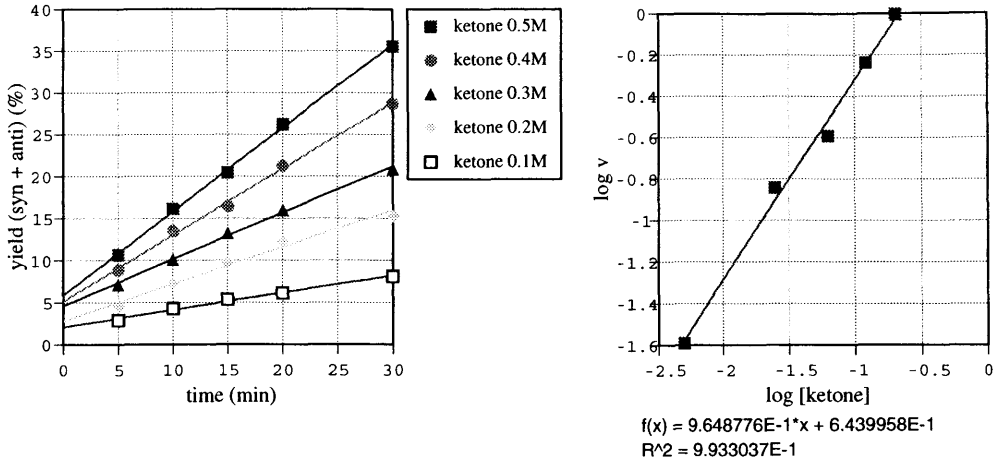

Figure (S3-5)-5. Reaction profile in various ketone concentration.

Table (S3-5)-3. Numerical Data for Plots in Figure (S3-5)-5.

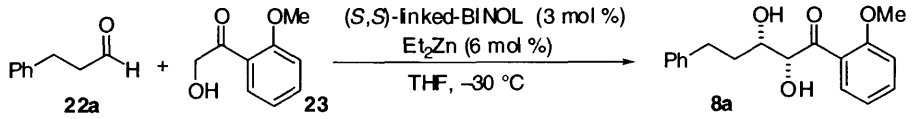

Ketone **23** 0.1M					
time (min)	5	10	15	20	30
yield (%)	2.9	4.3	5.3	6.1	8.1
			f(x) = 2.037297E-1*x + 2.084324E+0		
			R^2 = 9.922099E-1		
Ketone **23** 0.2M					
time (min)	5	10	15	20	30
yield (%)	4.5	7.4	9.8	12.3	15.3
			f(x) = 4.310811E-1*x + 2.942703E+0		
			R^2 = 9.794171E-1		
Ketone **23** 0.3M					
time (min)	5	10	15	20	30
yield (%)	7.1	10.1	13.2	16.0	20.9
			f(x) = 5.531351E-1*x + 4.617838E+0		
			R^2 = 9.968595E-1		
Ketone **23** 0.4M					
time (min)	5	10	15	20	30
yield (%)	8.9	13.5	16.4	21.3	28.7
			f(x) = 7.885946E-1*x + 5.136486E+0		
			R^2 = 9.971096E-1		
Ketone **23** 0.5M					
time (min)	5	10	15	20	30
yield (%)	13.9	19.1	24.8	32.3	42.6
			f(x) = 9.967838E-1*x + 5.859459E+0		
			R^2 = 9.986959E-1		

(S3-5)-D: Initial rate kinetics on aldehyde concentration.

Procedure for the aldol reaction with 0.2 M aldehyde 22a concentration.

To a stirred solution of (*S*,*S*)-linked-BINOL **10**(19.74 mg, 6.7w/w% diethyl ether and hexane included, 0.03 mmol) in THF (0.9 mL) at –20 ℃, was added Et,Zn (60 μL, 0.06 mmol, 1.0 M in hexanes). After stirring for 30 min at –20 °C, a solution of **23** (322.3 mg, 2.0 mmol) in THF (4.7 mL) was added. The resulting mixture was cooled to –30 ℃, and **22a** (1.0 mmol) was added. The reaction mixture was stirred at –30 ℃. Sampling and determination of chemical yields were carried out by the same procedure as described in section (S3-5)-A.

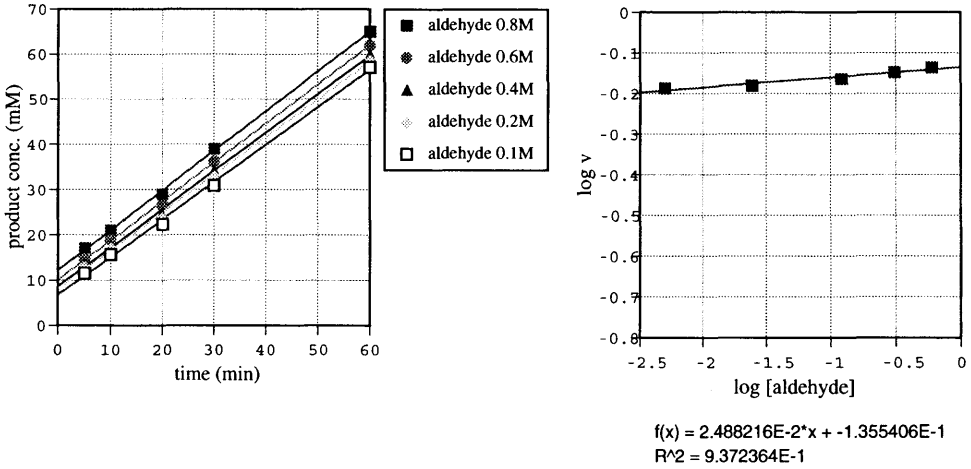

Figure (S3-5)-6. Reaction profile in various aldehyde **22a** concentration.

Table (S3-5)-4. Numerical Data for Plots in Figure (S3-5)-6.

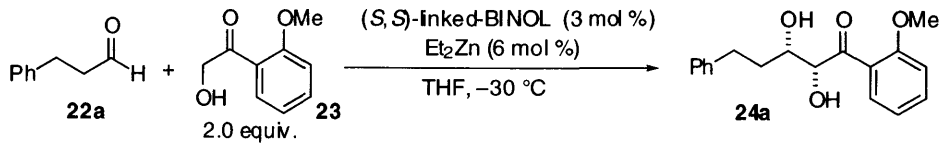

aldehyde **22a** 0.1M						
time (min)		5	10	20	30	60
product (mM)		11.54	15.68	22.3	30.9	57.1
						f(x) = 8.290789E-1*x + 6.783026E+0
						R^2 = 9.979334E-1
aldehyde **22a** 0.2M						
time (min)		5	10	20	30	60
product (mM)		13.0	17.1	23.8	33.0	58.8
						f(x) = 8.347105E-1*x + 8.256237E+0
						R^2 = 9.983519E-1
aldehyde **22a** 0.4M						
time (min)		5	10	20	30	60
product (mM)		13.4	13.8	24.6	34.1	59.9
						f(x) = 8.485789E-1*x + 8.697526E+0
						R^2 = 9.988500E-1
aldehyde **22a** 0.6M						
time (min)		5	10	20	30	60
product (mM)		14.8	18.9	26.7	36.2	62.0
						f(x) = 8.626316E-1*x + 1.015021E+1
						R^2 = 9.994864E-1
aldehyde **22a** 0.8M						
time (min)		5	10	20	30	60
product (mM)		17.1	21.0	29.0	39.0	65.0
						f(x) = 9.100000E-1*x + 1.190600E+1
						R^2 = 9.988273E-1

(S3-6) Optimization of the Direct Aldol Reaction with a New Et_2Zn/(*S*,*S*)-linked-BINOL = 4/1–MS 3A System

General Procedure for Catalytic Asymmetric Aldol Reaction of Ketone 23 Promoted by Et_2Zn/(*S*,*S*)-linked-BINOL = 4/1 with MS 3A System (For aldehyde 22a and 22b):

MS 3A (200 mg) in a test tube was activated prior to use under reduced pressure (ca. 0.7 kPa) at 160 ℃ for 3h. After cooling, a solution of (*S*,*S*)-linked-BINOL (1.6 mg, 4.1w/w% diethyl ether and hexane included, 0.0025 mmol) in THF (0.6 mL) was added under Ar. The mixture was cooled down to –20 ℃. To the mixture was added Et_2Zn (10

μL, 0.01 mmol, 1.0 M in hexanes) at –20 °C. After stirring for 10 min at –20 °C, a solution of **23** (182.8 mg, 1.1 mmol) in THF (1.1 mL) was added. Aldehyde **22a** (1.0 mmol) was added and stirred at –20 °C The stirring was continued for 18 h at –20 °C and quenched by addition of 1 M HCl (2 mL). The mixture was extracted with ethyl acetate and the combined organic layers were washed with *sat. aq* $NaHCO_3$, brine and dried over $MgSO_4$. Evaporation of solvent gave a crude mixture of the aldol products. The diastereomeric ratios of the aldol products were determined by ^1H NMR of the crude product. After purification by silica gel flash column chromatography (hexane/acetone 8/1–4/1), **24a** was obtained (269.6 mg, 0.898 mmol, y. 90%, dr: *syn/anti* = 89/11, 96% ee(*syn*)).
Spectra data were collected after conversion into acetonide.

(2*R*, 3*S*)-2,3-Dihydroxy-2,3-*O*-isopropylidene-1-(2-methoxyphenyl)-6-phenyl-1-pentanone (from *syn*-24a) :

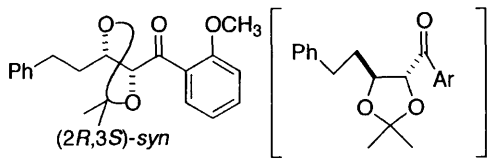

colorless oil; IR (neat) ν 2936, 1685, 1598, 1247 cm^{-1}; ^1H NMR ($CDCl_3$) δ 1.34 (s, 3H), 1.49 (s, 3H), 1.87-1.99 (m, 2H), 2.65 (ddd, *J* = 6.9, 9.8, 14.1Hz, 1H), 2.80 (ddd, *J* = 5.5, 10.0, 14.1 Hz, 1H), 3.82 (s, 3H), 4.21-4.23 (m, 1H), 4.95 (d, *J* = 6.7 Hz, 1H), 6.92 (brd, *J* = 8.3 Hz, 1H), 6.99 (ddd, *J* = 0.9, 7.5, 7.5 Hz, 1H), 7.10-7.12 (m, 2H), 7.14-7.17 (m, 1H), 7.22-7.25 (m, 2H), 7.42-7.48 (m, 2H); ^{13}C NMR ($CDCl_3$) δ 26.1, 27.5, 31.8, 35.6, 55.6, 77.7, 84.7, 110.3, 111.5, 120.8, 125.8, 127.5, 128.3, 128.3, 130.3, 133.3, 141.5, 157.8, 201.5; EI-MS *m/z* 340 [M^+], 135[$ArCO^+$]; $[\alpha]_D^{21}$ –39.4 (*c* 0.52, CH_2Cl_2) (92% ee); HPLC ((for diol) DAICEL CHIRALCEL OD, 2-propanol/hexane 20/80, flow 1.0 mL/min, detection at 254 nm) t_R 13.6 min (minor) and 15.9 min (major); HRMS (FAB) $[M+H]^+$ calcd for $C_{21}H_{25}O_4$, 341.1753; found, 341.1743. Ee was determined after cleavage of the acetonide. The absolute configuration of *syn*-**8a** was determined by HPLC analysis as shown in the scheme below. An authentic sample was prepared by using AD-mix-α.

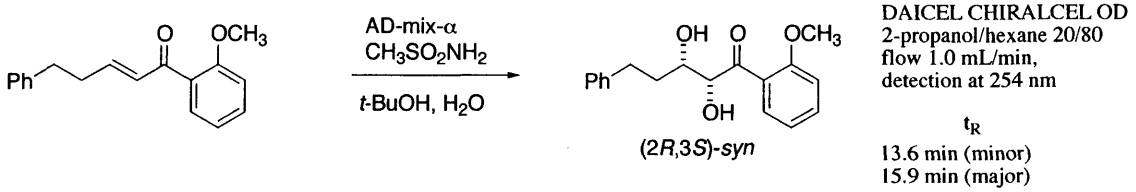

(2*R*, 3*S*)-3-Cyclohexyl-2,3-Dihydroxy-2,3-*O*-isopropylidene-1-(2-methoxyphenyl)-1-propanone (from *syn*-24b):

colorless oil; IR (neat) ν 2926, 1684, 1598, 1247 cm^{-1}; ^1H NMR ($CDCl_3$) δ 0.99-1.25 (m, 5H), 1.22 (s, 3H), 1.38 (s, 3H), 1.40-1.75 (m, 5H), 1.81-1.88 (m, 1H), 3.83 (s, 3H), 4.13 (dd, J = 6.4, 6.4 Hz, 1H), 4.94 (d, J = 6.4 Hz, 1H), 6.91 (brd, J = 8.5 Hz, 1H), 6.95 (ddd, J = 0.6, 7.6, 7.6 Hz, 1H), 7.40 (ddd, J = 1.5, 7.6, 8.5 Hz, 1H), 7.45 (dd, J = 1.5, 7.6 Hz, 1H) ; ^{13}C NMR ($CDCl_3$) δ 25.8, 25.8, 26.0, 26.3, 27.0, 28.1, 29.5, 40.9, 55.7, 82.1, 82.2, 109.9, 111.5, 120.6, 127.9, 130.1, 133.1, 157.9, 202.4; EI-MS *m/z* 318 [M^+], 135 [$ArCO^+$] ; $[\alpha]_D^{24}$ –28.6 (*c* 1.0, $CHCl_3$) (98% ee); HPLC (for diol) (DAICEL CHIRALCEL OD, 2-propanol/hexane 20/80, flow 1.0 mL/min, detection at 254 nm) t_R 6.5 min (minor) and 12.9 min (major); HRMS (FAB) $[M+H]^+$ calcd for $C_{19}H_{27}O_4$, 319.1904; found, 319.1908. Ee was determined after cleavage of the acetonide. The absolute configuration of *syn*-**24b** was determined by HPLC analysis as shown in the scheme below. An authentic sample was prepared by using AD-mix-α.

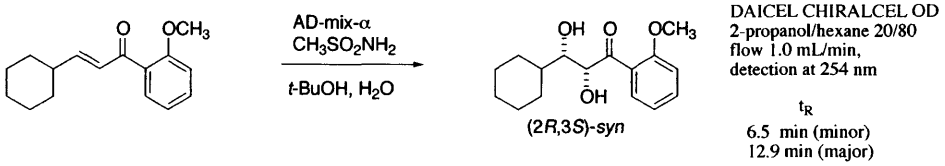

The general procedure was applied to aldehyde **22a** and **22b**. In the case of aldehyde **22c**, aldol adduct was directly converted into acetonide without aqueous work-up, because aldol adduct was unstable.

Procedure for aldehyde 22c:

MS3A (50 mg) in a test tube tube was activated prior to use under reduced pressure (ca. 0.7 kPa) at 160 °C for 3h. After cooling down to room temperature, argon gas was refilled to the test tube and a solution of (*S*,*S*)-linked-BINOL **10** (16.96 mg, 9.44 w/w% diethyl ether and hexane included, 0.025 mmol) in THF (0.4 mL) was charged. The resulting mixture was cooled to –20 °C, and was added Et_2Zn (100 μL, 0.1 mmol, 1.0M in hexanes). After stirring for 20 min at this temperature, a solution of **23** (166.2 mg, 1.0 mmol) in THF (2.1 mL) and **22c** (98.0 μL, 0.5 mmol) was added successively. The stirring was continued for 15 h at this temperature and was added $TsOH \cdot H_2O$ (0.2 mg) in dimethoxypropane (8.0 mL) to the reaction mixture and warmed up to room temperature. After stirring for 11 h at this temperature, quenched with saturated aqueous $NaHCO_3$. The mixture was extracted with ethyl acetate and was added 1M aqueous HCl (10 mL) to the

combined organic layers, then concentrated to half volume under reduced pressure (acetone and dimethoxypropane was removed). The resulting residue was washed with saturated aqueous $NaHCO_3$ and brine and dried over $MgSO_4$. Evaporation of solvent gave a crude mixture of aldol products. The resulting crude residue was purified by flash silica gel column chromatography (ethyl acetate/hexane = 1/15) to afford *syn*-**24c** (148.9 mg, y. 75%, 92% ee).

(2*R*, 3*S*)-5-Benzyloxy-2,3-dihydroxy-2,3-*O*-isopropylidene-4,4-dimethyl-1-(2-methoxyphenyl)-1-pentanone (*syn*-24c): 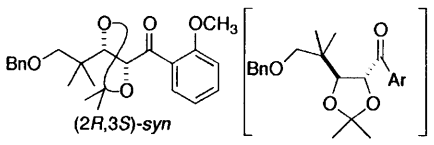

colorless oil; IR (neat) ν 1644, 1240, 1149, 1049 cm^{-1}; ^1H NMR ($CDCl_3$) δ 0.96 (s, 3H), 0.97 (s, 3H), 1.18 (s, 3H), 1.38 (s, 3H), 3.27 (s, 2H), 3.77 (s, 3H), 4.37 (s, 2H), 4.50 (d, J = 6.1 Hz, 1H), 5.18 (d, J = 6.1 Hz, 1H), 6.89 (d, J = 8.2 Hz, 1H), 6.94 (dd, J = 7.6, 7.6 Hz, 1H), 7.19-7.32 (m, 5H), 7.40 (ddd, J = 1.8, 7.6, 8.2 Hz, 1H), 7.50 (dd, J = 1.8, 7.6 Hz, 1H); ^{13}C NMR ($CDCl_3$) δ 20.1, 21.3, 25.5, 26.7, 37.1, 55.8, 73.1, 76.9, 79.9, 82.0, 109.4, 111.7, 120.5, 127.2, 127.3, 128.1, 130.4, 133.1, 138.8, 158.2, 202.5; ESI-MS *m/z* 421 $[M+Na]^+$; $[\alpha]_D^{25}$ –31.5 (*c* 1.4, $CHCl_3$) (92% ee); HPLC (DAICEL CHIRALCEL OD, 2-propanol/hexane 20/80, flow 1.0 mL/min, detection at 254 nm) t_R 5.2 min (minor) and 7.1 min (major); HRMS (FAB) $[M+H]^+$ calcd for $C_{24}H_{31}O_5$, 399.2165; found, 399.2160.

(S3-6) Optimization of the Direct Michael Reaction with a New Et_2Zn/(*S*,*S*)-linked-BINOL = 4/1–MS 3A System

General Procedure for Asymmetric Michael Reaction of 2-Hydroxy-2'-methoxyacetophenone (23) with Enones 25 Catalyzed by Et_2Zn/(*S*,*S*)-linked-BINOL 10 = 4/1 with MS 3A System:

Procedure with 0.02 mol % ligand loading (substrate/ligand = 5000):

MS3A (2.0 g) in a flask was dried at 160 ℃ under vacuum (0.7 KPa) for 3h. After cooling down to room temperature, argon gas was refilled to the flask and a solution of (*S*,*S*)-linked-BINOL **10** (1.5 mg, 0.0025 mmol) in THF (1.0 mL) was charged. The resulting mixture was cooled to –20 °C, and was added Et_2Zn (10 μL, 0.01 mmol, 1.0 M in hexanes). After stirring for 10 min at –20 ℃, and then a solution of ketone **23** (13.75 mmol) in THF (6.9 mL) was added. The mixture was warmed up to room temperature and **25a** (1.04 mL, 12.5 mmol) was added. The stirring was continued for 13 h at room temperature and quenched with aq. 1 M HCl. The mixture was extracted with ethyl acetate and the combined organic layers were washed with brine and dried over $MgSO_4$. The

solvent was evaporated and the residue was purified by flash silica gel column chromatography (acetone/hexane = 1/10–1/5) to afford **26** (2.66 g, 90% yield, 91% ee).

(S3-8) Construction of Chiral Tetrasubstituted Carbon Stereocenter:

General Procedure for Asymmetric Michael Reaction of *rac*-2-Hydroxy-2'-methoxypropiophenone (*rac*-27) with Vinyl Ketones (25) Catalyzed by Et_2Zn/(*S*,*S*)-linked-BINOL 10 = 4/1 with MS 3A:

MS3A (30 mg) in a test tube was dried at 160 ℃ under vacuum (0.7 KPa) with vigorous stirring for 3h. After cooling down to room temperature, argon gas was refilled to the test tube and a solution of (*S*,*S*)-linked-BINOL **10** (10.17 mg, 9.44 w/w% diethyl ether and hexane included, 0.015 mmol) in THF (0.4 mL) was charged. The resulting mixture was cooled to –20 ℃, and was added Et_2Zn (60 μL, 0.06 mmol, 1.0 M in hexanes). After stirring for 20 min at this temperature, a solution of **27** (270.3 mg, 1.5 mmol) in THF (0.46 mL) and **25a** (25 μl, 0.3 mmol) was added successively. The stirring was continued for 16 h at this temperature and quenched with saturated aqueous NH_4Cl. The mixture was extracted with ethyl acetate and the combined organic layers were washed with brine and dried over Na_2SO_4. The solvent was evaporated and the resulting crude residue was purified by flash silica gel column chromatography (acetone/hexane = 1/8) to afford **32a** (65.8 mg, 88% yield, 96% ee).

(2*R*)-2-Hydroxy-1-(2-methoxyphenyl)-2-methyl-1,5-hexanedione (32a):

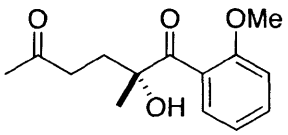

colorless solid; IR (KBr) ν 3510, 1685, 1600 cm^{-1}; ^1H NMR (C_6D_6) δ 1.38 (s, 3H), 1.64 (s, 3H), 2.00-2.06 (m, 1H), 2.27-2.39 (m, 3H), 3.11 (s, 3H), 4.09 (s, 1H), 6.34 (brd, *J* = 7.7 Hz, 1H), 6.69-6.73 (m, 1H), 6.98-7.02 (m, 1H), 7.23 (dd, *J* = 1.5, 7.7, 1H); ^{13}C NMR (C_6D_6) δ 25.4, 29.3, 33.5, 38.0, 54.9, 79.8, 111.4, 121.2, 128.9, 129.9, 131.5, 156.2, 206.9, 210.6; ESI-MS *m/z* 273 $[M+Na]^+$; HRMS (FAB) $[M+H]^+$ calcd for $C_{14}H_{19}O_4$, 251.1283; found, 251.1275; $[\alpha]_D^{29}$ +1.1 (*c* 0.81, $CHCl_3$) (91% ee); HPLC (TMS ether)(DAICEL CHIRALCEL OD, 2-propanol/hexane 1/99, flow 1.0 mL/min, detection at 254 nm) t_R 14.9 min (minor) and 17.6 min (major).

(2*R*)-2-Hydroxy-1-(2-methoxyphenyl)-5-(4-methoxyphenyl)-2-methyl-1,5-pentanedione (32b):

colorless oil; IR (neat) ν 3489, 1675, 1600 cm^{-1}; ^1H NMR (C_6D_6) δ 1.45 (s, 3H), 2.28 (ddd, *J* = 5.8, 9.8, 14.3 Hz, 1H), 2.55 (ddd, *J* = 5.2, 9.5, 14.3 Hz, 1H), 3.01 (ddd, *J* = 5.2, 9.8, 12.1 Hz, 1H), 3.09-3.17 (m, 1H), 3.13 (s, 3H), 3.22 (s, 1H), 4.31 (brs, 1H), 6.36 (d, *J* = 8.3 Hz, 1H), 6.62-6.65 (m, 2H), 6.72 (dd, *J* = 7.6, 7.6 Hz, 1H), 7.02 (ddd, *J* = 1.8, 7.6, 8.3 Hz, 1H), 7.23 (dd, *J* = 1.8, 7.6 Hz, 1H), 7.88-7.93 (m, 2H); ^{13}C NMR (C_6D_6) δ 25.6, 33.2, 34.2, 54.9, 55.1, 80.1, 111.3, 113.9, 121.0, 128.7, 129.9, 130.6, 130.6, 131.4, 156.3, 163.6, 198.0, 210.9; ESI-MS *m/z* 365 $[M+Na]^+$; HRMS (FAB) calcd for $C_{20}H_{23}O_5$ 343.1540 $[M+H]^+$, found 343.1535; $[\alpha]_D^{26}$ +6.2 (*c* 3.2, $CHCl_3$) (90% ee); HPLC (TMS ether) (DAICEL CHIRALCEL OD, 2-propanol/hexane 1/99, flow 1.0 mL/min, detection at 254 nm) t_R 30.2 min (minor) and 36.4 min (major).

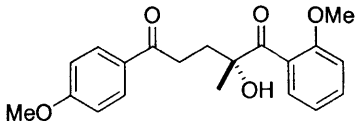

(2*R*)-2-Hydroxy-1-(2-methoxyphenyl)-2-methyl-5-phenyl-1,5-pentanedione (32c):

colorless oil; IR (neat) ν 3493, 1686, 1598, 1488 cm^{-1}; ^1H NMR (C_6D_6) δ 1.42 (s, 3H), 2.26 (ddd, *J* = 5.8, 9.8, 14.3 Hz, 1H), 2.52 (ddd, *J* = 5.0, 9.8, 14.3 Hz, 1H), 2.98 (ddd, *J* = 5.0, 9.8, 17.4 Hz, 1H), 3.06-3.13 (m, 1H), 3.08 (s, 3H), 4.15 (s, 1H), 6.33 (brd, *J* = 8.2 Hz, 1H), 6.70 (dd, *J* = 7.6, 7.6 Hz, 1H), 6.97-7.05 (m, 3H), 7.10-7.13 (m, 1H), 7.21 (dd, *J* = 1.5, 7.6 Hz, 1H), 7.84-7.86 (m, 2H); ^{13}C NMR (C_6D_6) δ 25.6, 33.4, 34.0, 55.1, 80.0, 111.4, 121.1, 128.3, 128.6, 128.7, 129.8, 131.3, 132.7, 137.5, 156.2, 199.2, 210.5; ESI-MS *m/z* 335 $[M+Na]^+$; $[\alpha]_D^{28}$ +2.9 (*c* 1.3, CH_2Cl_2) (93% ee); HPLC (TMS ether)(DAICEL CHIRALPAK AD, 2-propanol/hexane 1/99, flow 1.0 mL/min, detection at 254 nm) t_R 16.6 min (minor) and 23.9 min (major); HRMS (FAB) $[M+H]^+$ calcd for $C_{19}H_{21}O_4$, 313.1434; found, 314.1426.

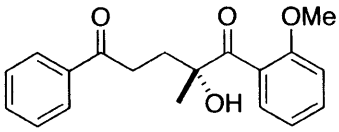

(2*R*)-2-Hydroxy-1,5-bis(2-methoxyphenyl)-2-methyl-1,5-pentanedione (32d):

colorless oil; IR (neat) ν 3491, 1674, 1598, 1486 cm^{-1}; ^1H NMR (C_6D_6) δ 1.46 (s, 3H), 2.32 (ddd, *J* = 5.8, 9.8, 15.1 Hz, 1H), 2.56 (ddd, *J* = 5.2, 9.5, 15.1 Hz, 1H), 3.14 (s, 3H), 3.17-3.35 (m, 2H), 3.23 (s, 3H), 4.17 (s, 1H), 6.39 (brd, *J* = 8.5 Hz, 1H), 6.44 (brd, *J* = 8.5 Hz, 1H), 6.72 (ddd, *J* = 0.9, 7.6, 7.6 Hz, 1H), 6.74 (ddd, *J* = 0.9, 7.6, 7.6 Hz, 1H), 7.03 (ddd, *J* = 0.9, 7.6, 8.5 Hz, 1H), 7.08 (ddd, *J* = 0.9, 7.6, 8.5 Hz, 1H), 7.24 (dd, *J* = 1.8, 7.6 Hz, 1H), 7.84 (dd, *J* = 1.8, 7.6 Hz, 1H); ^{13}C NMR (C_6D_6) δ 25.6, 34.4, 38.9, 55.0, 55.1, 80.1, 111.4, 111.8,

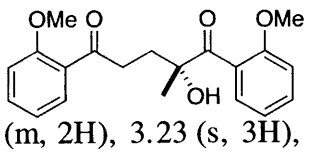

120.8, 121.0, 128.7, 129.1, 130.1, 130.7, 131.3, 133.2, 156.3, 158.3, 201.5, 211.0; ESI-MS *m/z* 365 $[M+Na]^+$; $[\alpha]_D^{28}$ +8.2 (*c* 1.8, CH_2Cl_2) (91% ee); HPLC (TMS ether)(DAICEL CHIRALCEL OD–H, 2-propanol/hexane 1/99, flow 1.0 mL/min, detection at 254 nm) t_R 19.9 min (major) and 22.5 min (minor); HRMS (FAB) $[M+H]^+$ calcd for $C_{20}H_{23}O_5$, 343.1540; found, 343.1545.

(2*R*)-2-Hydroxy-1-(2-methoxyphenyl)-2-methyl-5-(4-bromophenyl)-1,5-pentanedione (32e):

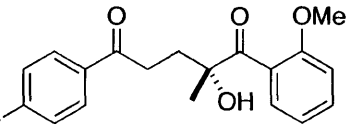

colorless oil; IR (neat) ν 3487, 1685, 1585, 1487 cm^{-1}; ^1H NMR (C_6D_6) δ 1.41 (s, 3H), 2.21 (ddd, *J* = 5.5, 9.5, 15.1 Hz, 1H), 2.47 (ddd, *J* = 5.5, 9.8, 15.1 Hz, 1H), 2.83 (ddd, *J* = 5.5, 9.8, 17.4 Hz, 1H), 2.95 (ddd, *J* = 5.5, 9.5, 17.4 Hz, 1H), 3.07(s, 3H), 4.11 (s, 1H), 6.32 (brd, *J* = 8.3 Hz, 1H), 6.71 (ddd, *J* = 0.9, 7.4 7.4 Hz, 1H), 6.99 (ddd, *J* = 1.8, 7.4, 8.3 Hz, 1H), 7.13-7.17 (m, 2H), 7.21 (dd, *J* = 1.8, 7.4 Hz, 1H), 7.46-7.49 (m, 2H); ^{13}C NMR (C_6D_6) δ 25.6, 33.3, 33.9, 55.1, 79.9, 111.4, 121.1, 128.3, 128.8, 129.7, 129.8, 131.5, 131.9, 136.1, 156.2, 198.1, 210.3; ESI-MS *m/z* 413, 415 $[M+Na]^+$; $[\alpha]_D^{28}$ –3.4 (*c* 0.82, CH_2Cl_2) (93% ee); HPLC (TMS ether)(DAICEL CHIRALCEL OD, 2-propanol/hexane 1/99, flow 1.0 mL/min, detection at 254 nm) t_R 18.8 min (minor) and 25.3 min (major); HRMS (FAB) $[M+H]^+$ calcd for $C_{19}H_{20}O_4Br$, 391.0540; found, 391.0537.

(2*R*)-2-Hydroxy-1-(2-methoxyphenyl)-2-methyl-1,5-heptanedione (32f):

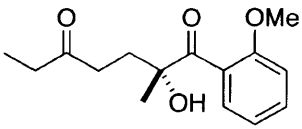

colorless oil; IR (neat) ν 3491, 1704, 1599, 1488 cm^{-1}; ^1H NMR (C_6D_6) δ 0.89 (t, *J* = 7.3 Hz, 3H), 1.39 (s, 3H), 2.03-2.10 (m, 1H), 2.27-2.41 (m, 3H), 3.11 (s, 3H), 4.05 (s, 1H), 6.33 (brd, *J* = 8.2 Hz, 1H), 6.71 (dd, *J* = 7.3, 7.6 Hz, 1H), 6.99 (ddd, *J* = 1.8, 7.6, 8.2 Hz, 1H), 7.24 (dd, *J* = 1.8, 7.3, 1H); ^{13}C NMR (C_6D_6) δ 7.92, 25.4, 33.5, 35.7, 36.7, 55.0, 79.8, 111.4, 121.1, 128.9, 129.9, 131.4, 156.2, 209.5, 210.6; ESI-MS *m/z* 287 $[M+Na]^+$; $[\alpha]_D^{29}$ +1.4 (*c* 2.3, CH_2Cl_2) (91% ee); HPLC (TMS ether)(DAICEL CHIRALCEL OD, 2-propanol/hexane 1/99, flow 1.0 mL/min, detection at 254 nm) t_R 13.0 min (minor) and 15.7 min (major); HRMS (FAB) $[M+H]^+$ calcd for $C_{15}H_{21}O_4$, 265.1434; found, 265.1440.

Reaction Profiles of 1,4-Addition Reaction with Optically Active Ketone

(*S*)-27 (99% ee) Catalyzed by (a) Et_2Zn/(*R*,*R*)-linked-BINOL and (b) Et_2Zn/(*S*,*S*)-linked-BINOL.

Optically active ketone 27 was obtained by the following procedure.

MS3A (400 mg) in a test tube was dried at 160 ℃ under vacuum with vigorous stirring for 3h. After cooling down to room temperature, argon gas was refilled to the test tube and a solution of (*R*,*R*)-linked-BINOL **10** (136.4 mg, 9.1 w/w% diethyl ether and hexane included, 0.2 mmol) in THF (3.0 mL) was charged. The resulting mixture was cooled to –20 ℃, and was added Et_2Zn (60 μL, 0.06 mmol, 1.0M in hexanes). After stirring for 20 min at this temperature, a solution of racemic **27** (1500 mg, 8.3 mmol) in THF (2.54 mL) and hydrocinnamaldehyde (526.7 μl, 4 mmol) was added successively. The stirring was continued for 24 h at this temperature and quenched with saturated aqueous NH_4Cl. The mixture was extracted with ethyl acetate and the combined organic layers were washed with brine and dried over Na_2SO_4. Evaporation of solvent gave a crude mixture and the remaining ketone **27** was isolated by flash silica gel column chromatography (acetone/hexane = 1/8) and successively conducted for asymmetric aldol reaction just described above. After repeating asymmetric aldol reaction for four times, optically pure **27** (572 mg, 99.3% ee, HPLC analysis: DAICEL CHIRALCEL OD, 2-isopropanol/hexane = 1/9, flow 1.0 mL/min, detection at 254 nm, t_R 7.4 min (major) and 10.2 min (minor)) was obtained.

Procedure for Michael reaction with optically active (*S*)-27 using (*S*,*S*)-linked-BINOL 10:

MS3A (30 mg) in a test tube was dried at 160 ℃ under vacuum (0.7 KPa) with vigorous stirring for 3h. After cooling down to room temperature, argon gas was refilled to the test tube and a solution of (*S*,*S*)-linked-BINOL **10** (10.17 mg, 9.44 w/w% diethyl ether and hexane included, 0.015 mmol) in THF (0.4 mL) was charged. The resulting mixture was cooled to –20 ℃, and was added Et_2Zn (60 μL, 0.06 mmol, 1.0M in hexanes). After stirring for 20 min at this temperature, a solution of (*S*)-**27** (135.2 mg, 0.75 mmol, 99.3% ee) in THF (0.46 mL) and **25a** (25 μl, 0.3 mmol) was added successively. Samples were taken at recorded times according to the following procedure: 0.05 mL of the reaction mixture was taken with a syringe filled with 0.1 mL of saturated aqueous NH_4Cl solution and was immediately poured onto saturated aqueous NH_4Cl (1.0 mL). The resulting mixture was extracted with ether. After evaporating solvents, the crude residue was analyzed by ^1H NMR (C_6D_6). Yields of the products **32a** were measured by comparison of integrated area of methyl proton at C-2 position of **32a** (singlet, 1.38 ppm) and methyl

proton at C-2 position of the **27** (doublet, 1.29 ppm).

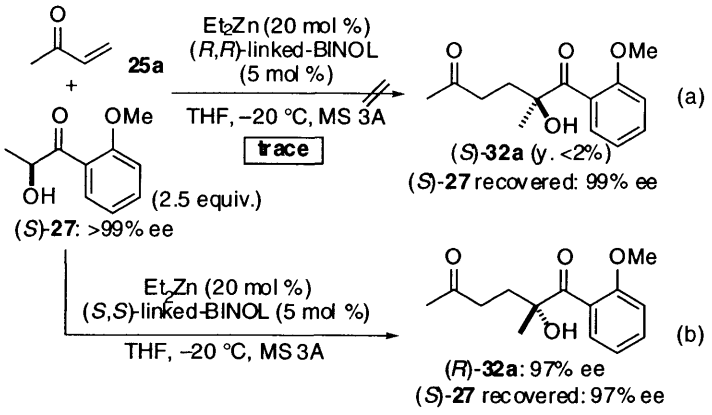

<reaction profile>

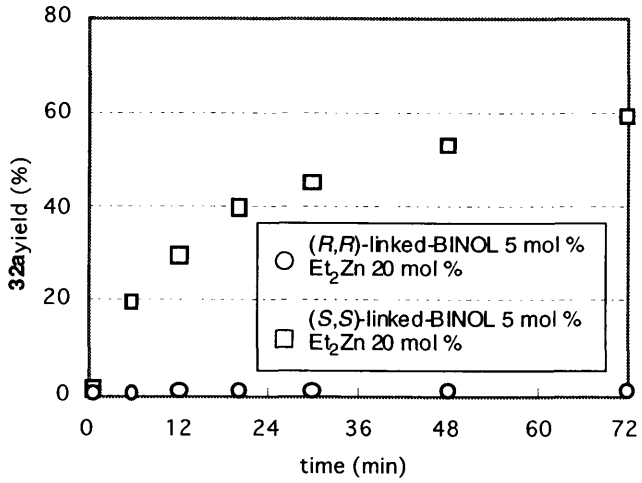

Figure (S3-8)-1. Reaction profiles of 1,4-addition reaction with optically active ketone (*S*)-**27** (99% ee) catalyzed by (a) Et2Zn/(*R*,*R*)-linked-BINOL and (b) Et2Zn/(*S*,*S*)-linked-BINOL.

Table (S3-8)-1. Numerical Data for Plots in Figure (S3-8)-1.

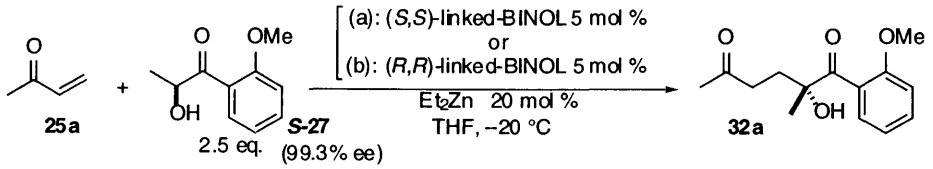

(a): (*S*,*S*)-linked-BINOL (5 mol %), Et_2Zn (20 mol %)

time (h)	1	6	12	20	30	48	72
yield (%)	1.46	19.67	29.32	39.56	45.04	53.24	59.1

(b): (*R*,*R*)-linked-BINOL (5 mol %), Et_2Zn (20 mol %)

time (h)	1	6	12	20	30	48	72
yield (%)	0.63	0.78	1.15	1.13	1.13	1.09	1.27

General Procedure for Catalytic Asymmetric Aldol Reaction of Ketone *rac*-27 Promoted by Et_2Zn/(*S*,*S*)-linked-BINOL 10 = 4/1 with MS 3A System:

MS 3A (30 mg) in a test tube was activated prior to use under reduced pressure (ca. 0.7 kPa) at 160 °C for 3h. After cooling, a solution of (*S*,*S*)-linked-BINOL (9.6 mg, 4.1w/w% diethyl ether and hexane included, 0.015 mmol) in THF (0.2 mL) was added under Ar. The mixture was cooled down to –20 °C. To the mixture was added Et_2Zn (60 μL, 0.06 mmol, 1.0 M in hexanes) at –20 °C. After stirring for 10 min at –20 °C, a solution of *rac*-**27** (270.3 mg, 1.5 mmol) in THF (0.24 mL) was added. After 5 min at – 20 °C, aldehyde **22a** (40 μL, 0.304 mmol) was added and stirred at –20 °C The stirring was continued for 16 h at –20 °C and quenched by addition of 1 M HCl (2 mL). The mixture was extracted with ethyl acetate and the combined organic layers were washed with *sat. aq* $NaHCO_3$, brine and dried over $MgSO_4$. Evaporation of solvent gave a crude mixture of the aldol products. The diastereomeric ratios of the aldol products were determined by ^1H NMR of the diastereomixture. After purification by silica gel flash column chromatography (hexane/acetone 8/1–4/1), **28a** was obtained (92.5 mg, 0.294 mmol, y. 97%, dr: *syn*/*anti* = 62/38, 87% ee(*syn*), 95% ee(*anti*)). Ee was determined by chiral HPLC analysis.

(2*R*, 3*S*)-2,3-dihydroxy-1-(2-methoxyphenyl)-2-methyl-5-phenyl-1-pentanone (*syn*-28a)

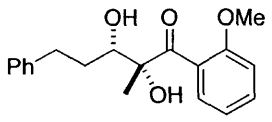

colorless oil; IR (neat) ν 3474, 1699, 1599 cm^{-1}; ^1H NMR (C_6D_6) δ 1.26 (s, 3H), 1.81-1.94 (m, 2H), 2.35 (brd, *J* = 8.8 Hz, 1H), 2.58 (ddd, *J* = 7.3, 9.1, 13.7 Hz, 1H), 2.92 (ddd, *J* = 4.8, 9.4, 13.7 Hz, 1H), 3.08 (s, 3H), 3.93-4.00 (m, 1H), 4.20 (s, 1H), 6.36 (brd, *J* = 8.3 Hz, 1H), 6.73 (dd, *J* = 7.4, 7.4 Hz, 1H), 6.96-7.07 (m, 2H), 7.11-7.16 (m, 4H), 7.47 (dd, *J* = 1.5, 7.3 Hz, 1H); ^{13}C NMR (C_6D_6) δ 14.2, 21.4, 32.5, 32.9, 55.2, 60.1, 74.4, 83.1, 111.4, 121.1, 126.1, 128.6, 128.7, 128.9, 129.7, 131.2, 142.7, 156.2, 170.2, 210.0; ESI-MS *m/z* 337 $[M+Na]^+$; HRMS (FAB) $[M+H]^+$ calcd for $C_{19}H_{23}O_4$, 315.1596; found, 315.1595; $[\alpha]_D^{28}$ –24.3 (*c* 1.4, CH_2Cl_2) (74% ee); HPLC (DAICEL CHIRALPAK AD, 2-propanol/hexane 20/80, flow 1.0 mL/min, detection at 254 nm) t_R 11.1 min (major) and 12.4 min (minor).

(2*R*, 3*R*)-2,3-dihydroxy-1-(2-methoxyphenyl)-2-methyl-5-phenyl-1-pentanone (*anti*-28a)

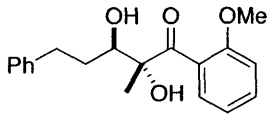

colorless solid; IR (KBr) ν 3490, 1672 cm^{-1}; ^1H NMR (C_6D_6)

δ 1.52 (s, 3H), 1.87-1.93 (m, 2H), 2.35 (brs, 1H), 2.73 (ddd, *J* = 8.3, 8.3, 13.7 Hz, 1H), 2.93 (s, 3H), 2.88-2.96 (m, 1H), 3.90-3.97 (m, 1H), 3.99 (brs, 1H), 6.26 (brd, *J* = 8.3 Hz, 1H), 6.65 (dd, *J* = 7.4, 7.4 Hz, 1H), 6.93-6.98 (m, 1H), 7.02-7.07 (m, 1H), 7.11-7.20 (m, 5H); ^{13}C NMR (C_6D_6) δ 22.3, 32.8, 34.1, 55.1, 75.2, 83.0, 111.4, 121.5, 126.0, 128.7, 129.1, 129.4, 131.7, 142.7, 156.2, 210.0; ESI-MS *m/z* 337 $[M+Na]^+$; $[\alpha]_D^{29}$ +9.1 (*c* 0.88, CH_2Cl_2) (85% ee); HPLC (DAICEL CHIRALPAK AD, 2-propanol/hexane 20/80, flow 1.0 mL/min, detection at 254 nm) t_R 10.4 min (minor) and 13.2 min (major); HRMS (FAB) $[M+H]^+$ calcd for $C_{19}H_{23}O_4$, 315.1596; found, 315.1591.

(2*R*, 3*S*)-2,3-dihydroxy-1-(2-methoxyphenyl)-2-methyl-6-phenyl-1-hexanone (*syn*-28d)

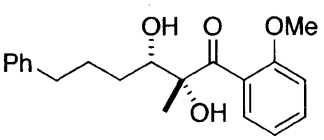

colorless oil; IR (neat) ν 3475, 1699, 1599 cm^{-1}; ^{1}H NMR (C_6D_6) δ 1.28 (s, 3H), 1.50-1.59 (m, 3H), 1.88-1.94 (m, 1H), 1.97 (d, *J* = 9.5 Hz, 1H), 2.45-2.52 (m, 2H), 3.07 (s, 3H), 3.90-3.95 (m, 1H), 4.12 (s, 1H), 6.36 (brd, *J* = 8.2 Hz, 1H), 6.73 (ddd, *J* = 0.9, 7.6, 7.6 Hz, 1H), 6.99 (ddd, *J* = 1.6, 7.6, 8.2 Hz, 1H), 7.04-7.08 (m, 3H), 7.14-7.18 (m, 2H), 7.50 (dd, *J* = 1.6, 7.6 Hz, 1H); ^{13}C NMR (C_6D_6) δ 21.5, 28.0, 30.4, 36.1, 55.2, 74.9, 83.0, 111.4, 121.1, 126.0, 128.5, 128.6, 128.7, 129.7, 131.0, 142.7, 156.1, 209.9; ESI-MS *m/z* 351 $[M+Na]^+$; HRMS (FAB) $[M+H]^+$ calcd for $C_{20}H_{25}O_4$, 329.1753; found, 329.1750; $[\alpha]_D^{29}$ +8.7 (*c* 0.85, CH_2Cl_2) (78% ee); HPLC (DAICEL CHIRALPAK AD, 2-propanol/hexane 20/80, flow 1.0 mL/min, detection at 254 nm) t_R 9.2 min (minor) and 11.9 min (major).

(2*R*, 3*R*)-2,3-dihydroxy-1-(2-methoxyphenyl)-2-methyl-6-phenyl-1-hexanone (*anti*-28d)

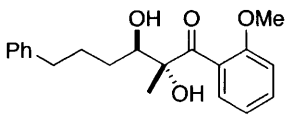

colorless oil; IR (neat) ν 3457, 1683, 1599 cm^{-1}; ^{1}H NMR (C_6D_6) δ 1.56 (s, 3H), 1.58-1.64 (m, 2H), 1.64-1.75 (m, 1H), 1.95-2.03 (m, 1H), 2.18 (brd, *J* = 8.0 Hz, 1H), 2.48-2.58 (m, 2H), 2.96 (s, 3H), 3.88 (s, 1H), 3.93 (ddd, *J* = 3.4, 8.0, 8.6 Hz, 1H), 6.28 (brd, *J* = 8.2 Hz, 1H), 6.71 (ddd, *J* = 0.6, 7.2, 7.3 Hz, 1H), 6.97 (ddd, *J* = 1.5, 7.2, 8.2 Hz, 1H), 7.04-7.08 (m, 3H), 7.13-7.17 (m, 2H), 7.24 (dd, *J* = 1.5, 7.3 Hz, 1H); ^{13}C NMR (C_6D_6) δ 22.5, 28.6, 31.8, 36.0, 55.1, 76.5, 83.0, 111.3, 121.5, 125.9, 128.6, 128.8, 129.5, 130.6, 131.6, 142.8, 156.1, 210.5; ESI-MS *m/z* 351 $[M+Na]^+$; HRMS (FAB) $[M+H]^+$ calcd for $C_{20}H_{25}O_4$, 329.1753; found, 329.1756; $[\alpha]_D^{29}$ –2.0 (*c* 0.49, CH_2Cl_2) (90% ee);

HPLC (DAICEL CHIRALPAK AD–H, 2-propanol/hexane 20/80, flow 0.8 mL/min, detection at 254 nm) t_R 12.5 min (major) and 14.2 min (minor).

(2*R*, 3*S*)-2,3-dihydroxy-1-(2-methoxyphenyl)-2-methyl-1-penanone (*syn*-28e)

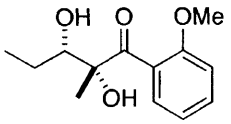

colorless oil; IR (neat) ν 3465, 1687, 1599 cm^{-1}; ^1H NMR (C_6D_6) δ 0.95 (t, J = 7.5 Hz, 3H), 1.30 (s, 3H), 1.44-1.56 (m, 2H), 1.98 (d, J = 9.5 Hz, 1H), 3.08 (s, 3H), 3.81 (ddd, J = 3.5, 9.5, 9.5 Hz, 1H), 4.12 (s, 1H), 6.37 (brd, J = 8.6 Hz, 1H), 6.73 (ddd, J = 0.6, 7.6, 7.6 Hz, 1H), 7.00 (ddd, J = 1.8, 7.6, 8.6 Hz, 1H), 7.51 (dd, J = 1.8, 7.6 Hz, 1H); ^{13}C NMR (C_6D_6) δ 10.6, 21.5, 23.8, 55.2, 76.5, 83.0, 111.4, 121.1, 128.5, 129.8, 131.0, 156.2, 210.0; ESI-MS *m/z* 261 $[M+Na]^+$; HRMS (FAB)(for carbonate) $[M+H]^+$ calcd for $C_{21}H_{25}O_5$, 265.1076; found, 265.1084; $[\alpha]_D^{29}$ +3.6 (*c* 0.56, CH_2Cl_2) (68% ee); HPLC (DAICEL CHIRALPAK AD, 2-propanol/hexane 20/80, flow 1.0 mL/min, detection at 254 nm) t_R xx 7.6 (minor) and 9.7 min (major).

(2*R*, 3*R*)-2,3-dihydroxy-1-(2-methoxyphenyl)-2-methyl-1-penanone (*anti*-28e)

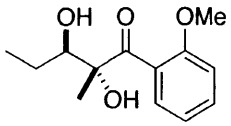

colorless oil; IR (neat) ν 3465, 1698, 1599 cm^{-1}; ^1H NMR (C_6D_6) δ 1.05 (t, J = 7.5 Hz, 3H), 1.51-1.67 (m, 2H), 1.55 (s, 3H), 2.16 (d, J = 7.9 Hz, 1H), 2.99 (s, 3H), 3.77-3.81 (m, 1H), 3.87 (s, 1H), 6.29 (brd, J = 8.6 Hz, 1H), 6.70 (ddd, J = 0.9, 7.4, 7.4 Hz, 1H), 6.97 (ddd, J = 1.8, 7.4, 8.2 Hz, 1H), 7.28 (dd, J = 1.8, 7.4 Hz, 1H); ^{13}C NMR (C_6D_6) δ 11.3, 22.5, 25.3, 55.1, 78.2, 83.0, 111.4, 121.5, 129.4, 130.6, 131.5, 156.1, 210.4; ESI-MS *m/z* 261 $[M+Na]^+$; HRMS (FAB)(for carbonate) $[M+H]^+$ calcd for $C_{21}H_{25}O_5$, 265.1076; found, 265.1077; $[\alpha]_D^{29}$ +4.4 (*c* 0.39, CH_2Cl_2) (86% ee); HPLC (DAICEL CHIRALPAK AD, 2-propanol/hexane 20/80, flow 1.0 mL/min, detection at 254 nm) t_R 6.7 min (major) and 8.0 min (minor).

(2*R*, 3*S*)-2,3-Carbonyldioxy-1-(2-methoxyphenyl)-2,5-dimethyl-1-hexanone (from *syn*-28f)

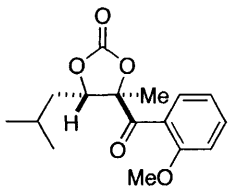

colorless oil; IR (neat) ν 1810, 1687, 1599 cm^{-1}; ^1H NMR ($CDCl_3$) δ 0.98 (d, J = 6.4 Hz, 3H), 1.01 (d, J = 6.4 Hz, 3H), 1.47-1.53 (m, 1H), 1.57 (s, 3H), 1.69-1.77 (m, 1H), 1.85-1.93 (m, 1H), 3.86 (s, 3H), 4.89 (dd, J = 2.8, 11.0 Hz, 1H), 6.94 (brd, J = 8.6 Hz, 1H), 7.01 (dd, J = 7.6, 7.6 Hz, 1H), 7.27 (dd,

J = 1.5, 7.6 Hz, 1H), 7.46 (ddd, J = 1.5, 7.6, 8.6 Hz, 1H); ^{13}C NMR ($CDCl_3$) δ 18.7, 21.5, 23.3, 25.1, 38.4, 55.6, 79.5, 88.3, 111.1 121.1, 126.9, 129.2, 133.3, 153.7, 157.1, 210.4; ESI-MS *m/z* 315 $[M+Na]^+$; $[\alpha]_D^{28}$ –4.4 (*c* 0.49, $CHCl_3$) (72% ee); HPLC (for diol)(DAICEL CHIRALPAK AD, 2-propanol/hexane 20/80, flow 0.6 mL/min, detection at 254 nm) t_R 12.6 min (major) and 14.4 min (minor); HRMS (FAB) $[M+H]^+$ calcd for $C_{16}H_{21}O_5$, 293.1384; found, 293.1381..

(2*R*, 3*R*)-2,3-Carbonyldioxy-1-(2-methoxyphenyl)-2,5-dimethyl-1-hexanone (from *anti*-28f)

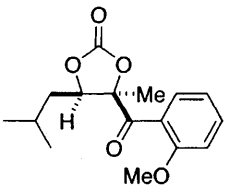

colorless oil; IR (neat) ν 1809, 1692, 1599 cm^{-1}; ^{1}H NMR ($CDCl_3$) δ 0.95 (d, J = 6.5 Hz, 3H), 0.96 (d, J = 6.8 Hz, 3H), 1.51-1.56 (m, 1H), 1.59-1.67 (m, 1H), 1.69 (s, 3H), 1.82-1.92 (m, 1H), 3.83 (s, 3H), 4.54 (dd, J = 2.8, 11.3 Hz, 1H), 6.91 (brd, J = 8.3 Hz, 1H), 7.00 (ddd, J = 0.6, 7.6, 7.6 Hz, 1H), 7.23 (dd, J = 1.8, 7.6 Hz, 1H), 7.45 (ddd, J = 1.8, 7.6, 8.3 Hz, 1H); ^{13}C NMR ($CDCl_3$) δ 21.3, 23.4, 25.2, 25.6, 39.4, 55.1, 84.3, 88.9, 110.8 121.1, 127.0, 129.2, 133.4, 153.5, 155.7, 202.6; ESI-MS *m/z* 315 $[M+Na]^+$; $[\alpha]_D^{28}$ +64.9 (*c* 0.59, $CHCl_3$) (87% ee); HPLC (for diol) (DAICEL CHIRALPAK AD, 2-propanol/hexane 20/80, flow 0.6 mL/min, detection at 254 nm) t_R 11.7 min (minor) and 13.4 min (major); HRMS (FAB) $[M+H]^+$ calcd for $C_{16}H_{20}O_5$, 293.1384; found, 293.1387.

(2*R*, 3*S*)-2,3-dihydroxy-5-(4-methoxy-benzyloxy)-1-(2-methoxyphenyl)-2-methyl-1-penanone (*syn*-28g)

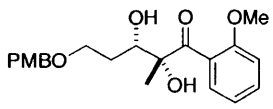

colorless oil; IR (neat) ν 3472, 1700, 1599 cm^{-1}; ^{1}H NMR (C_6D_6) δ 1.35 (s, 3H), 1.72-1.78 (m, 1H), 1.85-1.93 (m, 1H), 3.11 (s, 3H), 3.16 (d, J = 5.8 Hz, 1H), 3.29 (s, 3H), 3.40 (ddd, J = 4.6, 6.7, 9.2 Hz, 1H), 3.51 (ddd, J = 4.6, 6.7, 9.2 Hz, 1H), 4.10 (s, 1H), 4.20 (d, J = 11.5 Hz, 1H), 4.21 (d, J = 11.5 Hz, 1H), 4.23 (ddd, J = 2.5, 5.8, 10.1 Hz, 1H), 6.38 (d, J = 8.3 Hz, 1H), 6.72-6.78 (m, 3H), 6.98-7.02 (m, 1H), 7.10-7.15 (m, 2H), 7.61 (dd, J = 1.7, 7.3 Hz, 1H); ^{13}C NMR (C_6D_6) δ 21.3, 30.6, 54.8, 55.2, 68.4, 73.0, 74.6, 82.7, 111.3, 114.2, 120.9, 128.4, 128.4, 129.5, 130.2, 130.7, 156.4, 159.8, 210.2; ESI-MS *m/z* 397 $[M+Na]^+$; $[\alpha]_D^{25}$ +5.4 (*c* 0.88, $CHCl_3$) (86% ee); HPLC (DAICEL CHIRALPAK AD, 2-propanol/hexane 20/80, flow 1.0 mL/min, detection at 254 nm) t_R 18.5 min (minor) and 23.5 min (major); HRMS (FAB) $[M+H]^+$ calcd for $C_{21}H_{27}O_6$, 507.0778; found, 507.0775.

(2*R*, 3*R*)-2,3-dihydroxy-5-(4-methoxy-benzyloxy)-1-(2-methoxyphenyl)-2-methyl-1-penanone (*anti*-28g)

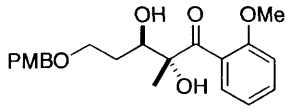

colorless oil; IR (neat) ν 3472, 1694, 1599 cm^{-1}; ^1H NMR (C_6D_6) δ 1.62 (s, 3H), 1.85-1.93 (m, 2H), 2.96 (brd, *J* = 3.6 Hz, 1H). 3.06 (s, 3H), 3.30 (s, 3H), 3.46 (ddd, *J* = 4.9, 6.4, 9.2 Hz, 1H), 3.60 (ddd, *J* = 4.6, 7.3, 9.2 Hz, 1H), 3.95 (s, 1H), 4.23 (s, 2H), 4.25-4.30 (m, 1H), 6.32 (brd, *J* = 8.3 Hz, 1H), 6.69-6.72 (m, 1H), 6.73-6.80 (m, 2H), 6.96-7.00 (m, 1H), 7.15-7.13 (m, 2H), 7.41 (dd, *J* = 1.5, 7.6 Hz, 1H); ^{13}C NMR (C_6D_6) δ 22.3, 32.3, 54.8, 55.2, 68.4, 73.0, 75.1, 82.7, 111.4, 114.2, 121.2, 129.0, 129.5, 130.9, 131.3, 156.3, 159.3, 210.4; ESI-MS *m/z* 397 $[M+Na]^+$; HRMS (FAB)(for carbonate) $[M+H]^+$ calcd for $C_{22}H_{25}O_7$, 401.1600; found, 401.1603; $[\alpha]_D^{25}$ –5.2 (*c* 0.54, $CHCl_3$)(95% ee); HPLC (DAICEL CHIRALCEL OJ, 2-propanol/hexane 20/80, flow 1.0 mL/min, detection at 254 nm) t_R 31.5 min (major) and 39.0 min (minor).

(2*R*, 3*S*)-5-benzyloxymethoxy-2,3-dihydroxy-1-(2-methoxyphenyl)-2-methyl-1-penanone (*syn*-28h)

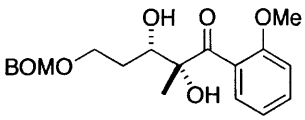

colorless oil; IR (neat) ν 3468, 2938, 1700, 1598 cm^{-1}; ^1H NMR (C_6D_6) δ 1.37 (s, 3H), 1.79-1.83 (m, 2H), 2.82 (d, *J* = 7.6 Hz, 1H), 3.10 (s, 3H), 3.58 (ddd, *J* = 5.5, 5.5, 10.6 Hz, 1H), 3.70-3.75 (m, 1H), 4.20 (s, 1H), 4.28 (ddd, *J* = 3.6, 7.6, 8.6 Hz, 1H), 4.42 (d, *J* = 12.2 Hz, 1H), 4.47 (d, *J* = 12.2 Hz, 1H), 4.52 (s, 2H), 6.38 (d, *J* = 8.3 Hz, 1H), 6.72 (dd, *J* = 7.6, 7.6 Hz, 1H), 6.99 (ddd, *J* = 1.5, 7.6, 8.3 Hz, 1H), 7.05-7.09 (m, 1H), 7.13-7.18 (m, 2H), 7.26-7.30 (m, 2H), 7.57 (dd, *J* = 1.5, 7.6 Hz, 1H); ^{13}C NMR (C_6D_6) δ 21.3, 30.7, 55.2, 65.5, 69.4, 73.3, 82.9, 94.7, 111.4, 120.9, 127.7, 128.1, 128.3, 128.5, 129.9, 130.9, 138.7, 156.3, 210.0; ESI-MS *m/z* 397 $[M+Na]^+$; HRMS (FAB) $[M+H]^+$ calcd for $C_{21}H_{27}O_6$, 375.1807; found, 375.1811; $[\alpha]_D^{25}$ –2.7 (*c* 0.41, $CHCl_3$) (87% ee); HPLC (DAICEL CHIRALPAK AD, 2-propanol/hexane 20/80, flow 1.0 mL/min, detection at 254 nm) t_R 11.8 min (minor) and 14.5 min (major).

(2*R*, 3*R*)-5-benzyloxymethoxy-2,3-dihydroxy-1-(2-methoxyphenyl)-2-methyl-1-penanone (*anti*-28h)

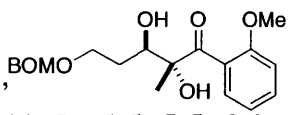

colorless solid; IR (KBr) ν 3496, 1679, 1596 cm^{-1}; ^1H NMR (C_6D_6) δ 1.60 (s, 3H), 1.79-1.86 (m, 1H), 1.96 (dddd, *J* = 2.1, 5.5, 8.2, 17.5 Hz, 1H), 2.68 (d, *J* = 6.7 Hz, 1H), 3.04 (s, 3H), 3.65 (ddd, *J* = 5.5, 5.5, 9.2 Hz, 1H), 3.79 (ddd, *J* = 4.5, 8.2, 9.2 Hz, 1H), 3.94 (s, 1H), 4.22 (ddd, *J* = 1.8, 6.7, 8.2

Hz, 1H), 4.45 (d, J = 12.0 Hz, 1H), 4.49 (d, J = 12.0 Hz, 1H), 4.56 (s, 2H), 6.31 (d, J = 8.6 Hz, 1H), 6.72 (dd, J =6.7, 7.6 Hz, 1H), 6.98 (ddd, J = 1.8, 6.7, 8.6 Hz, 1H), 7.06-7.09 (m, 1H), 7.13-7.17 (m, 2H), 7.28-7.30 (m, 2H), 7.38 (dd, J = 1.8, 7.6 Hz, 1H); ^{13}C NMR (C_6D_6) δ 22.3, 32.3, 55.1, 65.8, 69.3, 74.5, 82.7, 94.7, 111.3, 121.3, 127.7, 128.3, 128.5, 129.2, 130.5, 131.4, 138.7, 156.2, 210.3; ESI-MS *m/z* 397 $[M+Na]^+$; HRMS (FAB) $[M+H]^+$ calcd for $C_{21}H_{27}O_6$, 375.1807; found, 375.1804; $[\alpha]_D^{25}$ –0.3 (*c* 0.77, $CHCl_3$) (97% ee); HPLC (DAICEL CHIRALPAK AD, 2-propanol/hexane 20/80, flow 1.0 mL/min, detection at 254 nm) t_R 11.7 min (major) and 14.5 min (minor).

(2*R*, 3*S*)-4-benzyloxy-2,3-dihydroxy-1-(2-methoxyphenyl)-2-methyl-1-butanone (*syn*-28i)

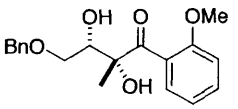

colorless oil; IR (neat) ν 3466, 1703, 1599 cm^{-1}; ^{1}H NMR (C_6D_6) δ 1.38 (s, 3H), 3.07 (d, J = 5.8 Hz, 1H), 3.13 (s, 3H), 3.60 (dd, J = 6.7, 9.7 Hz, 1H), 3.63 (dd, J = 4.3, 9.7 Hz, 1H), 4.16 (s, 1H), 4.23 (s, 2H), 4.27-4.30 (m, 1H), 6.39 (d, J = 8.3 Hz, 1H), 6.74 (dd, J = 7.4, 7.6 Hz, 1H), 6.99-7.09 (m, 2H), 7.10-7.16 (m, 4H), 7.50 (dd, J = 1.6, 7.4 Hz, 1H); ^{13}C NMR (C_6D_6) δ 21.7, 55.3, 71.1, 73.5, 74.3, 81.7, 111.4, 120.9, 127.9, 128.5, 128.6, 128.6, 130.0, 131.0, 138.5, 156.5, 209.7; ESI-MS *m/z* 353 $[M+Na]^+$; HRMS (FAB) $[M+H]^+$ calcd for $C_{19}H_{23}O_5$, 331.1545; found, 331.1542; $[\alpha]_D^{25}$ +1.3 (*c* 0.51, CH_2Cl_2)(85% ee); HPLC (DAICEL CHIRALPAK AD, 2-propanol/hexane 20/80, flow 1.0 mL/min, detection at 254 nm) t_R 12.0 min (minor) and 15.6 min (major).

(2*R*, 3*R*)-4-benzyloxy-2,3-dihydroxy-1-(2-methoxyphenyl)-2-methyl-1-butanone (*anti*-28i)

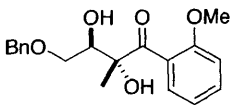

colorless oil; IR (neat) ν 3445, 1685, 1599 cm^{-1}; ^{1}H NMR (C_6D_6) δ 1.63 (s, 3H), 2.72 (brd, J = 7.3 Hz, 1H), 3.08 (s, 3H), 3.64 (dd, J = 4.6, 10.5 Hz, 1H), 3.70 (dd, J = 5.5, 10.6 Hz, 1H), 4.04 (s, 1H), 4.15 (d, J = 11.9 Hz, 1H), 4.19 (d, J = 11.9 Hz, 1H), 4.25-4.28 (m, 1H), 6.36 (brd, J = 8.3 Hz, 1H), 6.71 (ddd, J = 0.8, 7.4, 7.6 Hz, 1H), 6.98-7.12 (m, 6H), 7.36 (dd, J = 1.8, 7.6 Hz, 1H); ^{13}C NMR (C_6D_6) δ 22.8, 55.1, 72.0, 73.5, 74.6, 82.2, 111.4, 120.9, 127.9, 128.3, 128.5, 129.3, 130.2, 131.3, 138.3, 156.7, 209.6; ESI-MS *m/z* 353 $[M+Na]^+$; HRMS (FAB) $[M+H]^+$ calcd for $C_{19}H_{23}O_5$, 331.1545; found, 331.1540; $[\alpha]_D^{24}$ –2.6 (*c* 0.87, CH_2Cl_2)(92% ee); HPLC (DAICEL CHIRALCEL OD, 2-propanol/hexane 20/80, flow 1.0 mL/min, detection at 254 nm) t_R 9.7 min (minor) and 10.8 min (major).

Determination of the absolute configuration of the aldol product from hydroxyketone 27.

The absolute configuration of the aldol product *syn*-**28i** (from (*S*,*S*)-linked-BINOL) was determined after conversion to known compound ((2*R*,3*R*)-4-*O*-benzyl-2-methylbutane-1,2,3,4-tetraol) which was reported in *Tetrahedron Asymmetry*, **1997**, *8*, 559-577. The transformation was performed by following the Scheme (S3-8)-1. From optical resolution of the product, the absolute configuration of *syn*-**28i** was determined to be 2*R*,3*S*. Absolute configuration of other aldol products from hydroxyketone **27** was deduced to be 2*R*,3*S* by analogy.

Scheme (S3-8)-1. Determination of the Abosolute Configuration of Aldol Product from Hydroxypropiophenone **12.**

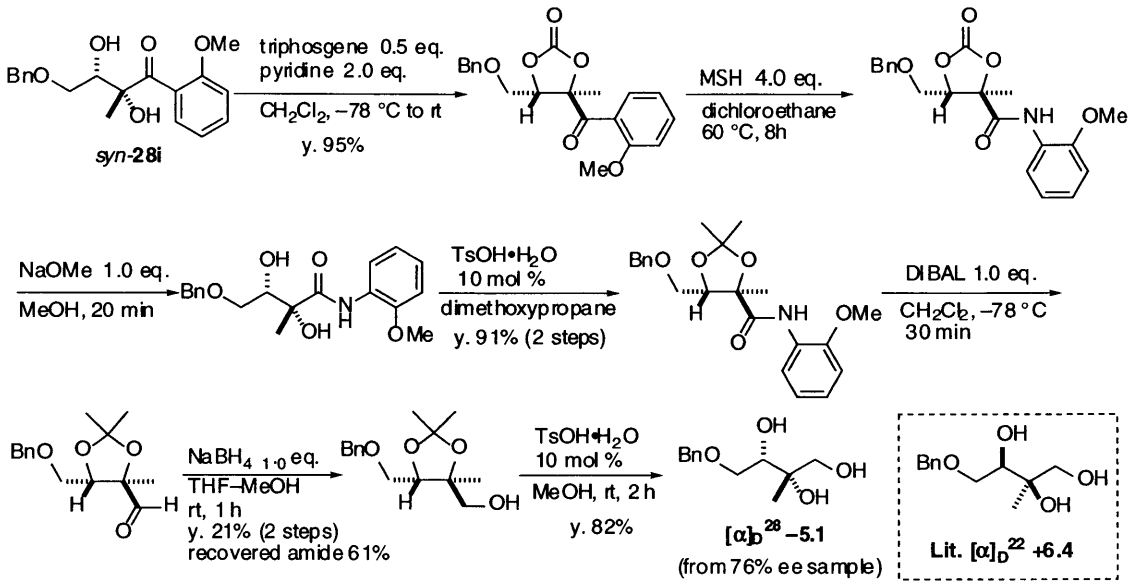

MSH: *O*-mesitylenesulfonylhydroxylamine.

General Procedure for Catalytic Asymmetric Aldol Reaction of Ketone *rac*-27 Promoted by Et_2Zn/(*S*,*S*)-Sulfur-linked-BINOL 35 = 4/1 with MS 3A System:

MS 3A (30 mg) in a test tube was activated prior to use under reduced pressure (ca. 0.7 kPa) at 160 ℃ for 3h. After cooling, a solution of (*S*,*S*)-Sulfur-linked-BINOL **35** (10.4 mg, 11.8w/w% diethyl ether and hexane included, 0.015 mmol) in THF (0.3 mL) was added under Ar. The mixture was cooled down to –20 °C. To the mixture was added Et_2Zn (60 μL, 0.06 mmol, 1.0 M in hexanes) at –20 ℃. After stirring for 10 min at –20 ℃, a solution of *rac*-**27** (270.3 mg, 1.5 mmol) in THF (0.24 mL) was added. After 5 min at –20 ℃, aldehyde **22a** (20 μL, 0.152 mmol) was added and stirred at –20 ℃ The stirring

was continued for 45 h at –20 ℃ and quenched by addition of 1 M HCl (2 mL). The mixture was extracted with ethyl acetate and the combined organic layers were washed with *sat. aq* $NaHCO_3$, brine and dried over $MgSO_4$. Evaporation of solvent gave a crude mixture of the aldol products. The diastereomeric ratios of the aldol products were determined by ^1H NMR of the diastereomixture. After purification by silica gel flash column chromatography (hexane/acetone 8/1–4/1), **28a** was obtained (38.8 mg, 0.129 mmol, y. 85%, dr: *syn/anti* = 35/65, 60% ee(*syn*), 92% ee(*anti*)). Ee was determined by chiral HPLC analysis.

Synthesis of (*S, S*)-Sulfur linked-BINOL 35:

Synthetic procedure for 3-bromomethyl-2,2'-bis(methoxymethyloxy)-1,1'-binaphthalene (**15**) was reported. See, chapter 2 (Matsunaga, S.; Das, J.; Roels, J.; Vogl, E. M.; Yamamoto, N.; Iida, T.; Yamaguchi, K.; Shibasaki, M. *J. Am. Chem. Soc.* **2000**, *122*, 2252).

3-Thioacetoxymethyl-2,2'-bis(methoxymethyloxy)-1,1'-binaphthalene (33)

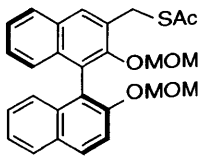

To a dark green solution of potassium thioacetate (1.14 g, 10 mmol) in DMF (20 mL) at 0 ℃ was added 3-bromomethyl-2,2'-bis(methoxymethyloxy)-1,1'-binaphthalene (**15**) (2.34 g, 5.0 mmol). The mixture was stirred at 0 ℃ for 10 min, then was diluted with diethyl ether. The organic layer was washed with H_2O, brine and was dried over $MgSO_4$. After evaporation of solvent, the residue was purified by silica gel flash column chromatography (hexane/ethyl acetate = 10/1 to 6/1) to afford **33** as colorless foam (2.23 g, 4.83 mmol, y. 97%). IR (neat) ν 2953 ,1688, 1240, 1149 cm^{-1}; ^1H NMR ($CDCl_3$) δ 2.37 (S, 3H), 3.01 (S, 3H), 3.17 (S, 3H), 4.47 (S, 2H), 4.49 (d, *J* = 5.8 Hz, 1H), 4.61 (d, *J* = 5.8 Hz, 1H), 5.03 (d, *J* = 7.1 Hz, 1H), 5.09 (d, *J* = 7.1 Hz, 1H), 7.11-7.15 (m, 2H), 7.18 (ddd, *J* = 7.9, 6.7, 1.3 Hz, 1H), 7.34 (ddd, *J* = 7.9, 6.7, 1.3 Hz, 1H), 3.88 (s, 3H), 4.73 (ddd, *J* = 3.0, 4.2, 8.0 Hz, 1H), 5.35 (d, *J* = 4.2 Hz, 1H), 7.00 (d, *J* = 8.5 Hz, 1H), 7.25 (ddd, *J* = 6.7, 6.7, 1.3 Hz, 1H), 7.36 (ddd, *J* = 6.7, 6.7, 1.3 Hz, 1H), 7.56 (d, *J* = 9.0 Hz 1H), 7.83-7.86 (m, 2H), 7.95 (d, *J* = 9.0 Hz, 1H), 7.99 (s, 1H); ^{13}C NMR ($CDCl_3$) δ 29.4, 30.4, 56.0, 56.9, 94.8, 99.3, 116.4, 120.5, 124.2, 125.1, 125.3, 125.4, 125.6, 126.2, 126.8, 127.8, 129.6, 129.8, 130.0, 130.8, 131.0, 133.5, 133.9, 152.5, 152.8, 195.6; EI-MS *m/z* 485 $[M+Na]^+$; HRMS (FAB) $[M+H]^+$ calcd for $C_{27}H_{27}O_5S$, 463.1579; found, 463.1580.

3,3''-(Thiodimethylene)-di-2,2'-bis(methoxymethyloxy)-1,1'-binaphthalene (34)

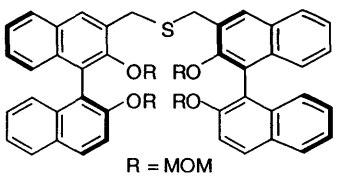

To a stirred solution of **33** (1.91 g, 4.13 mmol) in THF (12 mL)/CH_3OH (12 mL) at 0 ℃ was added $NaOCH_3$ (500 mg, 11.4 mmol). The mixture was stirred at 0 ℃ for 5 min, and then was quenched by adding *sat. aq.* NH_4Cl. The mixture was extracted with ethyl acetate (100 mL x 3). The combined organic layer was washed with brine, dried over $MgSO_4$. After evaporation of solvent, the residue was obtained as colorless solid. Because the intermediate thiol was not stable, the crude material was quickly subjected to the next step without further purification.

All the crude solid was dissolved in anhydrous THF (25 mL) and cooled down to 0 ℃. To a solution at 0℃ was added NaH in oil (200 mg, 5 mmol as 60% purity), and then 3-bromomethyl-2,2'-bis(methoxymethyloxy)-1,1'-binaphthalene (**15**) (2.0 g, 4.28 mmol). The mixture was stirred at 0℃ for 30 min, then was quenched by adding *sat. aq.* NH_4Cl. The mixture was extracted with ethyl acetate. The combined organic layer was washed with brine and was dried over $MgSO_4$. After evaporation of solvent, the residue was purified by silica gel flash column chromatography (hexane/ ethyl acetate = 5/1 to 2/1) to afford **34** as colorless foam (2.49 g, 3.08 mmol, y. 75% (2 steps)). IR (neat) ν 2927, 1240, 1149, 1049 cm^{-1}; ^1H NMR ($CDCl_3$) δ 2.80 (s, 6H), 3.15 (s, 6H), 4.14 (d, *J* = 13.6 Hz, 2H), 4.17 (d, *J* = 13.6 Hz, 2H), 4.54 (d, *J* = 5.5 Hz, 2H), 4.62 (d, *J* = 5.5 Hz,2H), 5.01 (d, *J* = 7.0 Hz,2H), 5.10 (d, *J* = 7.0 Hz,2H), 7.13-7.24 (m, 8H), 7.31-7.34 (m, 4H), 7.57 (d, *J* = 9.0 Hz, 2H), 7.78 (d, *J* = 8.0 Hz, 2H), 7.85 (d, *J* = 8.0 Hz, 2H), 7.74 (d, *J* = 9.0 Hz, 2H), 8.01 (s, 2H); ^{13}C NMR ($CDCl_3$) δ 31.8. 55.9, 56.6, 94.9, 99.3, 116.5, 120.8, 124.1, 125.0, 125.5, 125.6, 125.7, 125.9, 126.7, 127.7, 127.9, 129.6, 129.8, 129.8, 130.9, 131.8, 133.3, 134.0, 152.5, 152.9; EI-MS *m/z* 829 $[M+Na]^+$; HRMS (FAB) $[M+H]^+$ calcd for $C_{50}H_{47}O_8S$, 807.2991; found, 807.3017.

3,3''-(Thiodimethylene)-di-1,1'-bi-2-naphthol (35)

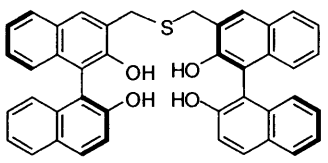

To a stirred solution of **34** (698.6 mg, 0.866 mmol) in CH_2Cl_2 (3 mL)/ CH_3OH (3 mL) was added $TsOH•H_2O$ (32 mg, 0.168 mmol). The mixture was stirred at 40 ℃ for 12 h. The mixture was then diluted with ethyl acetate, washed with *sat. aq* $NaHCO_3$, brine, dried over $MgSO_4$. After evaporation, the residure was purified by silica gel flash column chromatography (hexane/ diethyl ether = 2/1 to 1/1) to afford **35** as pale yellow solid (534.6 mg, containing 9.9 w/w% diethyl ether and hexane as determined by ^1H NMR, 0.764 mmol, y. 88%). IR (neat) ν 3499, 3057, 1383, 1210 cm^{-1}; ^1H NMR ($CDCl_3$) δ 4.04 (d, *J* = 13.9 Hz, 2H), 4.08 (d, *J* = 13.9 Hz, 2H), 4.98 (s, 2H), 5.54 (s, 2H), 7.08 (d, *J* = 8.5 Hz, 2H), 7.08 (d, *J* = 8.5 Hz, 2H), 7.20 (dd, *J* = 7.9, 7.9 Hz, 2H), 7.24 (dd, *J* = 7.9, 7.9 Hz, 2H), 7.29-7.35 (m, 6H), 7.79 (d, *J* = 7.9 Hz, 2H), 7.86 (d, *J* = 7.9Hz, 2H), 7.94 (d, *J* = 9.2 Hz, 2H), 7.96 (s, 2H); ^{13}C NMR ($CDCl_3$) δ 31.6, 111.4, 112.0,

117.8, 123.9, 124.2, 124.2, 124.3, 126.5, 127.2, 127.4, 128.0, 129.1, 129.4, 131.0, 131.2, 132.9, 133.4, 151.4, 152.5, 128.3; EI-MS *m/z* 653 $[M+Na]^+$; HRMS (FAB) $[M+H]^+$ calcd for $C_{42}H_{31}O_4S$, 631.1943; found, 631.1943. $[\alpha]_D^{25}$ +90.2 (*c* 1.0, $CHCl_3$).

References and Notes:

(1) (a) Noyori, R. *Asymmetric Catalysis in Organic Synthesis*, Wiley, New York, **1994**.(b) Jacobsen, E. N.; Pfaltz, A.; Yamamoto, H. Eds. *Comprehensive Asymmetric Catalysis*; Springer, Berlin, **1999**. (c) Ojima, I. Ed. *Catalytic Asymmetric Synthesis*, 2nd Ed., Wiley, New York, **2000**.

(2) For a general discussion of atom economy in organic synthesis, see: (a) Trost, B. M.; *Science* **1991**, *254*, 1471. (b) Trost, B. M.; *Angew. Chem., Int. Ed. Engl.* **1995**, *34*, 259.

(3) Review: (a) Shibasaki, M.; Yoshikawa, N. *Chem. Rev.* **2002**, *102*, 2187. (b) Shibasaki, M.; Kanai, M.; Funabashi, K. *Chem. Commun.* **2002**, 1989. (c) Shibasaki, M.; Kanai, M. *Chem. Pharm. Bull.* **2001**, *49*, 511. (d) Shibasaki, M. *Enantiomer*, **1999**, *4*, 513. (e) Shibasaki, M. *Chemtracts-Organic Chemistry*, **1999**, *12*, 979. (f) Shibasaki, M.; Sasai, H.; Arai, T. *Angew. Chem. Int. Ed. Engl.* **1997**, *36*, 1236.

(4) Sasai, H.; Suzuki, T.; Itoh, N.; Tanaka, K.; Date, T.; Okuma, K.; Shibasaki, M. *J. Am. Chem. Soc.* **1993**, *115*, 10372.

(5) (a) Yamada, Y. M. A.; Yoshikawa, N.; Sasai, H.; Shibasaki, M. *Angew. Chem., Int. Ed. Engl.* **1997**, *36*, 1871. (b) Yoshikawa, N.; Yamada, Y. M. A.; Das, J.; Sasai, H.; Shibasaki, M. *J. Am. Chem. Soc.* **1999**, *121*, 4168.

(6) (a) Arai, T.; Yamada, Y. M. A.; Yamamoto, N.; Sasai, H.; Shibasaki, M. *Chem. Eur. J.* **1996**, *2*, 1368. (b) Sasai, H.; Emori, E.; Arai, T.; Shibasaki, M. *Tetrahedron Lett.* **1996**, *37*, 5561. (c) Arai, T.; Sasai, H.; Yamaguchi, K.; Shibasaki, M. *J. Am. Chem. Soc.* **1998**, *120*, 441 and references therein.

(7) Arai, T.; Sasai, H.; Aoe, K.; Okamura, K.; Date, T.; Shibasaki, M. *Angew. Chem. Int. Ed. Engl.* **1996**, *35*, 104.

(8) (a) Arai, T.; Bougauchi, M.; Sasai, H.; Shibasaki, M. *J. Org. Chem.* **1996**, *61*, 2926. (b) Gröger, H.; Saida, Y.; Sasai, H.; Yamaguchi, K.; Martens, J.; Shibasaki, M. *J. Am. Chem. Soc.* **1998**, *120*, 3089 and references therein.

(9) Yamakoshi, K.; Harwood, S. J.; Kanai, M.; Shibasaki, M. *Tetrahedron Lett.* **1999**, *40*, 2565.

(10) Emori, E.; Arai, T.; Sasai, H.; Shibasaki, M. *J. Am. Chem. Soc.* **1998**, *120*, 4043.

(11) (a) Bougauchi, M.; Watanabe, S.; Arai, T.; Sasai, H.; Shibasaki, M. *J. Am. Chem. Soc.* **1997**, *119*, 2329. (b) Nemoto, T.; Ohshima, T.; Shibasaki, M. *J. Am. Chem. Soc.* **2001**, *123*, 2725 and references therein. (c) Nemoto, T.; Ohshima, T.; Shibasaki, M. *J. Am. Chem. Soc.* **2001**, *123*, 9474. (d) Nemoto, T.; Kakei, H.; Gnanadesikan, V.; Tosaki, S.-y.; Ohshima, T.; Shibasaki, M. *J. Am. Chem. Soc.* **2002**, *124*, 14544. (e) Kinoshita,

T.; Okada, S.; Park, S.-R.; Matsunaga, S.; Shibasaki, M. *Angew. Chem. Int. Ed.* in press.
(12) (a) Iida, T.; Yamamoto, N.; Sasai, H.; Shibasaki, M. *J. Am. Chem. Soc.* **1997**, *119*, 4783. (b) Iida, T.; Yamamoto, N.; Matsunaga, S.; Woo, H-G.; Shibasaki, M. *Angew. Chem. Int. Ed.* **1998**, *37*, 2223.
(13) Morita, T.; Arai, T.; Sasai, H.; Shibasaki, M. *Tetrahedron Asymmetry*, **1998**, *9*, 1445.
(14) (a) Yamada, K.-i.; Harwood, S. J.; Gröger, H.; Shibasaki, M. *Angew. Chem. Int. Ed.* **1999**, *38*, 3504. (b) Yamada, K.-i.; Moll, G.; Shibasaki, M. *Synlett* **2001**, 980.
(15) (a) Hamashima, Y.; Sawada, D.; Kanai, M.; Shibasaki, M. *J. Am. Chem. Soc.* **1999**, *121*, 2641. (b) Hamashima, Y.; Sawada, D.; Nogami, H.; Kanai, M.; Shibasaki, M. *Tetrahedron*, **2001**, *57*, 805.
(16) (a) Hamashima, Y.; Kanai, M.; Shibasaki, M. *J. Am. Chem. Soc.* **2000**, *122*, 7412. (b) Hamashima, Y.; Kanai, M.; Shibasaki, M. *Tetrahedron Lett.* **2001**, *42*, 691. (c) Yabu, K.; Masumoto, S.; Yamasaki, S.; Hamashima, Y.; Kanai, M.; Curran, D. P.; Shibasaki, M. *J. Am. Chem. Soc.* **2001**, *123*, 9908. (d) Masumoto, S.; Suzuki, M.; Kanai, M.; Shibasaki, M. *Tetrahedron Lett.* **2002**, *43*, 8647.
(17) (a) Takamura, M.; Hamashima, Y.; Usuda, H.; Kanai, M.; Shibasaki, M. *Angew. Chem. Int. Ed.* **2000**, *39*, 1650. (b) Takamura, M.; Hamashima, Y.; Usuda, H.; Kanai, M.; Shibasaki, M. *Chem. Pharm. Bull.* **2000**, *48*, 1586. (c) Nogami, H.; Matsunaga, S.; Kanai, M.; Shibasaki, M. *Tetrahedron Lett.* **2001**, *42*, 279. (d) Masumoto, S.; Usuda, H.; Suzuki, M.; Kanai, M.; Shibasaki, M. *J. Am. Chem. Soc.* **2003**, *125*, 5634.
(18) (a) Takamura, M.; Funabashi, K.; Kanai, M.; Shibasaki, M. *J. Am. Chem. Soc.* **2000**, *122*, 6327. (b) Takamura, M.; Funabashi, K.; Kanai, M.; Shibasaki, M. *J. Am. Chem. Soc.* **2001**, *123*, 6801. (c) Funabashi, K.; Ratni, H.; Kanai, M.; Shibasaki, M. *J. Am. Chem. Soc.* **2001**, *123*, 10784.
(19) (a) Tian, J.; Yamagiwa, N.; Matsunaga, S.; Shibasaki, M. *Angew. Chem. Int. Ed.* **2002**, *41*, 3636. (b) Tian, J.; Yamagiwa, N.; Matsunaga, S.; Shibasaki, M. *Org. Lett.* **2003**, *5*, 3021.
(20) Reviews: (a) Sawamura, M.; Ito, Y. *Chem. Rev.* **1992**, *92*, 857. (b) Steinhagen, H.; Helmchen, G. *Angew. Chem. Int. Ed. Engl.* **1996**, *35*, 2339. (c) van den Beuken, E. K.; Feringa, B. L. *Tetrahedron*, **1998**, *54*, 12985. (d) Rowlands, G. J. *Tetrahedron*, **2001**, *57*, 1865. For selected examples of recent bifunctional asymmetric catalysts, see: (a) Yamanaka, M.; Ito, H.; Noyori, R. *J. Am. Chem. Soc.* **2000**, *122*, 1466. (b) Ready, J. M.; Jacobsen, E. N. *J. Am. Chem. Soc.* **2001**, *123*, 2687. (c) McCleland, B. W.; Nugent, W. A.; Finn, M. G. *J. Org. Chem.* **1998**, *63*, 6656. (d) Sundararajan, G.; Prabagaran, N.

Org. Lett. **2001**, *3*, 389. (e) Blake, A. J.: Cunningham, A.; Ford, A.; Teat, S. J.; Woodward, S. *Chem. Eur. J.* **2000**, *6*, 3586. (f) DiMauro, E. F.; Kozlowski, M. C. *Org. Lett.* **2001**, *3*, 1641 and references cited therein. (g) Watanabe, M.; Murata, K.; Ikariya, T. *J. Am. Chem. Soc.* **2003**, *125*, 7508. (h) France, S; Guerin, D. J.; Miller, S. J.; Lectka, T. *Chem. Rev.* **2003**, *103*, 2985 and references therein.

(21) Review: (a) Pu, L. *Chem. Rev.* **1998**, *98*, 2405. (b) Chen, Y.; Yekta, S.; Yudin, A. K. *Chem. Rev.* **2003**, *103*, 3155. (c) Kocovsky, P.; Vyskocil, S.; Smrcina, M. *Chem. Rev.* **2003**, *103*, 3213. See, also ref 1.

(22) Sasai, H.; Arai, T.; Satow, Y.; Houk, K. N.; Shibasaki, M. *J. Am. Chem. Soc.* **1995**, *117*, 6194. See also, ref 3d, 5b, 6a, 7, 8b, 11.

(23) (a) Matsunaga, S.; Das, J.; Roels, J.; Vogl, E. M.; Yamamoto, N.; Iida, T.; Yamaguchi, K.; Shibasaki, M. *J. Am. Chem. Soc.* **2000**, *122*, 2252. For preliminary studies on carbon-linked-BINOLs, see; (b) Vogl, E. M.; Matsunaga, S.; Kanai, M.; Iida, T.; Shibasaki, M. *Tetrahedron Lett.* **1998**, *39*, 7917.

(24) For related works by other groups concerning linked-BINOLs and polymer-BINOLs, see; (a) Ishitani, H.; Kitazawa, T.; Kobayashi, S. *Tetrahedron Lett.* **1999**, *40*, 2161 and references therein. They independently reported the same carbon-linked-BINOL ligand at the same time with Shibasaki's report. (b) Yu, H.-B.; Hu, Q.-S.; Pu, L. *J. Am. Chem. Soc.* **2000**, *122*, 6500 and references therein. (c) Arai, T.; Hu, Q.-S.; Zheng, X.-F.: Pu, L.; Sasai, H.; *Org. Lett.* **2000**, *2*, 4261. (d) Cunningham, A.; Dennis, M. R.; Woodward, S. *J. Chem. Soc., Perkin Trans I*, **2000**, 4422 and references therein. (e) Chow, H.-F.; Ng, M.-K. *Tetrahedron Asymmetry*, **1996**, *7*, 2251. (f) Meng, Y.; Slaven IV, W. T.; Wang, D.; Liu, T.-J.; Chow, H.-F.; Li, C.-J. *Tetrahedron Asymmetry*, **1998**, *9*, 3693.

(25) Helgeson, R. C.; Tarnowski, T. L.; Cram, D. J. *J. Org. Chem.* **1979**, *44*, 2538.

(26) Sugasawa, K.; Shindo, M.; Noguchi, H.; Koga, K. *Tetrahedron Lett.* **1996**, *37*, 7377 and references cited therein.

(27) Review: Matsunaga, S.; Ohshima, T.; Shibasaki, M. *Adv. Synth. Catal.* **2002**, *344*, 4.

(28) (a) Kim, Y. S.; Matsunaga, S.; Das, J.; Sekine, A.; Ohshima, T.; Shibasaki, M. *J. Am. Chem. Soc.* **2000**, *122*, 6506. (b) Takita, R.; Ohshima, T.; Shibasaki, M. *Tetrahedron Lett.* **2002**, *43*, 4661.

(29) Matsunaga, S.; Ohshima, T.; Shibasaki, M. *Tetrahedron Lett.* **2000**, *41*, 8473.

(30) (a) Kumagai, N.; Matsunaga, S.; Yoshikawa, N.; Ohshima, T.; Shibasaki, M. *Org. Lett.* **2001**, *3*, 1539. (b) Yoshikawa, N.; Kumagai, N.; Matsunaga, S.; Moll, G.; Ohshima, T.; Suzuki, T.; Shibasaki, M. *J. Am. Chem. Soc.* **2001**, *123*, 2466.

(31) Reviews for direct catalytic asymmetric aldol reactions: (a) Alcaide, B.; Almendros, P.

Eur. J. Org. Chem. **2002**, 1595. (b) List, B. *Tetrahedron* **2002**, *58*, 5573.
(32) Kumagai, N.; Matsunaga, S.; Shibasaki, M. *Org. Lett.* **2001**, *3*, 4251.
(33) For selected examples of X-ray structures of bimetallic achiral zinc complexes, see: (a) Kaminskaia, N. V.; Spingler, B.; Lippard, S. J. *J. Am. Chem. Soc.* **2000**, *122*, 6411. (b) Koike, T.; Inoue, M.; Kimura, E.; Shiro, M. *J. Am. Chem. Soc.* **1996**, *118*, 3091. (c) Abe, K.; Izumi, J.; Ohba, M.; Yokoyama, T.; Okawa, H. *Bull. Chem. Soc. Jpn.* **2001**, *74*, 85 and references therein.
(34) CIF file of crystal **29** was deposited to CCDC (CCDC 186559).
(35) Coldspray ionization mass spectrometry (CSI-MS) method enables the direct observation of labile species in solution phase: Sakamoto, S.; Fujita, M.; Kim, K.; Yamaguchi, K. *Tetrahedron*, **2000**, *56*, 955 and references therein.
(36) In general, it is true that observed major species is not always an active species. However, it seems at least sure that some Zn-rich complex should be an actual active species as supported by kinetics in the following paragraph.
(37) (a) Trost, B. M.; Ito, H.; Silcoff, E. R. *J. Am. Chem. Soc.* **2001**, *123*, 3367. (b) Trost, B. M.; Ito, H. *J. Am. Chem. Soc.* **2000**, *122*, 12003.
(38) Judging from initial rate kinetic data alone, the possibility that the enolization step would be the rate determining step can not completely be ruled out. Considering the drastic additive effects of MS 3A to accelerate the reaction (see, section 3-3: second generation system with MS 3A), I believe it more reasonable to assume that rate limiting step would be the product dissociation step.
(39) For the beneficial effects of additional achiral base to enhance the reaction rate of bifunctional asymmetric catalysis, see ref 6a and 19a.
(40) For precedent examples where activated molecular sieves had a key role to accelerate the catalyst turn over step (the product dissociation step), see ref. 12.
(41) For a review of catalytic enantioselective synthesis of chiral quaternary centers, see: Corey, E. J.; Guzman-Perez, A. *Angew. Chem., Int. Ed.* **1998,** *37,* 388.
(42) For excellent achievements in catalytic asymmetric hydrogenation of ketones, see review: Noyori, R.; Ohkuma, T. *Angew. Chem., Int. Ed.* **2001,** *40,* 40.
(43) Optically active ketone **27** (99% ee), was prepared as shown in the scheme below. Starting from the racemic ketone **27** aldol reaction with (*R, R*)-linked-BINOL was repeated by using recovered ketone **27** each time. After four times direct aldol reaction and recovery processes, ketone **27** was recovered in high ee (>99% ee).